The chemical synthesis of natural and novel β-acid derivatives for biological evaluation as anticancer and antibacterial agents

Tucknott , Matthew L.

2013

THE FOLLOWING HAVE NOT BEEN COPIED ON INSTRUCTION FROM THE UNIVERSITY

Figure 8 page 11

Figure 10 page 14

Figure 13 page 17

Chapter 8: Appendix

Declaration

The content of this thesis is, to the best of my knowledge, original research except for that work which has been duly referenced.

Matthew Lee Tucknott

Acknowledgements

I must first recognise the tremendous generosity of Professor Elizabeth Tyrrell, who upon hearing I was available to take on a new research project made great efforts to contact me and offer me the position. She has provided excellent supervision, support, encouragement and guidance through this project whilst also being highly respectful of my personal life. I am also indebted to Dr Roland Archer, who's own PhD research was also concerned with the hop acids of *Humulus lupulus* and he too provided excellent supervision and guidance, along with a sense of humour to alleviate even the most difficult of days; his withdrawal from the university and therefore the group to embark on a new position. The departure of Roland was met by the arrival to the group of Dr Alex Sinclair, who has an equally impressive sense of humour and a knowledge of chemistry which I can currently only marvel upon.

I must also extend gratitude to my friends and fellow research students;, Jason Cranfield, Ravtej Thatti, Beena Shah and Dr Baljit Gatora, Dr Leon Whiteman, and Dr Peter Brawn. The laboratory has been a welcoming environment even when the work has tested my patience. I will sorely miss the excellent (!) music, the banter and camaraderie shared between us all.

I must also extend my thanks to the excellent technical staff of Kingston University, in particular Dr Jean Marie Peron for his ever-maximum enthusiasm for NMR spectroscopy and the manner in which he has always tried his best to help. Of equal special mention is Jan Dowler, the microbiology technician who made the microbiology studies possible – her patience in teaching me the fundamentals of microbiology enabled me to complete a large and significant portion of this research.

Finally, I cannot end this section of my thesis without mention of my beautiful and wonderful wife, Maria. Without her support and enduring patience, I would have lost perspective and motivation; a PhD is not a trivial activity to undertake, and with help from her I have remained enthusiastic, motivated and organised; successfully completing this research of which I am very proud.

Abstract

The Tyrrell group has, in recent years, developed a strong interest in the chemical synthesis and biological activity of the hop bitter acids lupulone **1**, humulone **2** and their naturally occurring congeners, **1a-d** and **2a-d**. Previous work focused on investigating the chemistry of the α-acid humulone **2**, demonstrating the propensity of this compound to have a cytotoxic effect against the SK-MES lung cancer cell line and the MCF-7 breast cancer cell line. This thesis documents the recent research concerning the synthesis, the anticancer and antibacterial activity of the β-acid lupulone **1**, its naturally occurring congeners **1a-d** and further, novel, non-naturally occurring compounds. We resumed the group's previous collaboration with the Colston and Pirianov research group at St Georges, where the anticancer studies were performed.

The synthesis centred on a Friedel-Crafts acylation of phloroglucinol **32**, followed by a C-trialkenylation reaction between the acylphloroglucinol and an allyl bromide. We conducted experiments that focused upon the choice of base and solvent for the trialkenylation reaction, concluding that liquid ammonia as both the base and solvent offered the most efficient route to the β-acids. It was shown that aliphatic allylic bromides lend themselves to the reaction, although some derivatives require purification by column chromatography in addition to recrystallisation. In contrast, aromatic allyl bromides did not participate in the alkenylation reaction.

We further investigated an alternate C-alkenylation reaction involving the di-lithiation of 1,3,5-trimethoxybenzene. We discovered that by including copper (I) iodide in the reaction, prenyl bromide **23** and allyl bromide **41** could be successfully coupled. We also discovered that our 2nd generation β-acids **42a-g** could participate in a ring-closing metathesis reaction, forming novel spirocyclic compounds **50a-b**.

Our antibacterial studies showed that β-acids are effective against Gram-positive bacteria, but not Gram-negative bacteria in accordance with published observations. We took our investigations further and found that β-acids are effective against multidrug-resistant *Staphylococcus aureus*, even where the commercially available ciprofloxacin **67** was not.

Our anticancer studies showed that of the compounds tested, non-natural derivative **1g** featuring a cyclopropyl ring was most effective against the MCF-7 and MDA-MB-231 breast cancer cell lines, and non-natural derivative **1j** was most effective against the DU145 and PC3 prostate cancer cell lines.

Abbreviations

ADP: Adenosine Diphosphate

ATP: Adenosine Triphosphate

BSAC: British Society for Antimicrobial Chemotherapy

CCC: Counter Current Chromatography

^{13}C-NMR: Carbon-13 Nuclear Magnetic Resonance spectroscopy

DCM: Dichloromethane

DEA: Diethylamine

DIEA: Diisopropylethylamine

DMF: Dimethylformamide

DMSO: Dimethylsulphoxide

DNA: Deoxyribonucleic Acid

FT-NMR: Fourier-Transform Nuclear Magnetic Resonance

GC-MS: Gas Chromatography-Mass Spectrometry

H. lupulus: *Humulus lupulus*

^{1}H-NMR: Proton Nuclear Magnetic Resonance spectroscopy

HPLC: High Performance Liquid Chromatography

HSQC: Heteronuclear Single Quantum Correlation spectroscopy

IC_{50}: Inhibitory Concentration 50 i.e. the lowest concentration of a drug required to kill 50% of a given sample of viable cells.

IR: Infra-Red Spectroscopy

IPA: Isopropylamine

Lb: *Lactobacillus*

MIC: Minimum Inhibitory Concentration i.e. the lowest concentration of a drug that will still prevent the growth of bacteria.

Mpt: Melting Point

MSSA: Methicillin or Multidrug-Sensitive *Staphylococcus aureus*

MSRA: Methicillin or Multidrug Resistant *Staphylococcus aureus*

MTT: (3-(4,5-dimethylthiazol-2-yl)-2,5-diphenyltetrazolium bromide

PARP: Poly-((Adenosine diphosphate) Ribose)-Polymerase

RBF: Round-Bottomed Flask

RCM: Ring-Closing Metathesis

SAR: Structure Activity Relationship

TLC: Thin Layer Chromatography

1,3,5-TMB: 1,3,5-trimethoxybenzene

TMEDA: Tetramethylethylenediamine

TNF-α: Tumor Necrosis Factor Alpha

TRAIL: TNF-related apoptosis-inducing ligand

VRSA: Vancomycin-Resistant *Staphylococcus aureus*

ZoI: Zone of Inhibition

Table of Contents

Chapter One:

Aims and Introduction

1.1 Research Objectives

The aims of this research project were:

(i) To develop a synthesis of the hop β-acid lupulone **1**;

(ii) To investigate the synthesis of β-acid derivatives, forming a small library of compounds derived from lupulone **1**;

(iii) To assess the antibacterial activity of both lupulone **1** and the derivatives against a range of bacteria;

(iv) To assess the anticancer activity of the lupulone **1** and derivatives against a range of cancer cell lines;

(v) To establish any potential structure activity relationship (SAR);

(vi) To investigate the mechanism by which lupulone **1** and any active derivatives cause cellular death in cancer cell lines.

Our rationale for evaluating the novel hop acids against these targets were based upon the known anticancer activity of hops[1] and their bacteriostatic/bacteriocidal role in the manufacture of beer[2]. The chemical syntheses made use of existing literature methods, optimised further to facilitate the wider synthesis of novel derivatives providing opportunities for in-depth analyses of the biological modes of action.

1.2 Background Information

The introduction of hops into the beer brewing process was historically intended to prevent spoilage of the beverage, and to promote a bitter flavour. The commonly used beer hop plant, *Humulus lupulus*, has been the subject of wide investigations in order to evaluate the chemical components giving rise to its pharmacological properties; this has lead to the classification of two distinct classes of extractable compounds – the β-acids of which lupulone **1** belongs and the α-acids of which humulone **2** belongs. These compounds also have naturally occurring analogues **1a-1d** and **2a-2d** (**Table 1**).

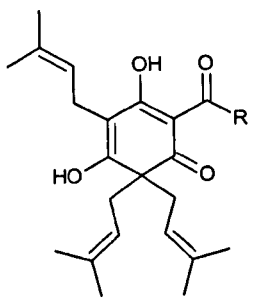

1, 1a-d

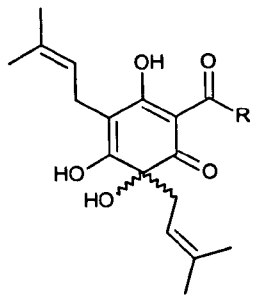

2, 2a-d

R =	Name
$CH_2CH(CH_3)_2$	n-lupulone **1** / n-humulone **2**
$CH(CH_3)_2$	Colupulone **1a** / Cohumulone **2a**
CH_2CH_3	Postlupulone **1b** / Posthumulone **2b**
$CH_2CH_2CH(CH_3)_2$	Prelupulone **1c** / Prehumulone **2c**
$CH(CH_3)CH_2CH_3$	Adlupulone **1d** / Adhumulone **2d**

Table 1

The assignment of "alpha" and "beta" to the naming of the two distinct classes of hop bitter acids is not due to the structural and chemical differences between the classes of compounds, but their importance to the brewing industry. The α-acids are important to the flavour and frothing properties of the final brewed

product, and as such are more important to the brewing manufacturers, hence their designation as the primary, or "alpha" component. Furthermore, most varieties of hop plants contain a greater proportion (by weight) of α-acids relative to the β-acids

1.2.1 Biosynthesis of the Hop Bitter Acids

Hop acids originate in the lupin glands of the hop flowering cone, the female part of the hop plant. These glands secrete α-acids, β-acids and a number of related compounds[3]. The biosynthetic pathway leading to the production of lupulone **1**, humulone **2** and their natural derivatives **1a-d** and **2a-d** has been extensively studied[4-9], revealing much about the intricate mechanism evolved by the hop plant.

The first stage of biosynthesis is the formation of an acylphloroglucinol derivative **3**, which occurs through a polyketide synthesis *via* a valerophenone synthase enzyme involving malonic acid **4**[4], bound to a cysteine-containing co-enzyme (**Figure 1a**). The resulting polyketide **6** is then coupled to a fatty acid **7**, affording the thioester **8** which undergoes cyclisation to form polyketide **9**, a tautomer of the acylphloroglucinol **3** (**Figure 1b**).

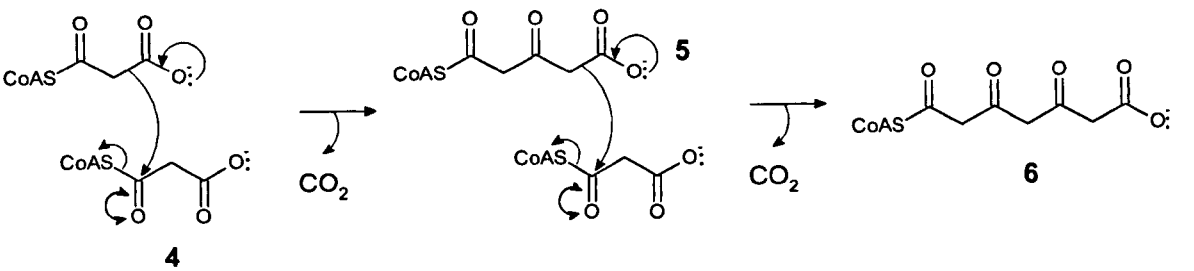

Figure 1a

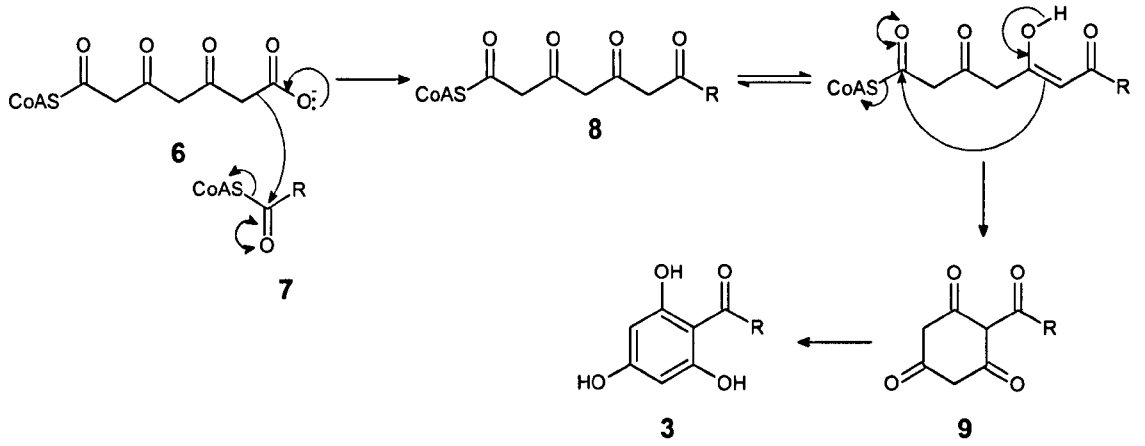

Figure 1b

The biosynthesis continues with the regiospecific introduction of a dimethylallyl (prenyl) moiety onto **3**, catalysed first by a membrane-bound prenyl transferase enzyme HIPT-1[5], generating the monoprenylated derivative **10**. It is not understood if this same enzyme catalyses the second prenylation to give deoxyhumulone derivatives **11**, or if other prenyl transferase enzymes are involved (**Figure 2**).

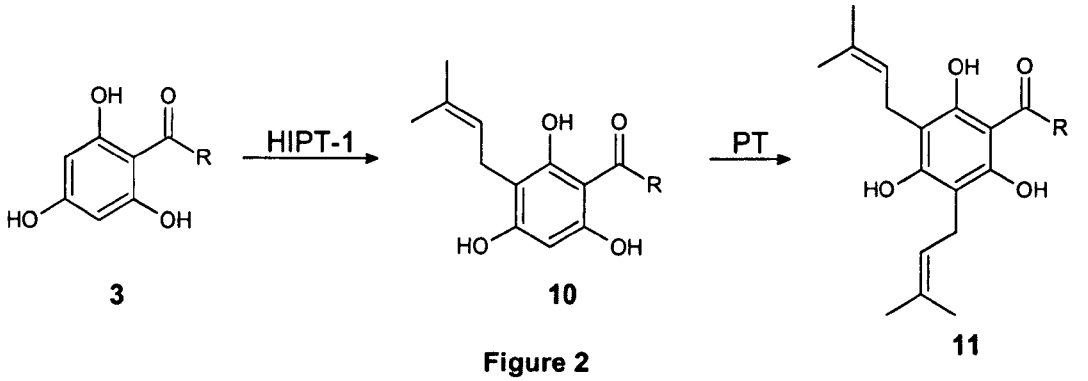

Figure 2

At this point in the biosynthesis, there is strong evidence suggesting that the oxidation of deoxyhumulone derivatives **11** occurs with molecular oxygen to give humulone **2** and derivatives **2a-d**[6, 7]; however, little is understood on how the third prenylation occurs to obtain lupulone **1** and derivatives **1a-d**[5, 8, 9]. Speculation still exists with two proposed hypotheses; a third prenylation occurs

with deoxyhumulone derivatives **11**, or there is a reduction of humulone **2** and derivatives **2a-d** at the tertiary hydroxyl moiety (**Figure 3**).

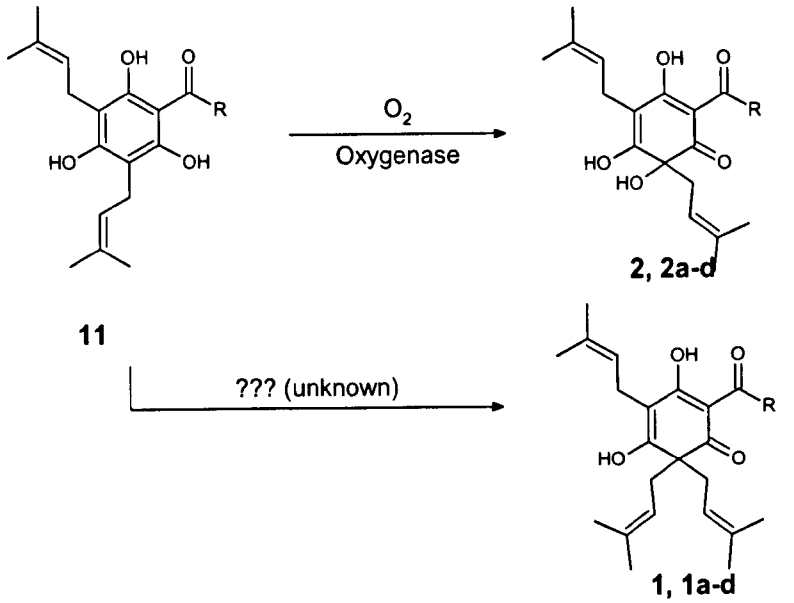

Figure 3

1.2.2 Isolation of the Hop Acids from Humulus lupulus

The historical process[10] of isolating the α-acids and β-acids begins with immersing dried hop cones in methanol to extract the compounds, followed by removal of methanol and centrifugation of the resulting material in cold (4 °C) water. This results in a hop extract free of fatty and waxy material. The following step to isolate the α-acids occurs by complexation with lead acetate ($Pb(OAc)_2$) in methanol, which forms a precipitate that is then filtered off. Removal of methanol, followed by addition of hexane and extraction into 1M sodium hydroxide solution allows isolation of the β-acids – acidification of the alkaline solution will yield a mixture of the β-acids as a waxy solid. The lead salts of the α-acids can be further purified by addition of 10% methanolic sulphuric acid to a hexane suspension of these lead salts, followed by selective complexation of α-acids using *ortho*-phenylenediamine. Acidification of the complex in diethyl ether yields the α-acids.

More contemporary methods of isolating hop acids involve the use of extracts from supercritical carbon dioxide[11], which depending on the conditions employed can be highly selective for a particular desired extract. Furthermore, the conditions used are milder, and because solvent removal is comparatively easy, the yield of isolated hop acids is relatively high. There are also reports of the use of counter-current chromatography (CCC)[12], where a liquid-liquid phase of two immiscible liquids is used to separate out components of a mixture. This is achieved by altering the properties of one phase (e.g. polarity), whereby different components can be extracted, and then passed through a chromatographic separation column (analogous to high-performance liquid chromatography, HPLC) for further separation. Such a method is useful at gaining small quantities of pure compound (up to ~100 mg) for analytical purposes, but is not a useful method for the multigram-scale isolation of individual hop acids.

1.2.3 Chemistry of the β-Acids

Lupulone **1**, and the naturally occurring congeners **1a-1d**, are structurally intriguing molecules, proving to be elusive to chemical synthesis and derivatization; this is mainly due to the known sensitivity towards pH[13, 14] and oxidation[15-17], enhanced by the potentially complicated keto-enol tautomeric patterns[18] (**Figure 4**).

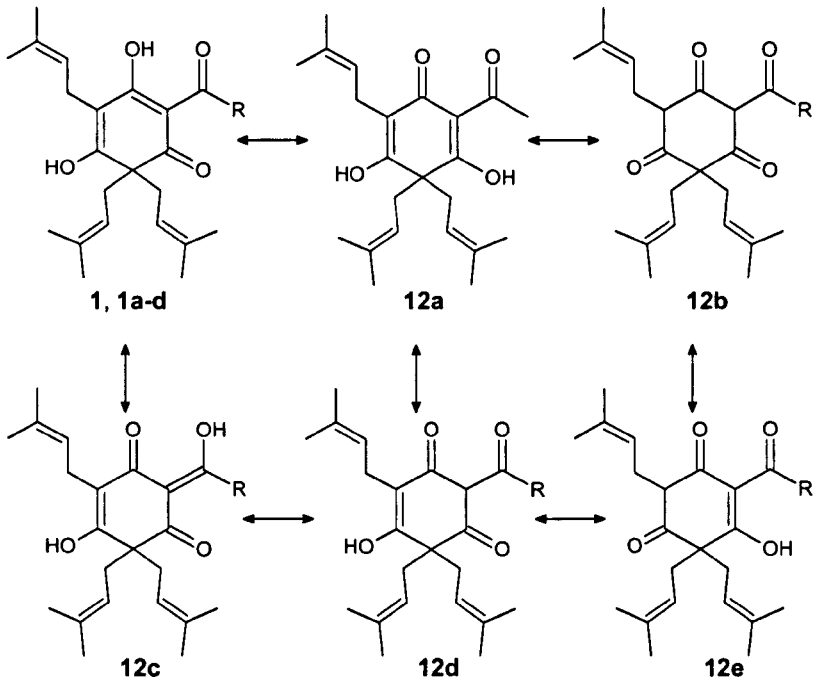

Figure 4: *Possible tautomeric forms of lupulone **1**,and compounds **1a-1d***

Non-protic solvents give rise to a mixture of tautomers, for example a chlorinated solvent such as chloroform will show a 70:30 mixture of isomer **1** and **12a**, whereas polar, protic solvents such as methanol will give rise to **1** in almost 100%[18]. In conditions of low pH, the β-acids tend to undergo degradation[13] (**Figure 5**) to generate deoxyhumulones **11** followed by intramolecular cyclisation[13, 14].

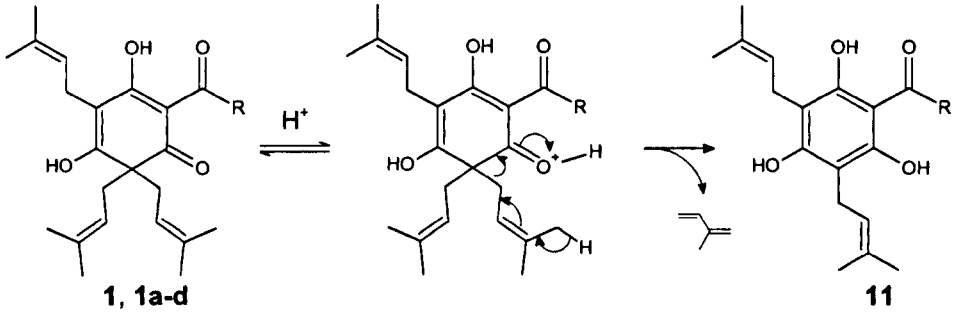

Figure 5

Howard et al[13] reported that the degradation to **11** was accompanied by an odour reminiscent of isoprene, suggesting that simple cleavage of one prenyl

unit is occurring. The intramolecular cyclisation (**Figure 6**) can generate two products, since after the initial cyclisation to give **13a**, the second can occur through attack of either remaining phenoxy group on the remaining prenyl side-chain, giving **13b** (*via* route 'a') and **13c** (*via* route 'b').

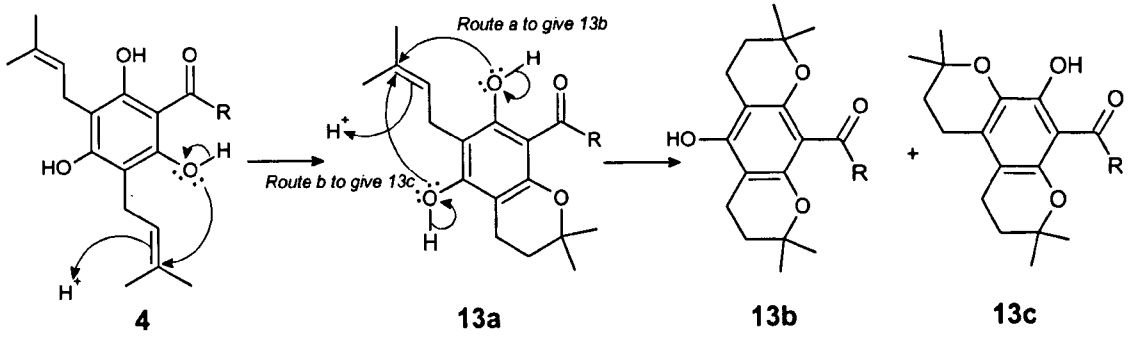

Figure 6

Oxidation of the β-acids gives rise to hulupones **14** through loss of the secondary prenyl unit, proceeded by ring contraction[19, 20] (**Figure 7**).

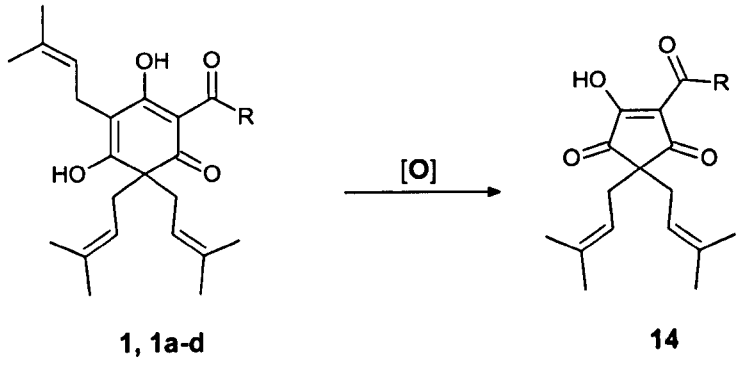

Figure 7

An extensive search of the literature revealed no reported mechanism by which this occurs, but synthetic preparation of cohulupone **14a** was reported by Wright[16], by exposing a solution of colupulone **1a** in cyclohexane to oxygen and sodium sulphite (**Scheme 1a**). Coates *et al*[17] demonstrated that cohulupone **14a** could be generated from colupulone **1a** in cyclohexane through exposure to

oxygen alone; further to this, an additional oxidation product **15** was formed (**Scheme 1b**), known to be present in batches of dried and stored hops which have been allowed to 'age' in air[17].

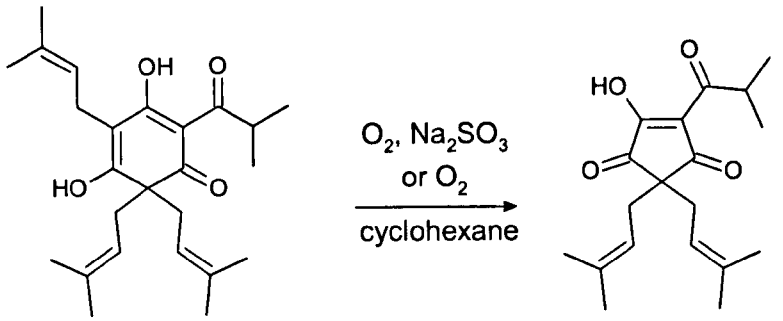

1a **14a**

Scheme 1a

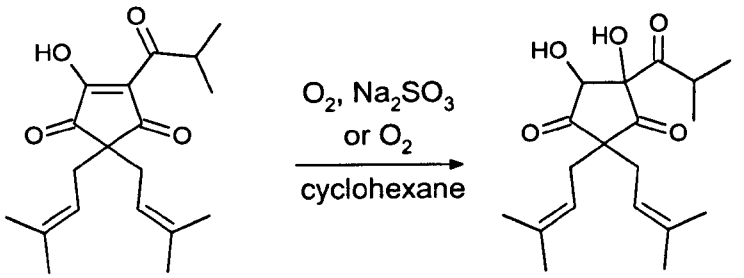

14a **15**

Scheme 1b

The sensitivity of the β-acids towards pH and oxygen is an important concern not only when handling them in synthetic work, but also when considering them as therapeutic agents. Oxygen-free storage at a neutral or weakly alkaline pH should decrease the rate of degradation, preserving the compound and its activity.

1.2.4 Antibacterial Activity

Bacteria are categorised as either Gram-positive or Gram-negative through the results of the Gram's differential staining procedure. Those bacteria which

remain permanently stained are termed "Gram-positive" and those bacteria where the stain is readily washed away are termed "Gram-negative"[21]. The differences between the two types are due to the construction of the cellular wall[22] (**Figure 8**). Gram-positive cells lack the relatively impermeable porin protein layer present in Gram-negative bacteria, hence they are potentially easier to eradicate with antibiotics as compounds are more likely to traverse the membrane into the intracellular space, where it can then exert an effect on the cell and either prevent replication, or induce cell death.

Figure 8: *The Porin protein wall gives Gram negative (right) bacteria its resistance to some drugs[23]. This relatively impermeable wall is not present in Gram-positive bacteria (left).*

The Gram staining procedure is commonly performed[24] as follows:

- The sample is placed in solution of the chemical dye "crystal violet" **16** (**Figure 9**) for one minute, and then rinsed quickly with deionised water.
- The sample is then placed in a 70% ethanol / 30% water solution containing 2% iodine and 3% potassium iodide.

- The sample is then counterstained by immersion in a solution of safranin **17** (**Figure 9**) to enhance the contrast of stained bacteria to non-stained bacteria, before rinsing again with deionised water.
- The bacteria present can be visualised under a microscope to determine if the dye has been retained or not.

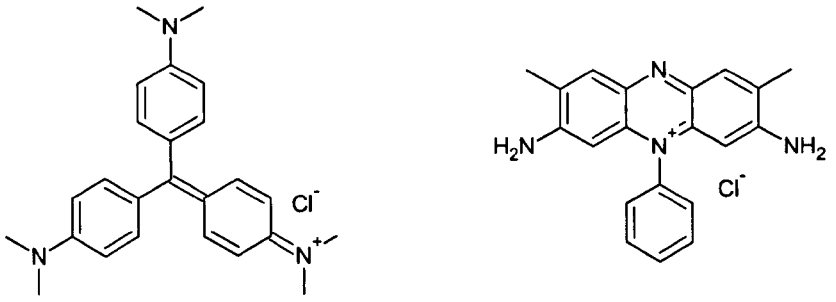

16 **17**

Figure 9

The triarylmethyl dye **16** interacts with the peptidoglycan component of the bacterial walls, which extends from the inner bilipid cytoplasmic membrane preventing leakage of the intracellular material into the extracellular space. Gram-positive bacteria can readily absorb the dye, but Gram-negative bacteria have a much more complex cellular wall and cannot retain the dye. The outermost cell wall layer consists of polysaccharides, and proceeding inwards gives way to a protein layer containing porins and receptor proteins, then a peptidoglycan layer (much thinner than that of the Gram-positive bacteria) and finally the bilipid layer of the cytoplasmic membrane.

1.2.4.1 Antibacterial Action of Hop Acids

The introduction of the hop plant *H. lupulus* into the brewing process resulted in the retention of the yeast performance which can otherwise be reduced by the growth of bacteria[2], particularly the lactic acid genus *Lactobacillus brevis* and

other *Lactobacillus* (*Lb*) species. Whilst this particular bacterium is considered a "healthy" bacteria i.e. can promote a healthy gastrointestinal tract in humans, it spoils the brewed beer product. As a result, the focus of the scientific research concerning the antibacterial properties of the hop plant has centred around *Lb. brevis*, and from these studies[2, 25, 26] significant advancements have been made to further the understanding of the mode of antibacterial action of β-acids and α-acids.

In the case of the antibacterial activity of the *β*-acids and the *α*-acids, there are no reports that we are aware of showing activity against Gram-negative bacteria; the body of evidence suggests activity only against Gram-positive bacteria[27, 28], such as the *Lb* species responsible for much of the beer spoilage. The mode of action[2, 25, 26] of the hop acids has been generally considered to be due to an ionophoric / protonophoric effect, where the hop acid diffuses across the cell membrane to the intracellular space. Here, the pH is higher, causing the hop acid to dissociate, releasing protons (H^+) to the intracellular medium, lowering the intracellular pH. The resulting anionic hop-acid species associates with divalent cations (e.g. Mg^{2+}, Ca^{2+}) *via* chelation, and diffuses back across the cell membrane to the extracellular medium; there is no change in the overall electrical charge distribution (**Figure 10**).

Figure 10: *Illustration of a hop-sensitive cell*[2]*. The hop acid dissociates within the bacterial cell, decreasing intracellular pH; chelated metal ions are "smuggled" back out of the cell.*

The resulting decrease in intracellular pH, and therefore the decrease in the pH difference (ΔpH, the "transmembrane proton gradient") between the intra- and extra- cellular medium disrupts the proton motive force. Protons are not expelled from the intracellular space (in order to conserve the electrical charge) and this corrupts the production of adenosine triphosphate (ATP), a molecule intrinsically required for cellular function, and hence bacterial death soon follows.

Studies on the antibacterial properties of the hop acids have extended beyond investigations against *Lb* species. Battacharya et al[29] assessed the ability of iso-humulone and a mixture of β-acids to cause growth inhibition of *Streptococcus* (*Strep*) *mutans*, a species known to facilitate tooth decay through organic acid production on the tooth surface to which it is adhered. It was found that iso-humulone and the beta-acid mixture were capable of inhibiting growth of *Strep. mutans* at micromolar concentrations; additionally, it was shown that

the minimum inhibitory concentration (MIC) of the β-acid mixture was much lower (0.5 μM) than the much-studied iso-humulone **18** (2.0 μM) (**Figure 11**).

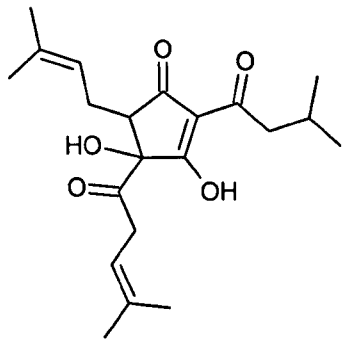

18

Figure 11

This is likely to be due to the greater lipophilicity of the beta-acid mixture over the iso-humulone facilitating an enhanced rate of passive transport across the lipophilic cell membrane to the intracellular space. The lipophilic properties of a given compound may be determined by a partition experiment between water and octanol (octanol being a reasonable approximation of the phospholipids that constitute the majority of cellular walls); the ratio of concentration of the compound of interest between the immiscible liquids allows a measurement of the compounds lipophilic or hydrophilic properties (i.e. a greater concentration of compound in the octanol layer relates to a more lipophilic compound, and vice-versa for a compound more soluble in water). The enhanced antibiotic activity of β-acids over both α-acids and iso-α-acids has also been documented by Yamaguchi *et al*[30], who showed that against five bacteria commonly implicated in the onset of the skin condition *Acne vulgaris* (*Proponobacterim acnes, Staphylococcus* (*Staph*) *epidermidis, Staph aureus, Staph pyogenes* and *Kocuria rhizophila*), the β-acid mixture used in their study was, in 4 out of 5 cases, the most potent; against *P. acnes* and *Staph. pyogenes* the MIC was

found to be 0.1 and 0.3 µg/ml respectively. The only other compound to exhibit similar or stronger activity was xanthohumol **19** (**Figure 12**), another compound isolated from *H.lupulus*.

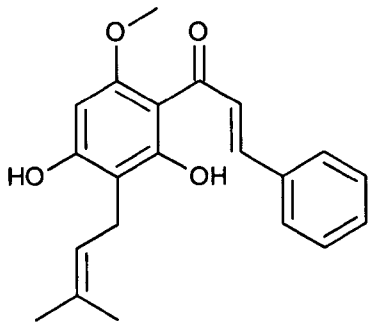

19

Figure 12

The general theory that β-acids have greater antibacterial strength in comparison to α-acids is further supported by Larson et al[31], who showed that the β-acids are strong growth inhibitors of *Listeria monocytogenes*, exhibiting activity at 0.3 µg/ml. Additionally, a mixture of β- and α-acids presented lower inhibition at this concentration; α-acids alone were not reported to have growth inhibitory properties at concentrations lower than 10 µg/ml.

1.2.4.2 Antibacterial Resistance and Methicillin-Resistant Staphylococcus aureus (MRSA)

Whilst the antibacterial / antimicrobial effects of hop acids are indeed promising and exciting, it has been observed that in the case of *Lactobacillus* species, there is a propensity to develop resistance to the antibacterial effects of hop acids[2]. This is generally considered to be caused by an increased ability to expel protons released from the invading hop-acid through upregulated ATPase (i.e. greater presence of ATPase, a membrane-bound protein able to expel protons to the extra-cellular medium), and there is evidence that another

membrane bound protein, HorA, can expel the hop acid before it has reached the intracellular area[32] (**Figure 13**).

Figure 13: *Illustration of a hop-resistant cell[2]. The hop acid can be caught by HorA in the cell membrane, and expelled. The proton pumps are upregulated, and ATP is replenished more efficiently, furthering the resistance to pH increase.*

To our knowledge, there are no reports of resistance accruement by other bacteria species to hop acids, since most reports focus on the initial antibacterial effects of these compounds and not their long-term efficacy. There is scope, then, to investigate the antibacterial effects against other bacteria species which are known to have acquired resistance to many examples of commercially available and clinically used antibiotics.

In recent years, there have been extensive reports of the increasing existence of methicillin- and multidrug-resistant *Staphylococcus aureus* (MRSA) bacteria. Methicillin **20a** belongs to the penicillin class of antibiotics **20**, which

have a core, 4-membered β-lactam cyclic structure fused to a 5-membered heterocycle common to all penicillin derivatives (**Figure 14**).

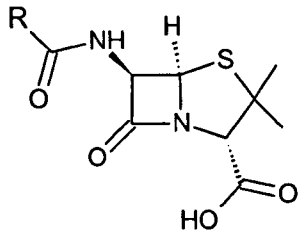

20

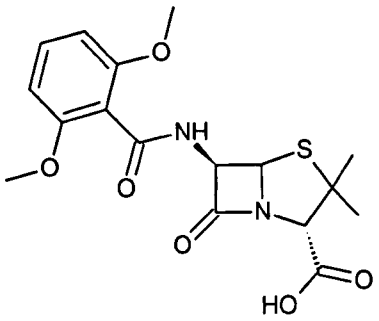

20a

Figure 14

The β-lactam core is also central to the mode of action of closely related cephalosporins **21**, for example cephamycin **21a**, the difference being the presence of a 6-membered heterocyclic ring fused with the β-lactam core functionality (**Figure 15**).

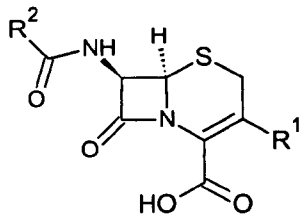

21

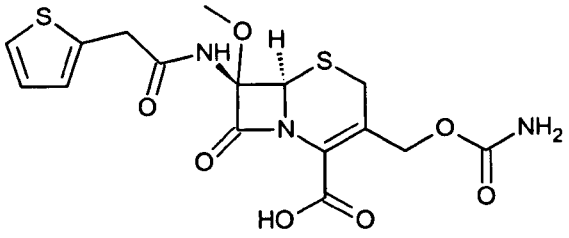

21a

Figure 15

Both the penicillins **20** and cephalosporins **21** class of β-lactam antibiotics target a transpeptidase enzyme, involved in the final stages of the biosynthesis of the peptidoglycan cell membrane layer, where the enzyme catalyses the cross-linking of peptides to create this outer-membrane wall. A serine residue in the enzyme active site binds to a C-terminal group of an amino acid residue *via* the

hydroxyl unit. This ester bond reacts further with an incoming amine from a lysine amino acid residue of the other peptide to form a cross-link between both peptide clusters[33, 34] (**Figure 16**); hydrolysis by water of the peptide-transpeptidase ester bond is very slow, preserving the desired peptide bond formation.

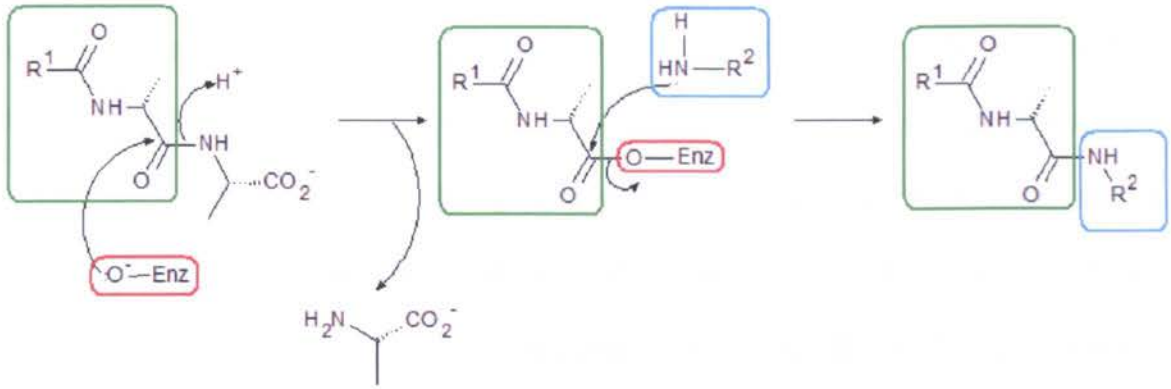

Figure 16: *The transpeptidase enzyme (red box) catalyses the cross-linking of peptides (green and blue boxes) to finalise the production of the bacterial cell wall.*

However, when a β-lactam antibiotic is introduced into the bacterium environment, it reacts readily with the serine residue at its hydroxyl group, forming a similar ester bond (**Figure 17**).

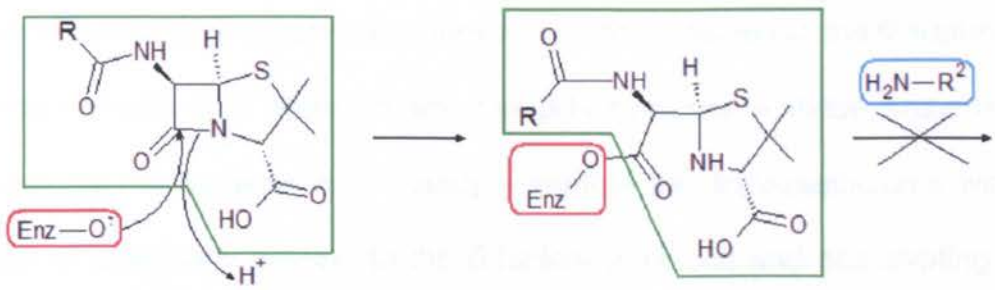

Figure 17: *The β-lactam antibiotic (green box) reacts at the transpeptidase enzyme (red box) to form a strong covalent bond, and due to the bulk of the heterocyclic ring the incoming peptide (blue box) cannot react further, thus cross-linking is prevented.*

The formation of this ester bond could be considered as energetically favourable with respect to the change in free energy of the system. The β-lactam ring is highly strained with respect to the bond angles, and is therefore in a high-energy state. The attack of the enzyme to form the resulting ester results in a relaxation of the previously strained bond angles; the formed ester is a more thermodynamically favourable system. Because of this, the reaction between the enzyme and the β-lactam antibiotics **20** and **21** is more favourable than with the natural substrate, where the change in free-energy of the system would not be so great since the natural substrate is already much more stable than the β-lactam antibiotics **20** and **21**. The continuing presence of the remaining heterocycle ring of the now bound antibiotic **20** or **21** induces steric hindrance; this prevents the lysine amino acid from getting close enough to cause hydrolysis of the ester[33, 35], hence a permanent covalent bond is formed. Since the transpeptidase enzyme can now no longer cross-link peptide clusters, the peptidoglycan membrane layer becomes weak, losing intracellular material. Furthermore, an increase in the intracellular pressure causes rupturing of the cell membrane; in effect, the cell "bursts"[34].

Resistance to β-lactam antibiotics is well-documented in the literature, and receiving considerable attention are the β-lactamases – these enzymes are produced by the bacteria and closely resemble the transpeptidases with the purpose of selectively binding to the β-lactam antibiotic and deactivating it. As with the transpeptidase enzyme, the lactamase will ring-open the β-lactam ring of the antibiotic *via* nucleophilic attack originating from a serine-bound hydroxyl unit[33, 34]. The enzymatic pocket, however, is of differing design; a nearby tyrosine unit is thought[33, 36] to allow proton transfer to occur, rendering efficient

and rapid hydrolysis of the serine-antibiotic ester by water possible. This releases an inactive derivative of the antibiotic, posing no threat to the transpeptidase enzymes which can continue their business of finalising the peptidoglycan membrane synthesis.

Another well-studied mechanism of resistance to β-lactam antibiotics concern slight, but significant changes in the structure and conformation of the binding site of the penicillin-binding proteins (PBPs)[37, 38]. Whilst these proteins are able to carry out their natural function related to the construction of the peptidoglycan layer, they undergo weaker binding with β-lactam antibiotics, hence the drug is not present long enough to exert its effect of inhibiting cell-wall synthesis.

Over the course of the development leading to alternative classes of compounds to combat MRSA infections, it has been found that *Staph aureus* can, and has, acquired resistance to many other commercially available, and clinically employed antibiotics[39]. Indeed, there is growing evidence for the emergence of vancomycin-resistant *Staphylococcus aureus* (VRSA)[40, 41], which is of concern since the high molecular weight glycopeptide antibiotic vancomycin is only recommended for use in cases of severe MRSA infection where other treatment options have failed[42]. The requirement for new classes of antibiotics to treat these multi-drug resistant "superbugs" is of growing importance; since *Staphylococcus* bacteria are Gram-positive, it would not be inconceivable that that hop acids should have an antibacterial effect against any *Staphylococcus* species, including drug-resistant strains of *Staphylococcus aureus*. We are unaware of any reports alluding to such activity, and have identified this as an area deserving of investigation in order to begin a new course of study into the further antibacterial effects of hop acids.

1.2.5 Cancer and Hop Acids

1.2.5.1 Prevalence of Cancer as a Disease

Cancer Research UK[43] states that, during the year 2009, 320,200 people in the UK alone were diagnosed with one of the 200+ cancers given a distinct classification. It is estimated[44] that 1 in 3 individuals will contract some form of cancer during their lifetime; since the 1970's, diagnoses of cancer diseases have risen. For those diagnoses made, over half fall into the categories of breast, lung, prostate and bowel cancers[44], with breast cancer being the most commonly encountered cancerous disease[45]; significant advances in medicine have lead to an increase in the number of people surviving beyond 5 years from initial diagnosis from approximately 50% in 1971-1975 to approximately 80% in 2005-2009[46]. Prostate cancer is estimated to be the most common cancer diagnosed in males – in 2009 alone, approximately 40,800 diagnoses were made[47]. The survival rate beyond 5 years from initial diagnosis is estimated to be approximately 80%, however beyond 10 years this falls to approximately 70%. Overall, survival rates have increased from approximately 65% in the period 1971-1975 to approximately 90% in the period 2004-2009[48].

Whilst awareness of cancer has increased in the general population, and both diagnosis and treatment methods are constantly improving with time, there is still scope for the introduction of new treatments including chemotherapeutic strategies. For a given cancer, there are often subtypes pertaining to the aggression of that cancer, for example those types which readily metastasise, which are themselves highly aggressive and for which the mortality rate is relatively high.

1.2.5.2 Anticancer Activity of Hop Acids

There is a small but compelling body of evidence in the literature pertaining to the ability of hop acids to inhibit the proliferation of cancerous cells. Tobe *et al*[49] demonstrated the antiproliferative effects of humulone **2** against HL-60 (leukemic) cells, with a reduction in cell population amounting to 2 orders of magnitude after 20 hours incubation with humulone **2** at 100 µg/ml. Further to this, humulone **2** inhibits proliferation of leukemic cell lines U937, K562, HEL and KU812, and may make for an effective therapy against leukaemia when combined with vitamin D[50] vitamin D is known to be cytotoxic towards leukemic cells, however the adverse side-effects regarding calcium (bone) resorption put a limit to its clinical application[51]. Humulone, by contrast, inhibits bone resorption[50], countering the effects of vitamin D and potentially providing a unique combination therapy for patients with leukemia. Lupulone **1** has been observed to have enhanced anticancer activity with respect to the α-acids (humulones); Stephan *et al*[52] observed colupulone **1a** to inhibit growth of leukemic CEM and vinblastine-resistant CEM-V cells (vinblastine is a potent anticancer compound) with IC_{50} values for each cell line being 4.25 µM and 6.41 µM respectively – this contrasts well with carboplatin and cisplatin (both routinely prescribed anticancer drugs), with respective IC_{50} values of 12.6 µM and 0.90 µM respectively against CEM cells[53]. This study also introduced a synthetic derivative of colupulone **1a**, hexahydrocolupulone **22** (**Figure 18**), prepared by hydrogenation of colupulone **1a**; it returned lower IC_{50} values against CEM and CEM-V cell lines (1.85 µM and 2.77 µM respectively) than colupulone **1a**. This initially suggests that higher lipophilicity enables greater anticancer action, but may also be a result of increased resistance to

metabolisation due to less degree of unsaturation, allowing it to remain in the cell for a longer period of time before destruction and/or expulsion.

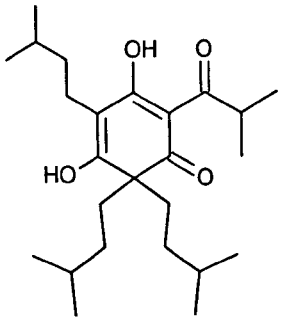

22

Figure 18

The literature is sparse when one seeks evidence directly comparing the anticancer activity of α-acids and β-acids, but a communication by Tyrrell *et al*[18] showed that against the SK-MES lung cancer cell line, humulone **2** and lupulone **1** had very similar antiproliferative properties. Furthermore, it was demonstrated that both hop acids had action against the MDA-MB-231 breast cancer cell lines - a result deserving of attention since this particular cell line is representative of an aggressive, hormone-independent breast cancer. For both cell lines, the data presented suggests that lupulone **1** is a more potent inhibitor of cancerous cell growth; IC_{50} values for SK-MES and MDA-MB-231 cell lines were 1.7 μmol / L and 4.0 μmol / L respectively; by comparison, humulone **2** had IC_{50} values of 2 μmol / L and 19 μmol / L respectively. In the case of the MDA-MB-231 cell line, this would indeed support a notion that greater lipophilicity results in enhanced anticancer effects. In the same publication, it was shown experimentally that when the caspase inhibitor V-ZAD was introduced along with the hop acids, cellular death did not occur. This suggests then that hop acids target caspase enzymes, triggering a cascade that results in apoptosis (programmed cellular death). However, this is only a very limited

amount of information, and does not reveal the intricacy of the activated mechanism by which apoptosis occurs. A detailed investigation by Chen and Lin[54] utilising the HL-60 cell line showed that in the presence of a mixture of hop acids, several cellular changes occur; the decrease in antiapoptotic protein Bcl-X_L (and also, but to a lesser extent, Bcl-2), and the increase in the proapoptotic protein Bax – the cell becomes activated towards apoptosis. It was also reported that the mitochondrial concentration of cytochrome c decreases with the subsequent increase in cytosolic cytochrome c, a known result of activated (oligomeric) Bax forming channels at the mitochondrial membrane, causing leakage of the internal components into the cystolic medium[55, 56]. Once cytochrome c is present, it can activate the protein Apaf1, readily receiving pro-caspase-9, cleaving aspartic acid residues to give the activated caspase 9 and forming an apoptosome, which cleaves the aspartic acid residues of pro-caspase-3 giving caspase-3. Caspase 3 will go on to cleave other cellular proteins – this is the intrinsic apoptotic caspase cascade (**Figure 19**)[55].

The evidence presented by Chen and Lin suggests that hop acids may activate both this intrinsic pathway and the alternative extrinsic pathway, activated externally by cytokine death ligands, such as FasL and tumor-necrosis factor alpha (TNF-α), that bind to membrane-bound death receptors. These acquire adaptor proteins, which in turn catalyse the formation of caspase-8 from procaspase-8. Caspase-8 will perform a similar task as caspase-9, facilitating the cleavage of procaspase-3 to generate caspase-3 (**Figure 20**).

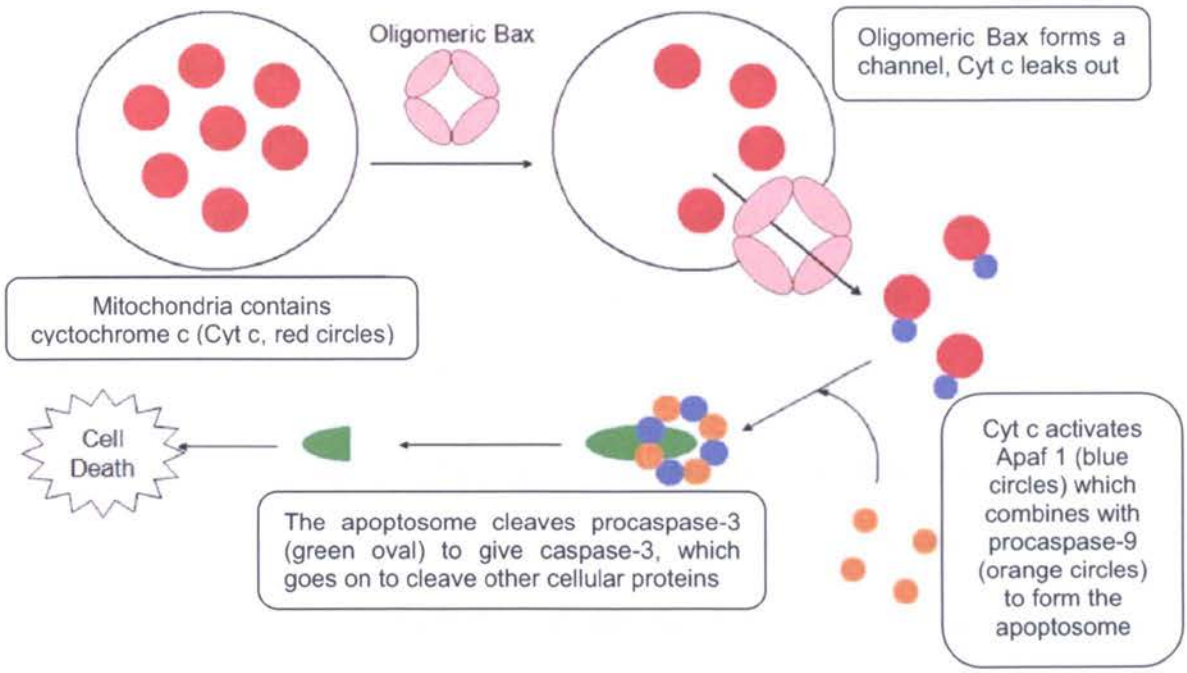

Figure 19: *The intrinsic apoptotic mechanism. Mitochondria contain cyctochrome c; upon induction of apoptosis, Bax proteins oligomerise to form channels that leak cytochrome c into the intracellular matrix. A caspase cascade with caspase-9 begins, causing destruction of other proteins.*

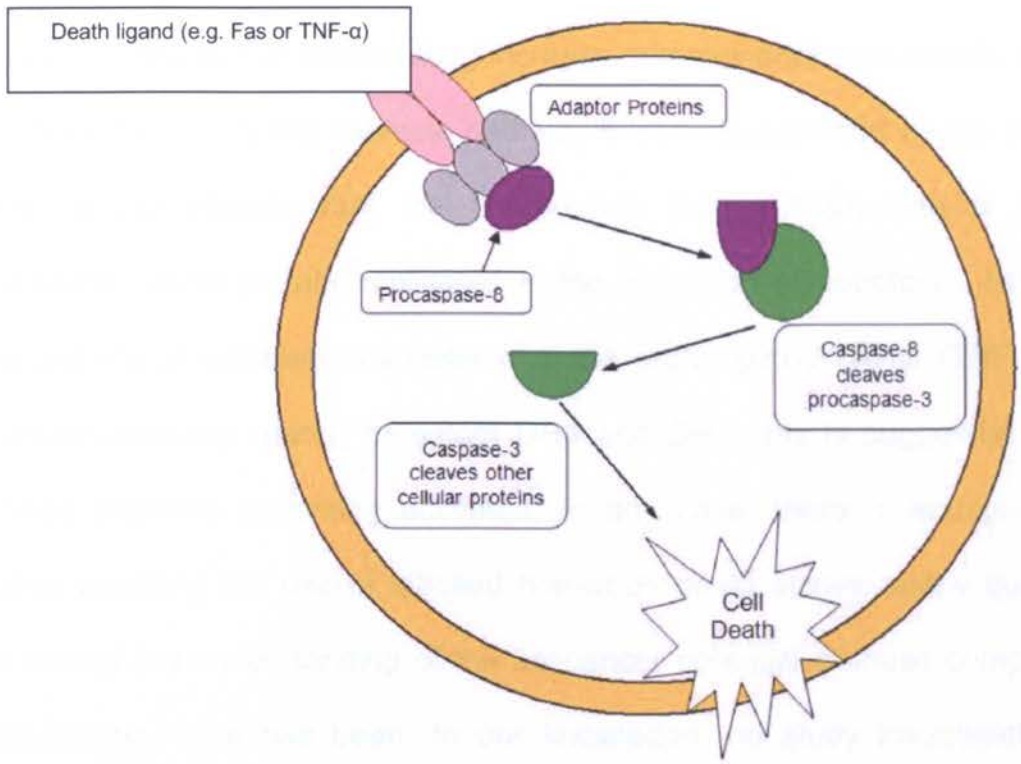

Figure 20: *The extrinsic apoptotic mechanism. Death ligands are received at the cell membrane by receptor ligands. Adaptor proteins then induce the caspase cascade starting with caspase-8.*

The activation of caspase-3 is an important point in the cascade, as amongst its many protein-cleaving abilities, it causes degradation of poly-(ADP-ribose)-polymerase (PARP), a molecule important for the repair of damaged DNA[57]. Chen and Lin showed the decreasing concentration of PARP, and the increase in a corresponding cleaved product, strongly suggesting the activation of the caspase-mediated apoptotic cell death pathway.

Whilst it is shown that hop acids provoke an apoptotic pathway to cell death, it is unclear how these compounds interact with cellular receptors to initialise the cascade, and which pathway (extrinsic or intrinsic) is triggered. Lamy *et al*[58] present some evidence demonstrating an increase in mitochondrial membrane permeability of SW620 (colon cancer) cells after 48 hours exposure to a mixture of β-acids. This would suggest an activation of the intrinsic pathway only, but the authors readily state they observed *both* pathways being activated, and also conclude that the resulting increase mitochondrial permeability may be a knock-on effect of the extrinsic pathway becoming activated by the β-acids. They do hypothesise that the compounds may interact with a surface membrane bound protein implicated in the activation of apoptosis, based on observations of increased expression of the proapoptotic TRAIL (TNF-related apoptosis-inducing ligand) receptors DR4 and DR5; this is suggestive of the extrinsic pathway becoming activated. In any case, there is ambiguity and studies involving the use of labelled hop-acids could answer many questions and further the understanding of the anticancer potential of these compounds. Furthermore, there has been, to our knowledge, no study investigating the anticancer potential of individual, naturally occurring hop acids and their comparison between each other; we aim to address this gap in the literature as

a major goal of this current research, with the addition of assessing the activity of non-natural derivatives.

1.2.6 Current Potential Uses and Applications of Hop Acids

The patent literature is home to many sources for the application of hop acids, the majority of which find use as antimicrobial agents. In the food industry, the use of a mixture of α-acids and β-acids to control bacterial growth in sugar production is reported[59], and the use of a mixture of β-acids has also been reported for the inhibition of bacterial growth on the surfaces of solid foodstuffs[60, 61]. Ethanol production for use in vehicle fuel can be complicated by the growth of ethanol-resistant bacteria, which has been controlled[62] by the introduction of α-acids, β-acids and their respective isomers generated through exposure to heat and other processes encountered during the traditional brewing process.

1.2.7 Chemical Synthesis of the Beta-Acids

The synthesis of lupulone **1** and its related congeners has undergone a great deal of investigation, most of which occurred between 1950 and 1980. Early work was conducted by Reidl[63] involving the reaction of acylphloroglucinols **3** with sodium ethoxide and 3,3-dimethylallyl bromide (prenyl bromide, **23**). This, however, gave rise to many products, ranging from mono-prenylated compounds to tetra-prenylated compounds **10**, **11**, **24** in addition to lupulone **1** and congeners **1a-d** (**Scheme 2**). Yields of lupulone **1** and the related triprenylated congeners were 5 – 30%[64] after chromatographic separation was used to isolate the components of the crude reaction product. The use of sodium ethoxide as the base is considered to be the problem in this reaction,

since the pK_a is too high leading to more proton extractions than is desired. This causes an over-consumption of prenyl bromide resulting in the wide dispersion of prenylated compounds.

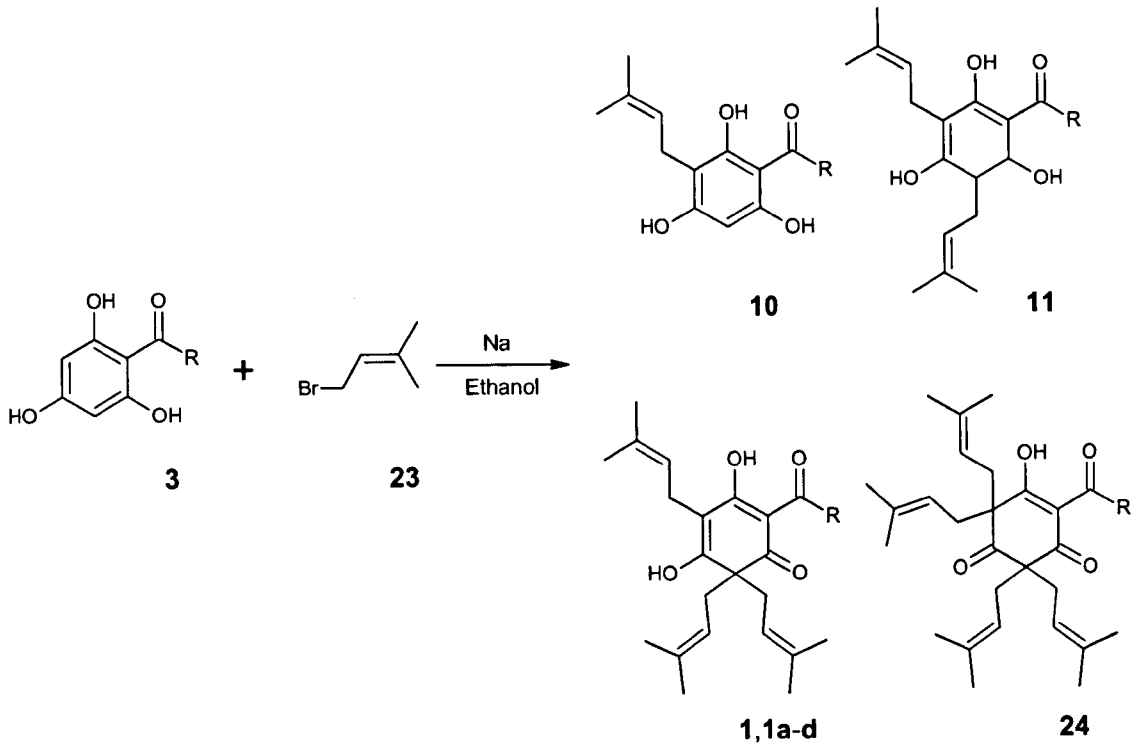

Scheme 2

Clearly, the requirement for a more controlled and efficient synthesis of the *beta*-acids was required and this was demonstrated by Drewett and Laws[65]. They observed that performing the reaction in liquid ammonia, the triprenylated compounds **1** and **1a-d** could be selectively generated, and purification was achieved by a simple recrystallisation. Yields of the purified ammonia-solvated reaction product were significantly improved to 60 – 70%, *via* a reliable and repeatable methodology. The pK_A of ammonia (~ 35-36) must therefore be favourable for the trialkenylation in allowing β-acids to occur, but further alkenylation to give **24** would require a more basic environment, such as that encountered where sodium ethanoate was employed.

Considering the reaction mechanism, it is envisaged that it would likely proceed *via* a route not dissimilar to the biosynthetic pathway previously discussed (**Figure 2** and **Figure 3**); this would involve a stepwise addition of prenyl groups *via* a deoxyhumulone derivative **11** (**Figure 21**).

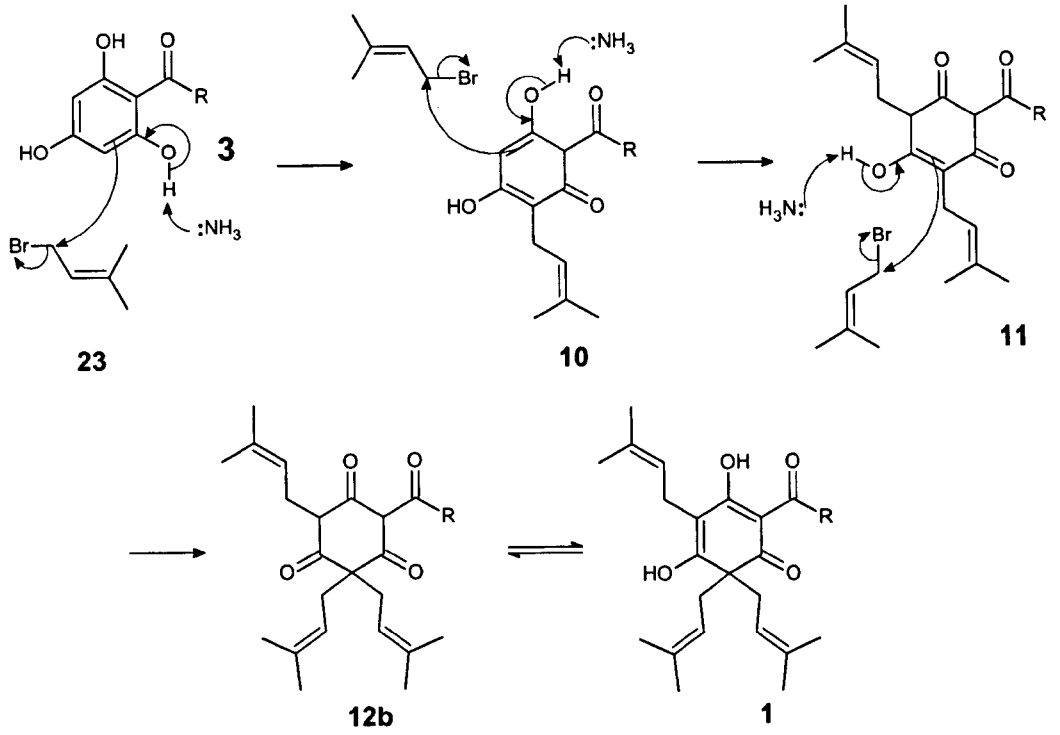

Figure 21

The initial acylphloroglucinol can be prepared simply and readily *via* a Friedel-Crafts acylation[66, 67], or the Hoesch reaction[68, 69]. The Friedel-Crafts reaction to form **27** (**Scheme 3**) is typified by the reaction of an aromatic compound **25** with an acyl chloride **26** in the presence of a Lewis acid, usually aluminium chloride.

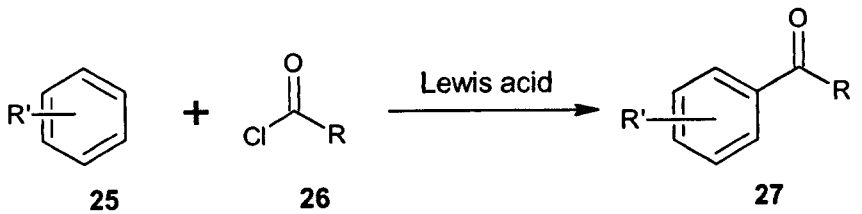

Scheme 3

Mechanistically, the acyl chloride **26** will coordinate to aluminium chloride through donation of a lone pair of electrons on the oxygen to the vacant d-orbital of the aluminium, forming an acylium ion **28**. Subsequent addition to the electron-rich aromatic substrate **25** forms intermediate **29**, where addition of water hydrolyses aluminium chloride to release the acylated product **27** (**Figure 22**).

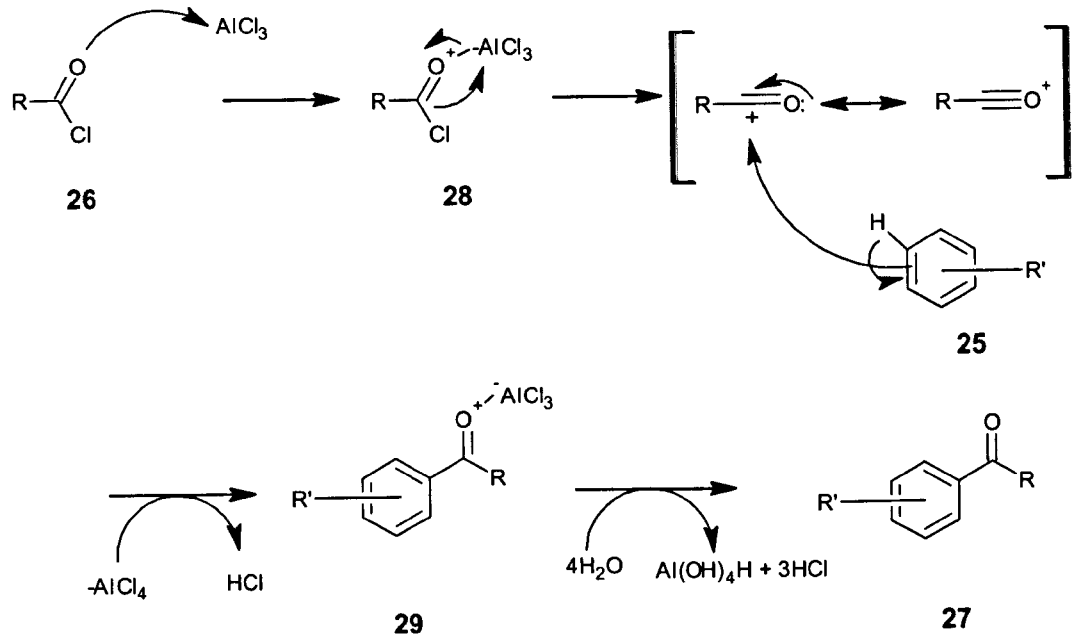

Figure 22

The limitations of this method lay with the Lewis acid; it is a common practice to have an excess of the Lewis acid (usually 1.5 – 2 mol eq) since it can remain coordinated to the oxygen atom of the acyl group, rendering it unavailable for further inclusion in the reaction. Furthermore, one has to be careful to control the addition of the acyl chloride with activated aromatics (for example, those with hydroxyl groups), since multiple substitutions may form. If one considers the resonance structures of phenol **30**, it is clearer to see how the electron density increases on the ring through a positive mesomeric effect – the

electrons of the phenolic oxygen can be delocalised into the aromatic ring, increasing the ring electron density (**Figure 23**).

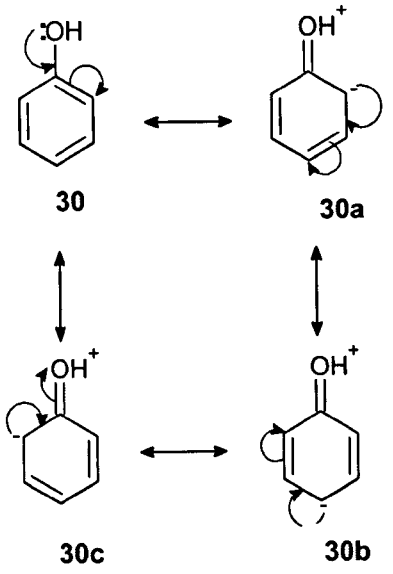

Figure 23

Extended substitution can be avoided by slow dropwise addition of the acyl chloride, and through using only the required molar equivalents, avoiding an excess. In practice, monosubstitution by acyl chloride **26** can deactivate the aromatic ring sufficiently to lower the chance of further substitutions occurring; if one considers the resonance structures of 1-phenylethanone **31**, it is clearer to see why the ring becomes deactivated, since electron density is drawn away from the ring and onto the acyl oxygen (**Figure 24**).

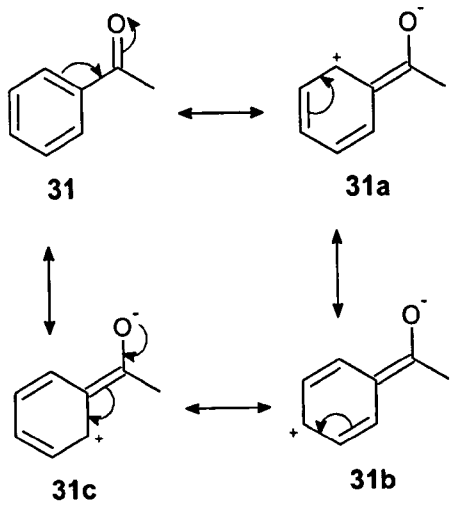

Figure 24

An alternative method to achieve acylated aromatic compounds is the Hoesch reaction. This is mediated by zinc chloride, and allows the coupling of a cyanoalkyl compound to the desired aromatic species. A representative procedure[70] involving phloroglucinol **32** involves the initial generation of a ketimine intermediate **33**, followed by hydrolysis with water to generate the desired acylphloroglucinol **3** (**Figure 25**).

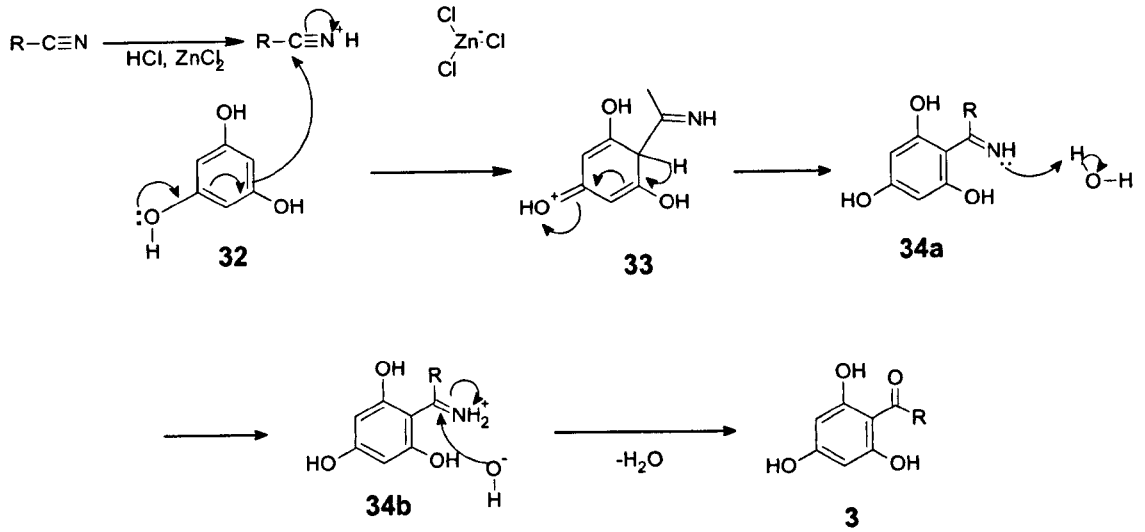

Figure 25

Protonation was historically[70] performed by passing hydrogen chloride gas through the reaction mixture, but more recent published procedures report the use of trifluoromethanesulphonic acid (triflic acid)[71, 72]; practically this may be both easier and safer since triflic acid is a liquid at room temperature.

Preparations of acylphloroglucinols **3** have been reported using both methods, but the majority of these compounds are prepared *via* the Friedel-Crafts acylation in the presence of aluminium chloride as the Lewis acid catalyst. The organic acids are widely available, and can be readily converted to the corresponding acyl chloride through reaction with oxalyl chloride[73] or thionyl chloride[74]. An efficient synthesis of acylphloroglucinols was included in the patent literature by Reininger and Hartl[75], with yields reported between 80 and 85 % using aluminium chloride and nitromethane in dichloromethane. The inclusion of nitromethane in the reaction serves to activate aluminium chloride and to facilitate the formation of a homogenous reaction mixture (i.e. a solution rather than a suspension); other procedures have employed nitrobenzene[76-79], however the boiling point of this alternative solvent is much higher than that of nitromethane, which prolongs the solvent-removal stage of a synthesis and can interfere with product purity due to residual nitrobenzene. Further to this, only one molar equivalent of nitromethane (with respect to aluminium chloride) is required. This further facilitates efficient isolation of the reaction product and may enable purer compound to be isolated due to the more complete removal of residual solvent. In contrast, nitrobenzene is often employed as the sole reaction solvent, or present in large excess as a co-solvent.

Chapter Two:

Chemical Syntheses

Results and Discussion

2.1 Friedel-Crafts Acylations

2.1.1 Initial Investigations with Aliphatic Acyl Chlorides

Our initial task was to investigate the conditions of the Friedel-Crafts acylation of phloroglucinol **32** (**Scheme 4**), adopting the synthetic method described by Reininger and Hartl[75].

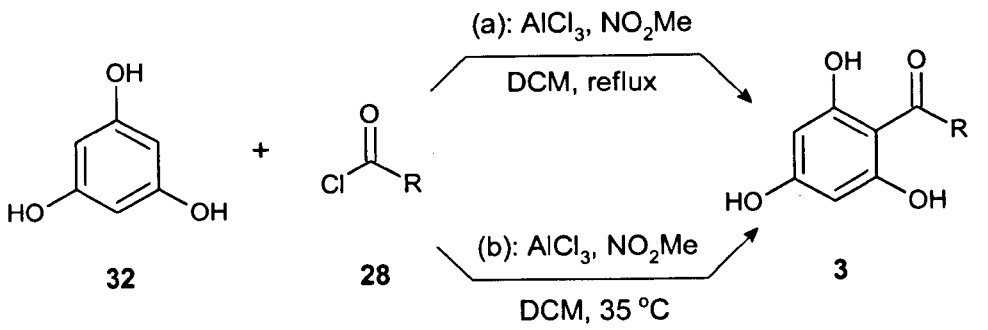

Scheme 4

According to the literature, the nitromethane served two purposes; firstly, it allowed the formation of a homogenous solution of phloroglucinol **32** and aluminium chloride, which are otherwise insoluble in dichloromethane. Secondly, nitromethane served to activate aluminium chloride through coordination[76]; dropwise addition of nitromethane to the stirred suspension of phloroglucinol **32** and aluminium chloride caused an exothermic reaction to ensue and the generation of acidic vapour was detected by placing a strip of pH indicator paper in the stream of the exhausting vapour. The following addition of the acyl chloride **28** gave rise to another exothermic reaction; a control experiment where nitromethane was omitted did not exhibit this characteristic, suggesting the inclusion of nitromethane allows an increase in the reactivity of the catalysing Lewis acid.

It was soon discovered that during conditions of reflux (route (a), **Scheme 4**), a resinous material was formed which could not be efficiently stirred in the reaction vessel; this lead to an inefficient and long work-up procedure in which the resin was broken down by stirring in 10% hydrochloric acid solution. Yields of the product were much lower than reported[75]. A lower reaction temperature of 35°C was attempted (route (b), **Scheme 4**), which prevented the formation of the resinous material and allowed for a more efficient work-up process. Yields were improved and a library of acylphloroglucinols **3a-f** with aliphatic side chains was soon compiled (**Table 2**).

Compound Number	R=	%Yield
3a	CH_3	53
3b	CH_2CH_3	51
3c	$CH_2CH_2CH_3$	74
3d	$CH(CH_3)_2$	46
3e	$CH_2CH(CH_3)_2$	74
3f	$CH_2CH_2CH(CH_3)_2$	56

Table 2

2.1.2 The Use of Cyclic Aliphatic Acyl Chlorides

Since we planned to study the structure-activity relationship (SAR) during our antibacterial and anticancer screening, we introduced aliphatic cyclic moieties onto the phloroglucinol ring to give acylphloroglucinols **3g-j** (**Table 3**); We were pleased to find the rings to be as stable toward the acylation reaction as those acyl chlorides used in producing **3a-e**, with a corresponding observation in yields which were consistent with that of **3a-e**.

Compound Number	R=	%Yield
3g	cyclopropyl	66
3h	cyclobutyl	46
3i	cyclopentyl	61
3j	cyclohexyl	55

Table 3

For the compounds **3i** and **3j**, the stability towards the reaction conditions was not surprising as the sp^3 carbon atom bond angle strain in cyclopentane and cyclohexane is not high rendering the ring relatively inert; our suprise came from observing that compounds **3g** and **3h** were also stable to the reaction conditions, and furthermore no degradation of the reaction product was observed. The cyclopropane and cyclobutane ring systems have highly-strained sp^3 carbon atom bond angles of 60^{O} and 90^{O} respectively, rendering them highly predisposed to ring-opening.

A common and recurring problem encountered during the work-up of the crude acylation products involved the efficient removal of the resulting aluminium compounds; these would sometimes precipitate out. Filtration proved to be a long process since the high density of the precipitate prevented a quick flow of liquid though the solid. It was found that incorporating washings of a 5% w/v solution of sodium potassium tartrate would allow the salts to be dissolved into the aqueous phase, but only after washing with water to remove the majority of the acid present.

2.1.3 The Use of Aromatic Acyl Chlorides

Our first major synthetic hurdle arose when attempting the acylation reaction with the aromatic acyl chloride benzoyl chloride **35** (**Scheme 5**), to generate **3k**.

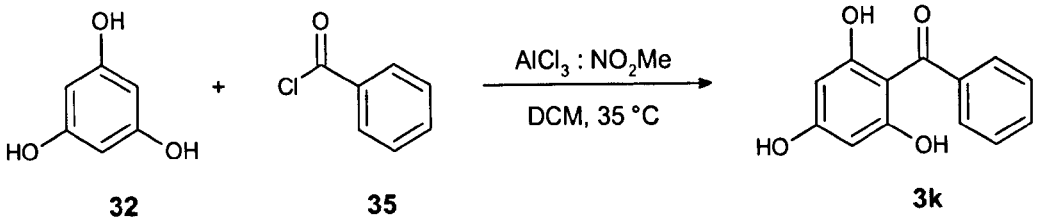

32 **35** **3k**

Scheme 5

The literature method[75] reports using the same conditions employed for the generation of aliphatic acylphloroglucinols **3a-j** and achieving similar yields, but when we attempted the reaction with our modified conditions, the isolated yield of **3k** was significantly reduced. Extended reaction times from 10 minutes to 30 minutes, then 1 hour, enabled improved yields, but we could never match that reported in the literature method. It was additionally found that purification was not efficient using the reported method of recrystallisation of the crude from water. Thin-layer chromatography (TLC) of the crude mixture obtained from the reaction revealed the presence of an intractable impurity that remained despite repeated recrystallisation steps. With this knowledge, purification was carried out by flash column chromatography[80] on silica gel, followed by recrystallisation from water. The isolated yield from this modified procedure was still substantially lower than that reported at 10% but the product obtained was of higher purity than before the introduction of chromatographic purification.

Our attempts to boost the yield involved:

- Pre-drying the phloroglucinol overnight at 100 ^{0}C under vacuum;

- Purification of aluminium chloride through vacuum sublimation onto a cold-finger;
- The generation of benzoyl chloride **35** from benzoic acid **36** as required, using oxalyl chloride **37**.

The conversion of benzoic acid to benzoyl chloride (**Scheme 5**) is catalysed by dimethylformamide (DMF), and it is entropically favoured due to the generation of carbon monoxide and carbon dioxide. No significant improvements in either the reduction of impurities or increase in yield was observed.

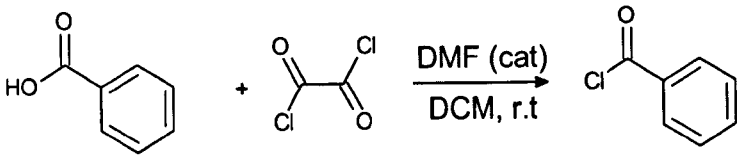

36 **37** **35**

Scheme 5

The reaction mechanism was again considered; the important step in the reaction is the formation of the acylium electrophile, so we changed the reaction procedure to form this species first by adding benzoyl chloride to a stirred solution of aluminium chloride and nitromethane in dichloromethane. Compared with a control experiment involving propionyl chloride, the addition of benzoyl chloride **35** gave rise to a gentle reaction where propionyl chloride addition was relatively violent, and required much more control. This highlights the reduced reactivity and enhanced stability of benzoyl chloride **35**. Stirring of the reaction mixture was continued for 2 hours to ensure conversion to the desired electrophilic intermediate, which was then transferred *via* syringe to a stirred suspension of phloroglucinol **32** and the reaction monitored by TLC analysis. After 2 hours, no more phloroglucinol appeared to be present. The work-up

procedure was followed by column chromatography and recrystallisation from water; the isolated yield had now improved to a more respectable 50%. We further investigated the scope of our optimised the Friedel-Crafts acylation involving aromatic acyl chlorides by using an activated compound, 4-methoxybenzoyl chloride **35a**, and a deactivated compound, 4-nitrobenzoyl chloride **35b**, giving **3l** and **3m** respectively (**Table 4**).

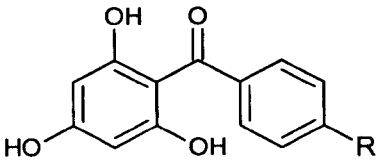

3k-l

Compound Number	R=	%Yield
3k	H	50
3l	OMe	50
3m	NO_2	30

Table 4

It was observed that the use of an activated benzoyl chloride derivative such as **35a** gave isolated yields of the product comparable with **3k**, while the use a deactivated benzoyl chloride derivative such as **35b** returned much reduced yields of **3m**. Indeed, in practice the addition of **35b** to the aluminium chloride-nitromethane solution gave rise to an unusually dark reaction mixture; this may be indicative of alternative and unwanted side-reactions occurring. This necessitated the use of flash column chromatography to isolate sufficiently pure samples of **3l** and **3m**.

2.1.4 Investigating the use of a Phloroglucinol Derivative

Whilst phloroglucinol **32** proved to be an excellent nucleophile with aliphatic acyl chlorides in our Friedel-Crafts reaction, it may be that where the relatively less reactive aromatic acyl chlorides were used, the ability of the hydroxyl groups to bind to aluminium chloride may have reduced and hence prevented product formation. To give aromatic acyl chlorides **35** and **35a-b** the best chance of reacting, the use of 1,3,5-trimethoxybenzene (1,3,5-TMB) **38** as the nucleophile was investigated. Upon isolation of the proposed intermediate product **39**, removal of the methyl groups using boron tribromide would then afford the desired compounds **3k-m** (**Scheme 6**).

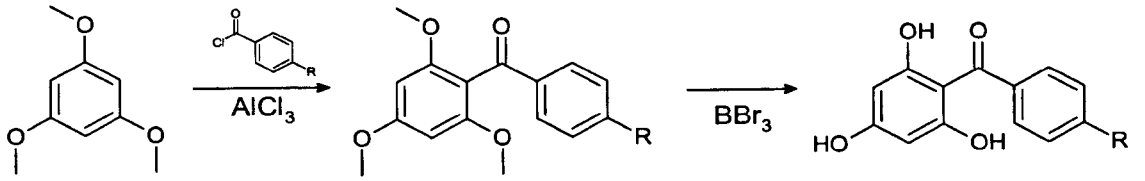

38 **39** **3k-m**

Scheme 6

A suitable procedure for both steps was discovered in the literature[81], with the notable observation that the authors allowed their reaction to proceed for 12 hours – much longer than reported by Reininger and Hartl[75] for their acylation of phloroglucinol **32** involving benzoyl chloride **35**. Benzoyl chloride **35** was stirred with $AlCl_3$ at $0^{\circ}C$, generating the reactive acylium ion complexed with the aluminium chloride. These highly reactive species are easily destroyed by water, so strict anhydrous conditions were employed. Dropwise transfer of the complex formed between **35** and $AlCl_3$ was added to a stirred and cooled solution of **38** was achieved by use of a dried syringe with a long needle; use of

a cannula needle was attempted, but the rate of transfer could not be controlled. The reaction was monitored by TLC analysis, and upon reaction completion purification by flash column chromatography was achieved to isolate **39**, with no need for further purification by recrystallisation. Demethylation was performed by the rapid addition of boron tribromide in one portion to a stirred and cooled suspension of **39**; we found it necessary to use 5 equivalents of BBr_3 to achieve full demethylation with an isolated yield of **3k** of 82%. Overall, we found no significant improvement in the yield of **3k** from the starting material **37**, compared to the route starting from phloroglucinol **32**. The Friedel-Crafts reaction involving **38** was repeated with 4-methoxybenzoyl chloride **35a,** 4-nitrobenzoyl chloride **35b** and 4-methylbenzoyl chloride **35c**, giving compounds **39a-c** (**Table 6**). We observed no significant improvment in the yield of the product where activated benzoyl chlorides **35a** and **35c** were used, but no reaction was observed where **35b** was used, hinting at a much-reduced level of activity of deactivated aromatic acyl chlorides (**Table 5**).

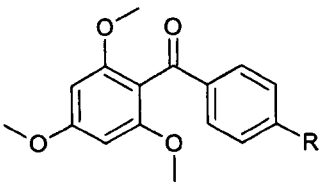

38 and **38a-c**

Compound Number	R=	%Yield
39	H	54
39a	OMe	54
39b	NO_2	No reaction
39c	Me	56

Table 5

2.2 C-Alkylation of Acylphloroglucinols

Upon the successful generation of acylphloroglucinols **3a–m**, we began our investigation into the C-alkenylation reaction. Although it was known to us that the desired tri-alkenylation product **1** could be produced in liquid ammonia[64, 65], there was scope to investigate the use of alkylamines (**Scheme 7**).

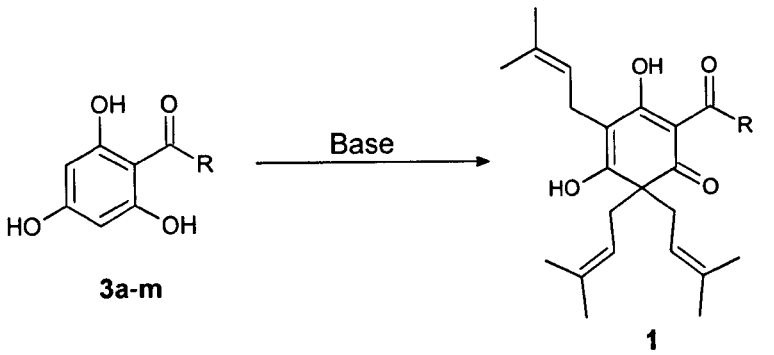

3a-m **1**

Scheme 7

This action could prove beneficial since the use of condensed liquid ammonia introduces some practical hurdles when considering the experimental set-up. One must consider how to safely condense the ammonia from a pressurized cylinder, how to sufficiently dry it over sodium and the transfer of this dried ammonia into a reaction vessel. The subsequent removal of ammonia upon completion of the reaction requires consideration as well. The proposed use of the alkylamines has advantages since they are liquid at room temperature, therefore they may be purified relatively easily and their removal involves a relatively trivial liquid-liquid extraction, employing dilute acid to draw the amine into the aqueous phase.

Initial investigations focussed upon the use of diethylamine (DEA) as the major reaction solvent, since a secondary amine was considered to be a strong enough base to promote tri-alkenylation without causing undesired tetra-

alkenylation as reported to occur with metal hydroxides[63]. The reaction procedure comprised of acylphloroglucinol **3b**, stirred in at room temperature, followed by the dropwise addition of prenyl bromide **23** with the aim of producing postlupulone **1b** (**Scheme 8**).

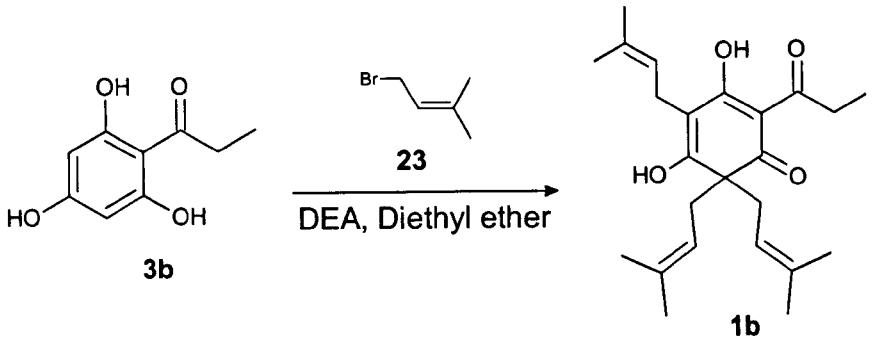

Scheme 8

It was immediately apparent that the desired product was not formed as the introduction of prenyl bromide **23** to the reaction caused an almost instant generation of a precipitate. A control reaction under the same conditions, excluding **3b** produced the same result. GC-MS analysis of the precipitate revealed it to be compound **40**, formed between DEA and **23** (**Scheme 9**).

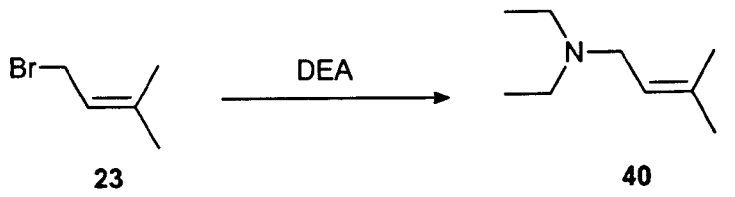

Scheme 9

Cooling the reaction to -78 °C did not lead to a desirable product forming, and so an alternative alkylamine base was sought in the form of isopropylamine (IPA). This has a lower pK_a than DEA, indicating a less basic character which was predicted to promote the formation of the desired product; again, room temperature studies lead to a product from a reaction between the base and **23**.

We opted this time to be more gradual in cooling the reaction, and a temperature of -42 °C produced the first positive observation *via* TLC analysis that the desired product was being formed. Isolation of this product, however, was proving problematic due to the presence of an unknown side-product; whilst the TLC allowed observation that the product was being produced, it provided no indication as to the relative abundance, hence it was concluded that **1b** was not being synthesised in great amounts, leading to degradation on the (acidic) column and thus averting isolation. Further reduction of the reaction temperature to -78 °C did not increase the formation of the product in appreciable amounts to aid easy isolation – column chromatography was proving a futile method to isolating the β-acids.

After extensive exploration of the possible C-alkenylation reaction using simple *N*-alkylated bases, we focused upon the use of ammonia. It is possible to obtain ammonia as part of an anhydrous methanolic solution, and so an experiment was prepared (alongside a control experiment using isopropylamine) to evaluate this as a viable procedure for the generation of **1e** (**Scheme 10**).

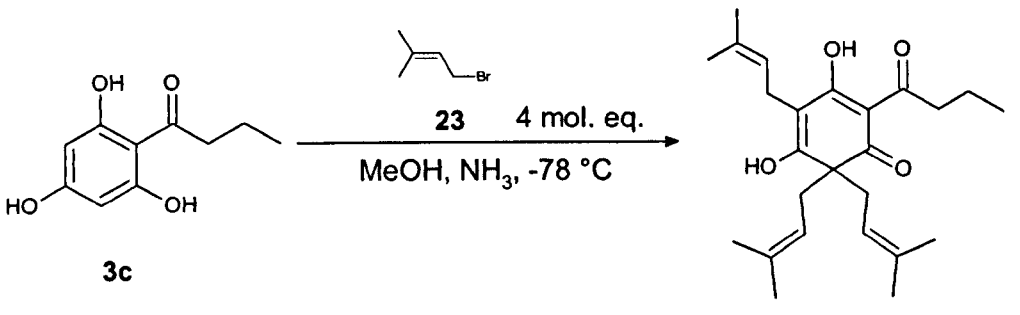

Scheme 10

The reaction was monitored by TLC analysis, using an authentic sample of lupulone **1** as a standard. It was observed that the formation of a potential

desired product occurred more rapidly in methanolic ammonia than previously observed when IPA was used. Workup of the reaction yielded a crude oil which was successfully recrystallised from hexane to give a pure sample of **1e**, albeit in low yield (9 %); this result was pleasing and validated the efforts made thus far into the synthesis of β-acids **1**. Repetition of the procedure however did not lead to an increase in yield beyond 11% - at this stage, an experiment involving the use of neat ammonia as the reaction was designed (**Figure 25**) and the practical challenges of such a procedure were undertaken.

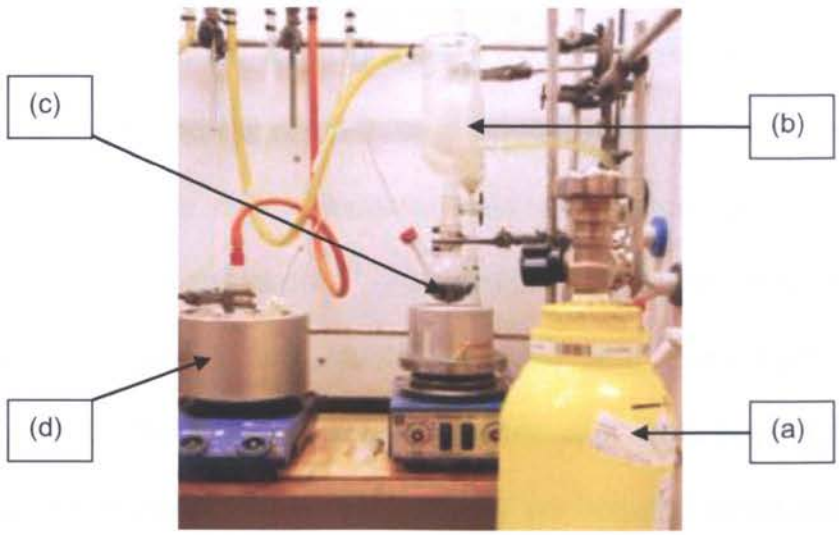

Figure 25: (a) *Ammonia cylinder.* (b) *Condensing tower.* (c) *Sodium-dried liquid ammonia.* (d) *Reaction vessel.*

The ammonia cylinder (a) was connected to a condensing tower, where a combination of dry ice and acetone in the cold finger (b) was used to condense the ammonia gas into a round-bottomed flask (RBF) also immersed in a dry ice / acetone bath. Upon sufficient condensation of ammonia into the RBF, sodium metal was added to the stirred ammonia to remove any water present; dryness is confirmed by a permanent deep-blue colour (c). The dried ammonia is transferred *via* cannula needle to the reaction vessel (d). This allows any

remaining lumps of sodium to be left behind, and the introduction of the reagents was then completed.

Removal of liquid ammonia (upon completion of the reaction) was a simple affair. A gas bubbler containing silicone oil was fitted, and the reaction mixture allowed to warm overnight to room temperature. The ammonia gas could evaporate gently without bumping and exit the reaction vessel, aided by a positive pressure of nitrogen gas. This preserved the reaction mixture, which could then be worked up. Acidification was required although this risked degradation of the product, working quickly avoided prolonged exposure of the desired compound and significant by-product formation was avoided. We initially found that the crude material was a viscous oil in keeping with previously reported observations[65]. The crude product was recrystallised first from hexane to give a fine crystalline solid and then from acetonitrile. Recrystallisation of the crude directly from acetonitrile was not initially possible, presumably due to residual substrate **23**. As we became more experienced in the procedure, we found that we could obtain post-work-up crude material as solids, which could then be readily recrystallised from acetonitrile without the need for the initial hexane step; this reduced the exposure of the products to heat and served to improve isolated yields.

Our initial concerns of using neat ammonia were soon found to be unwarranted, as the experimental procedure discussed was found to be efficient at producing high yields of lupulone **1** and its derivatives. The original papers[64, 65] describing the use of liquid ammonia in the production of β-acids recommended the use of approximately 200 ml ammonia per 1 g of acyl phloroglucinol; our optimised procedure subsequently used in this research

involved the use of only 50 ml ammonia per 1 g of acylphloroglucinol. Furthermore, the tolerance of the reaction towards non-anhydrous conditions was evaluated. Bench-grade, non-anhydrous diethyl ether was used, and the ammonia was not subjected to drying over sodium – no significant detriment to the overall yield of product was found. Whilst strict anhydrous conditions are not required, there must be some care taken to prevent too much water becoming included in the reaction. It is understood that acylphloroglucinols **3a–m** retain 1 mole-equivalent of water of crystallisation, and so thorough drying was necessitated using a drying pistol and a high vacuum. Using undried acylphloroglucinols resulted in reduced yields by 10-15%. With the conditions optimised, a small library of naturally occurring (**1**, **1a-f**) and synthetic (**1g-m**) β-acids were compiled (**Table 6**), which we termed the 1st generation β-acids.

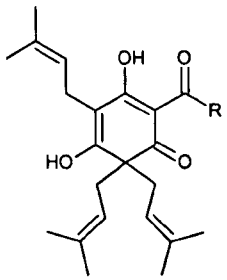

1, 1a-m

Compound Number	R=	%Yield	Compound Number	R=	%Yield
1	$CH_2CH(CH_3)_2$	53	**1h**	cyclobutyl	28
1a	$CH(CH_3)_2$	47	**1i**	cyclopentyl	26
1b	CH_2CH_3	63	**1j**	cyclohexyl	55
1c	$CH_2CH_2CH(CH_3)_2$	55	**1k**	phenyl	35
1e	$CH_2CH_2CH_3$	68	**1l**	*p*-methoxyphenyl	64
1f	CH_3	39	**1m**	*p*-nitrophenyl	25
1g	cyclopropyl	43			

Table 6

In some cases, the synthesis of a compound was only attempted once (for example, compounds **1f** and **1h**), owing to non-optimised yields. The aromatic derivatives **1k** and **1m** were observed to degrade quicker than other compounds – presumably the increased electron density resulted in compounds more prone to intramolecular reactions a well as oxidation during the work-up phase; yields could not be increased further.

2.2.1 NMR Studies of 1st Generation β-acid derivatives

NMR studies allowed us to positively confirm the formation of lupulone **1** and β-acid derivatives **1a-m**. It was observed that the resonances of the protons situated on the main body of the compound (i.e. the structure depicted in **1**) did not alter significantly between derivatives; the full ^{1}H-NMR of compound **1f** is illustrated (**Figure 26**).

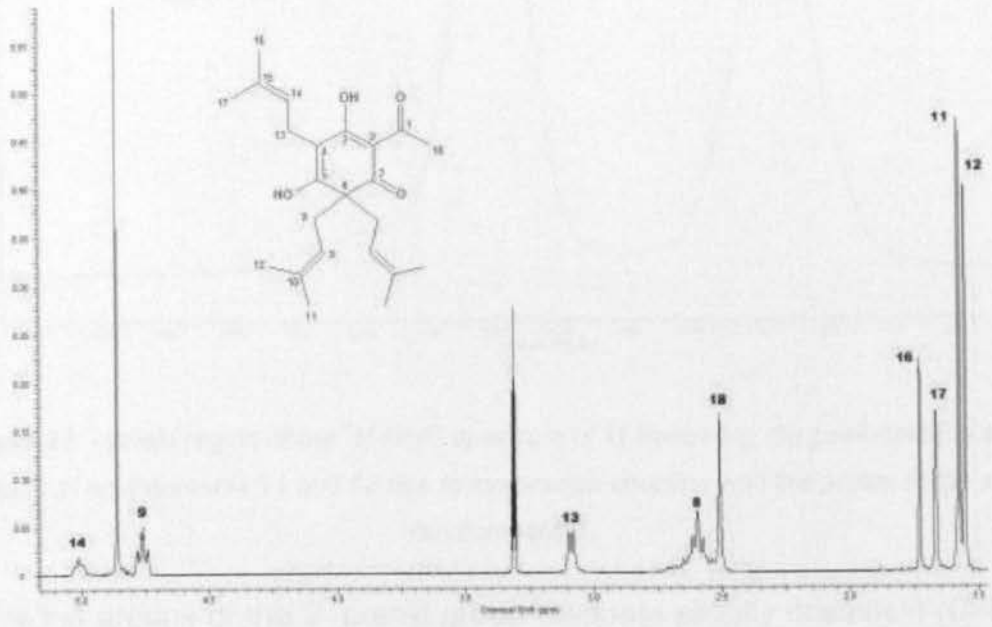

Figure 26: *^{1}H-NMR spectrum of* **1f** *(R = CH_3) illustrating a typical β-acid proton NMR spectrum*

The upfield region of the ^{1}H-NMR spectrum features the resonances attributed to the methyl groups of the geminal prenyl units (environments C-11 and C-12,

Figure 26). On some spectra, we could identify these as doublets with a coupling constant J = 1 (+/- 0.1) Hz, indicating the asymmetry of the dimethylallyl units. The coupling constant data facilitated the full assignment of the spectra. The long-range couplings (i.e. coupling through four bonds) for the methyl group *cis* to the allylic C-H proton, had a coupling constant of approximately 0.8 Hz for the methyl derivative **1f**. For the methyl group in the *trans* position to the allyl C-H proton, the coupling constant was slightly larger at 0.9 Hz (**Figure 27**).

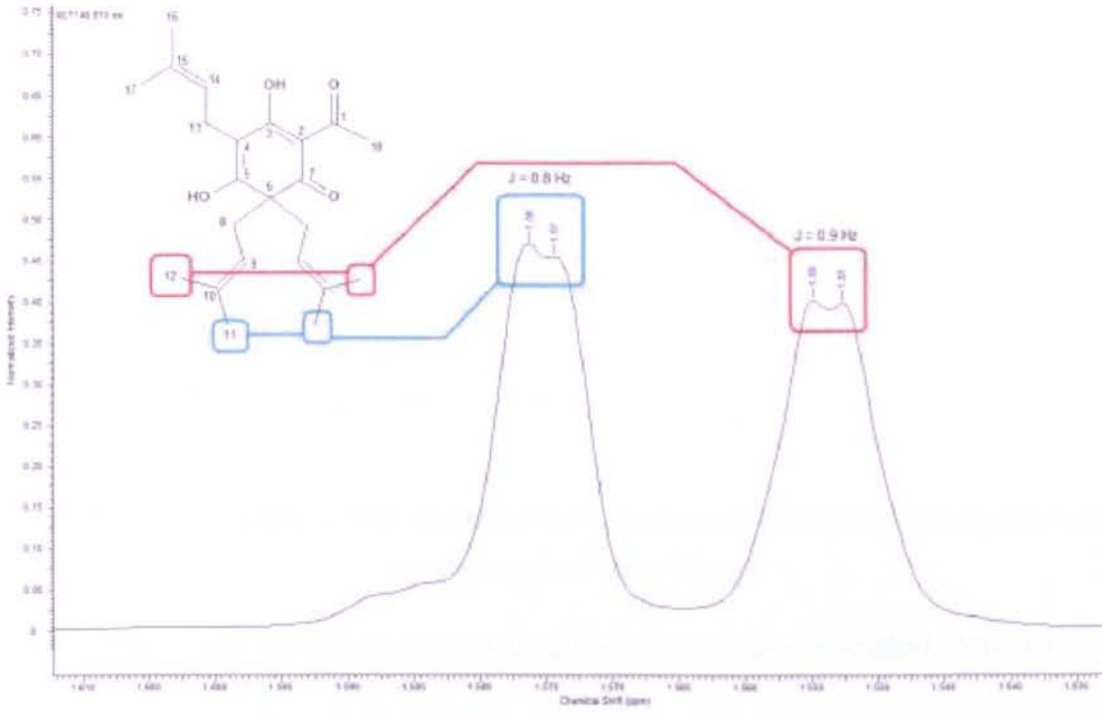

Figure 27: *Upfield region of the ^{1}H-NMR spectrum of* **1f** *illustrating the peak-splitting of the protons of environments 11 and 12 due to long-range coupling with the proton in the allylic environment 9.*

The methyl groups of the 2° prenyl group resonate slightly downfield (C-16 and C-17, **Figure 26**), and were observed in the ^{1}H-NMR spectra of all lupulone derivatives to be present as singlets, although a little broader than is usually encountered at the top of the peak. Further downfield, multiplets for the CH_2

proton environments are encountered; for the geminal CH_2 methylene protons (C-8), it is observed as a multiplet when using a 400 MHz instrument; finer peak structure of this environment was revealed (**Figure 28**) when spectra were obtained using a 600 MHz instrument.

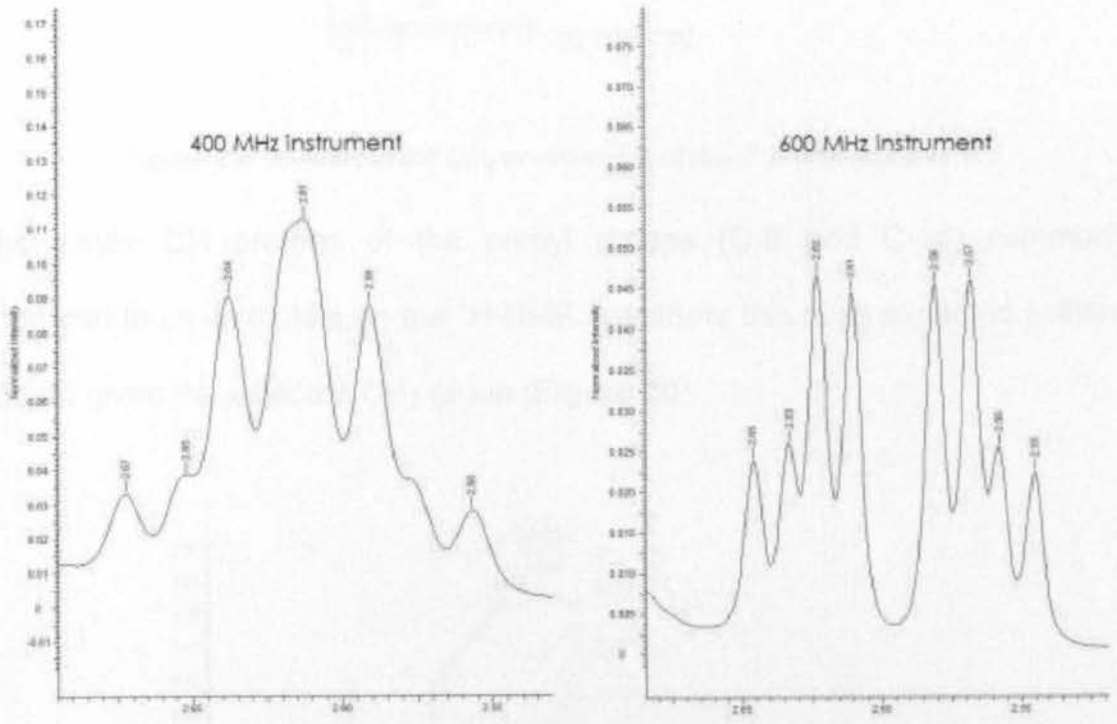

Figure 28: *400 MHz and 600 MHz ^{1}H-NMR of the CH_2 environment of the geminal prenyl units (environment 8,* **Figure 26***).*

The resolved peak structure of the 600 MHz spectrum revealed that the CH_2 unit has non-equivalent protons; the signal is split by the neighbouring vinylic CH, and then each (non-equivalent) proton of the methylene CH_2 splits those signals again. The methylene CH_2 unit of the 2° prenyl unit (C-13, **Figure 26**) are seen as a doublet, regardless of the instrument used (**Figure 29**).

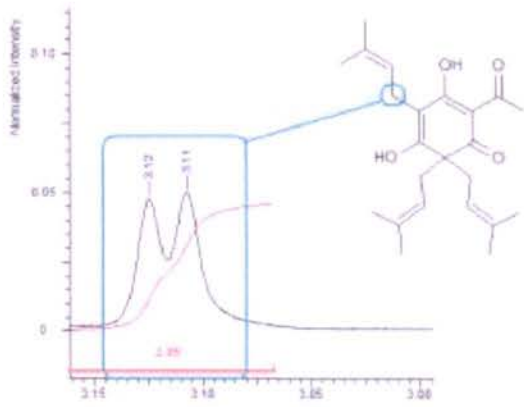

Figure 29: *^{1}H-NMR of the CH_2 environment of the 2^0 prenyl group of* **1f**

The vinylic CH protons of the prenyl groups (C-9 and C-14) commonly appeared to us as triplets on the ^{1}H-NMR spectrum; this is an expected splitting pattern given the adjacent CH_2 group (**Figure 30**).

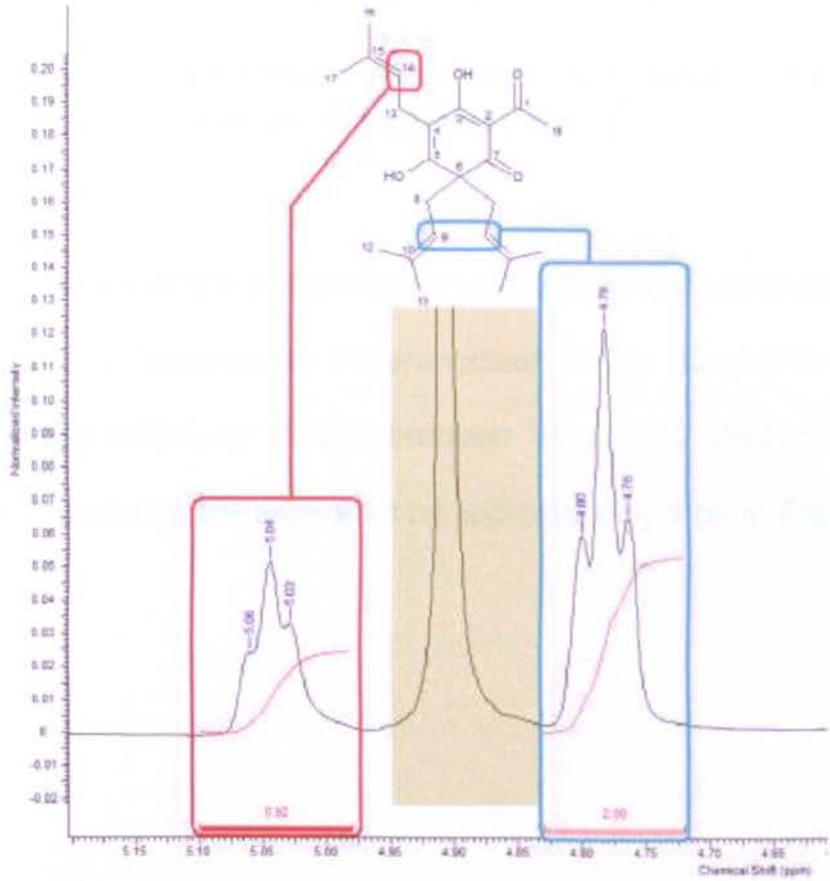

Figure 30: *^{1}H-NMR region showing the allylic CH triplet peak splitting patterns for hydrogen environments 9 and 14.*

At low NMR sample concentration, the larger of these triplets (integrating for 2H, the CH's of the geminal prenyl units) could be visualised as a more complex triplet of triplets (**Figure 31**).

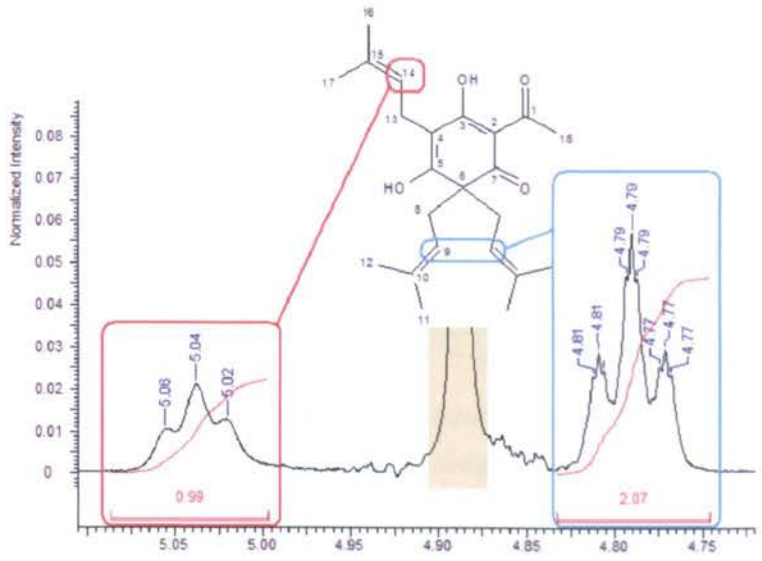

Figure 31: *^{1}H-NMR region showing the rarely observed triplet-of-triplet splitting pattern of hydrogen environment 9 (blue box).*

The non-equivalence of the prenyl methyl groups is further observed in the ^{13}C-NMR spectrum. 2-Dimensional Heteronuclear Single Quantum Correlation spectroscopy (2D-HSQC, or HSQC) between ^{1}H and ^{13}C showed that the *cis* and *trans* methyl groups are separated by approximately 8 ppm (**Figure 32**).

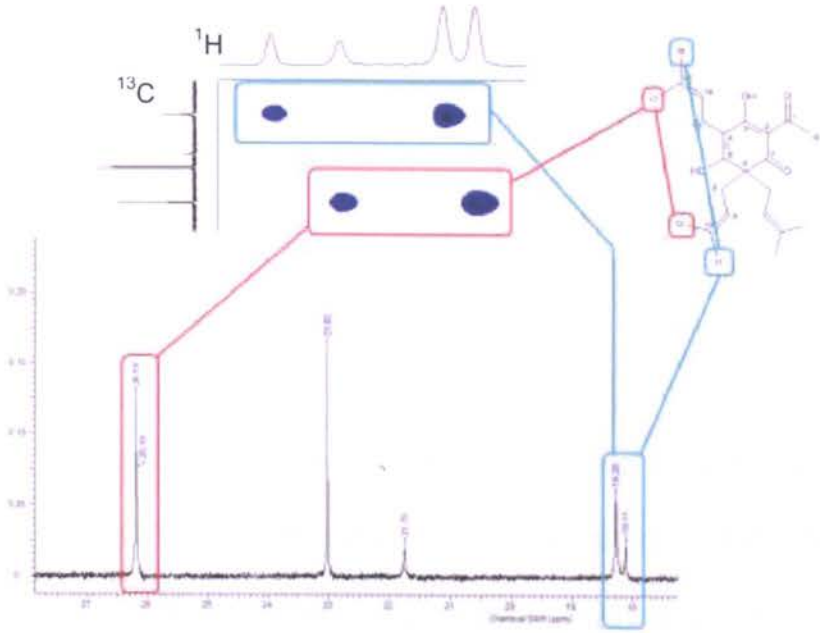

Figure 32: *HSQC spectrum (top) showing the non-equivalence of the cis/trans methyl groups on the prenyl units*

The methyl groups *cis* to the allylic CH_2 carbon were observed in a downfield position relative to the peak positions of the methyl groups *trans* to the allylic CH_2 carbon. Furthermore, it was observed that those groups on the geminal prenyl units were shifted slightly downfield compared to the respective (*cis* or *trans*) methyl group of the 2° prenyl group.

2.3 Synthesis of 2nd Generation β-Acid derivatives

As a result of our success in the development of the method for alkenylating acylphloroglucinols **3a-m** with prenyl bromide **23**, the use of alternate allylic bromides was explored for the synthesis of 2nd-generation β-acids. Allyl bromide **41** was investigated for its potential to C-alkenylate acylphloroglucinols **3a-m**. However, it was found early on that this modification required optimisation. The first attempt, using allyl bromide **41**, involved acylphloroglucinol **3e** (**Scheme 11a**) following the previously optimised procedure:

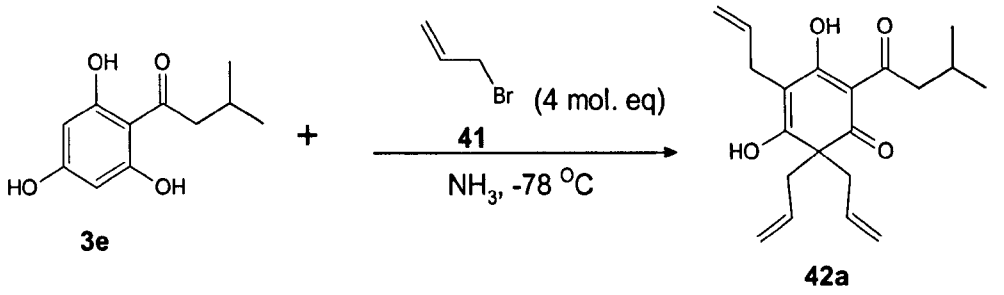

Scheme 11a

TLC analysis of the crude product mixture revealed that **3e** remained, and further analysis by GC-MS highlighted the desired product **42a** was dominant. Purification by flash column chromatography was attempted - while the suspected product was indeed isolated, it remained highly coloured and impure. Attempts at recrystallisation of the crude product from hexane failed, resulting in the reformation of the original crude oil upon cooling. An alternative where the crude was taken up in minimal warm methanol and water added upon cooling was also unsuccessful, again resulting in the recovery of the original crude oil. Unfortunately, long-term exposure to oxygen and repeated exposure to heat eventually destroyed the crude, and so the experiment was repeated using **3b**, with the first modification to the previous optimised procedure being an increase in the molar equivalents of allyl bromide **41** from 4 to 6 (**Scheme 11b**). This resulted in a higher conversion of starting material to desired product, as observed by gas chromatography-mass spectrometry (GC-MS) analysis. The next stage was to develop an improved method of purification, since simple recrystallisation of the crude semi-solid obtained was still not possible.

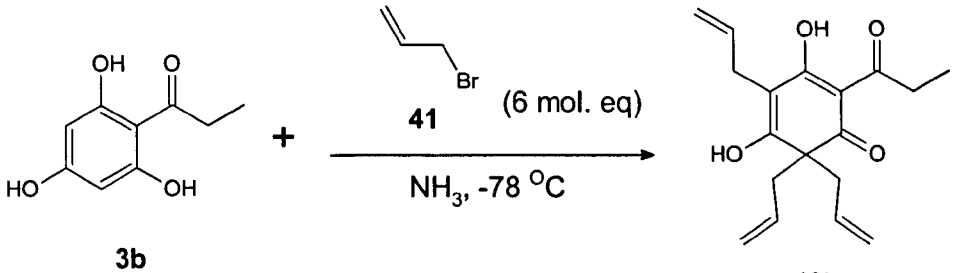

3b

42b

Scheme 11b

We had previously observed that acylphloroglucinols **3a-m** were not soluble in chlorinated solvents, whereas lupulone **1** and its derivatives **1a-m** were. With this in mind, chloroform and dichloromethane (DCM) were investigated for their use in purification of **42b** by column chromatography despite the known propensity of the C-alkenylated products to undergo degradation when exposed to acidic silica gel. In the case of chloroform, the addition of 1% v/v acetic acid was required in order to minimise streaking or tailing of the desired fraction. The eluted product still retained a dark colour indicative of residual impurities, but with care and the use of sonication, recrystallisation of crude **42b** from hexane was achieved. DCM was found to be a much better mobile phase for the procedure; no addition of acetic acid was required, and the isolated oily product soon solidified under vacuum or when left in a freezer. Recrystallisation from hexane was readily accomplished; the modified procedure proved to be repeatable, whereas the use of chloroform still gave rise to difficulty in isolating pure, crystalline products. Thus, optimisation of the purification procedure was achieved, and a small library of 2nd generation β-acids **42a-g** was generated (**Table 7**).

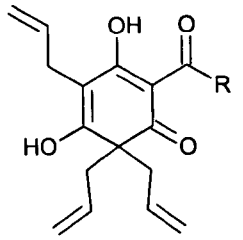

41

Compound Number	R=	%Yield (crude, pre-column)	%Yield (isolated, post-column)
42a	$CH_2CH(CH_3)_2$	-	22
42b	CH_2CH_3	58	16
42c	CH_3	87	43
42d	$CH_2CH_2CH_3$	-	49
42e	$CH(CH_3)_2$	73	39
42f	cyclopropyl	58	31
42g	cyclopentyl	68	14

Table 7

Yields were much lower than that for **1** and **1a-m**; this is likely to be due to the purification by column chromatography, where the compounds were exposed to an acidic environment for a significant amount of time, as well as prolonged exposure to oxygen, both promoting degradation of the compound.

2.3.1 NMR analysis of 2nd Generation β-Acids.

^{1}H and ^{13}C NMR analysis of the allyl bromide derivatives **42a-g** gave rise to interesting spectra, quite different to that of that observed for compounds **1** and **1a-m**. The allylic CH_2 groups were observed to be as much as they were for **1** and **1a-m**, in that the geminal methylene CH_2 groups (C-8) were a multiplet, and the 2° methylene CH_2 (C-11) was observed as a doublet (**Figure 33**).

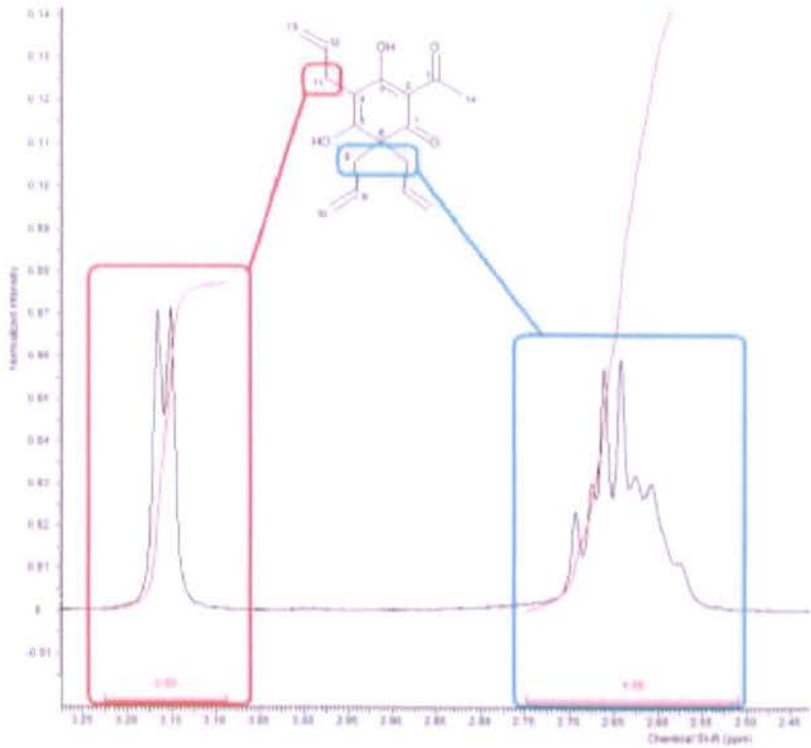

Figure 33: *^{1}H-NMR allylic CH_2 peak environments typical of compounds* **42a-g**.

The vinylic CH groups (C-9 and C-12) give rise to a complicated peak structure, deemed to be a doublet of doublet of triplets (**Figure 34**). This is due to coupling with the terminal, non-equivalent CH_2 protons (C-10 and C-13) as well as the methylene CH_2 groups (C-8 and C-11) bonded directly to the central polyphenolic core ring.

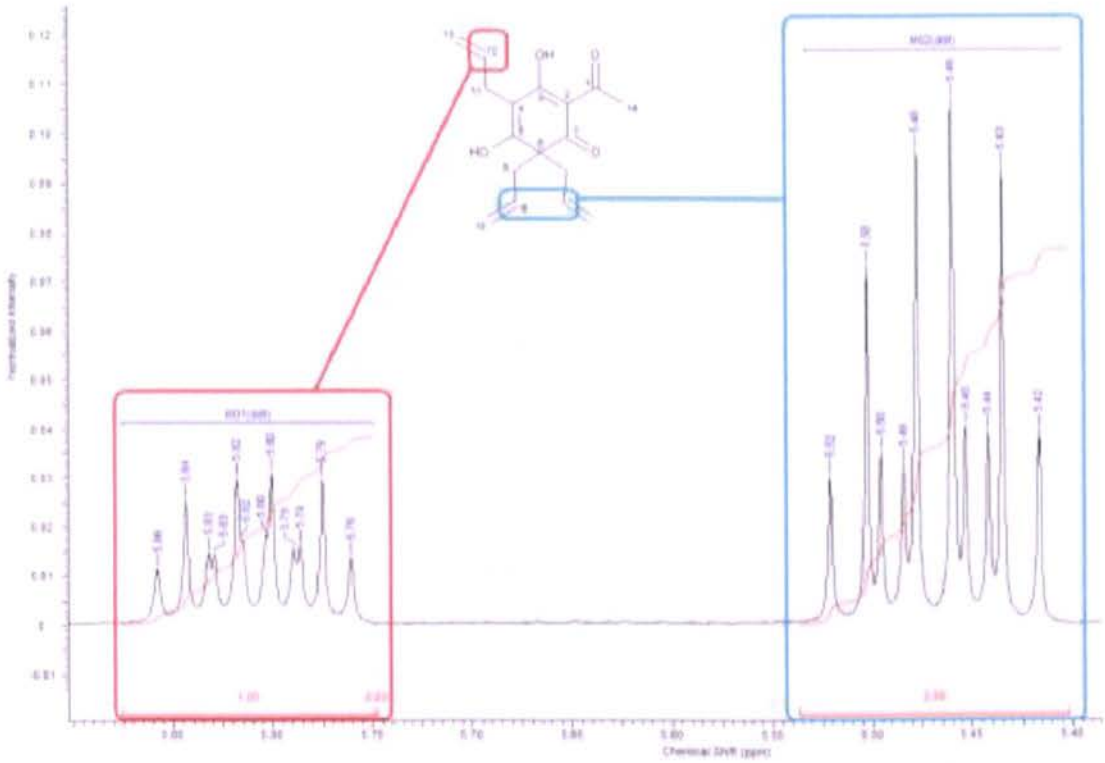

Figure 34: *^{1}H-NMR region showing the allylic CH peak structure typical to the ^{1}H-NMR spectra of compounds* **42a-g**.

Through the use of HSQC experiments, it was found that the vinylic CH_2 peak environments overlapped on the spectra, creating a complicated environment. Given the stronger intensity of the HSQC areas corresponding to a downfield position on the ^{13}C-NMR, these were attributed to the terminal geminal CH_2 environments (**Figure 35**).

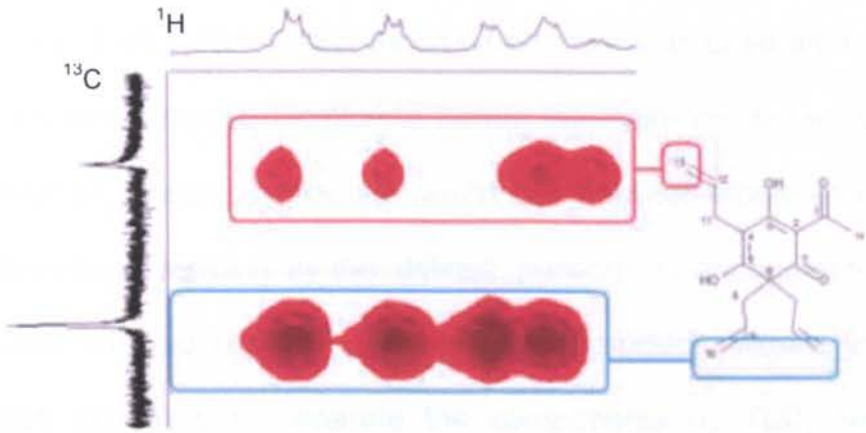

Figure 35: *HSQC spectrum area showing the overlapping peaks of the terminal allylic CH_2 groups typical of compounds* **42a-g**.

2.4 Further C-Alkenylation Attempts

We sought to further investigate the synthesis of β-acid derivatives with the use of crotyl bromide **43**. Two experiments were conducted with the aim of synthesising **44**, using the optimised conditions developed for the use of both prenyl bromide **23** and allyl bromide **40**.

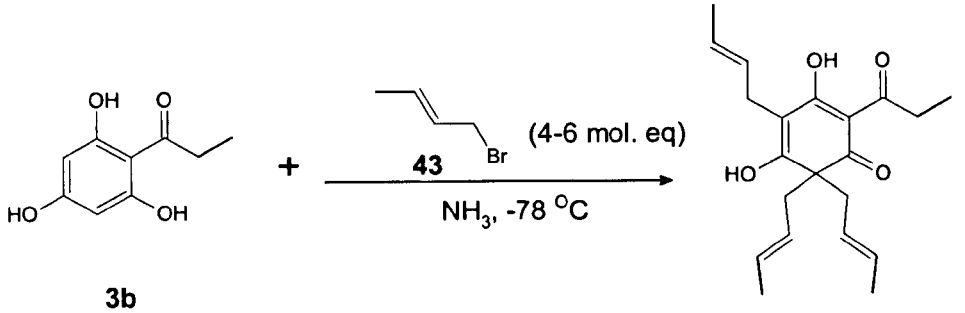

Scheme 11

In much the same way as we initially encountered when using allyl bromide **41**, compound **44** proved difficult to isolate. GC-MS analysis showed the loss of acylphloroglucinol **3b**, and the presence of a co-product with a similar retention time to the desired major product and molecular ion people matching **44** (*m/z* = 358). Indeed, the corresponding fragmentation pattern was almost exact, the only difference being the intensity of the fragments at *m/z* = 55 and 303. This could be due to a *cis / trans* effect as crotyl bromide was used as a mixture of *cis / trans* isomers, since purification to isolate the major *cis* isomer proved too great a challenge. These compounds, whilst not identical, would exhibit similar material properties resulting in the difficult purification encountered; indeed, where GC-MS showed two components in the product mixture, no solvent mixture could be found to separate the components by TLC, hence flash column chromatography with DCM as the eluent could only be used to remove

baseline impurities. Methods of recrystallisation were attempted, only to recover the product mixture in a yield of 23%.

In further exploration of the scope of the C-alkylation procedure, the use of both 3-bromocyclohexene **45** and 3-bromo-1-phenyl-propene **46** were investigated. **45** was observed to successfully couple with **3e** (**Scheme 13**) to generate the tetra-cyclic product **47**. Whilst purification of the product **47** again proved difficult, a ^{1}H-NMR of an impure sample was obtained indicating the presence of a product with the desired number of protons.

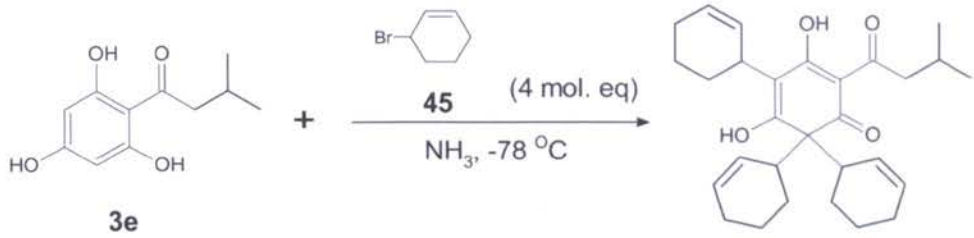

Scheme 13

Owing to the presence of the cyclohexene moieties, it was very difficult to attribute many of the resonances to specific proton environments on the molecular structure. Indicative general regions supporting the existence of **47** are shown (**Figure 36a** and **Figure 36b**).

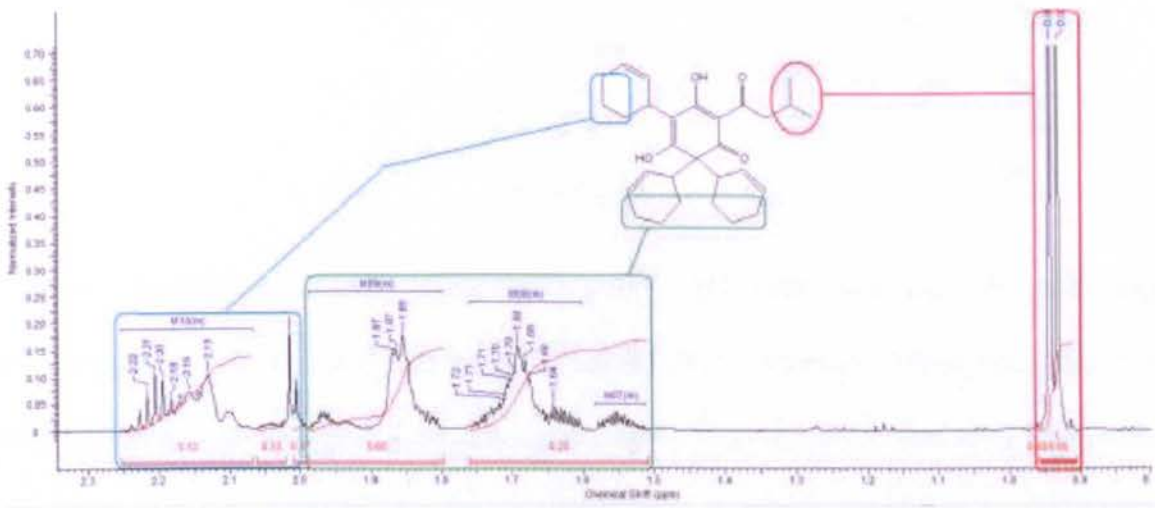

Figure 36a – *Upfield region of* ^{1}H-NMR *of* **47** *showing complicated multiplets for the* CH_2 *environments of the cyclohexene moieties (green and blue boxes).*

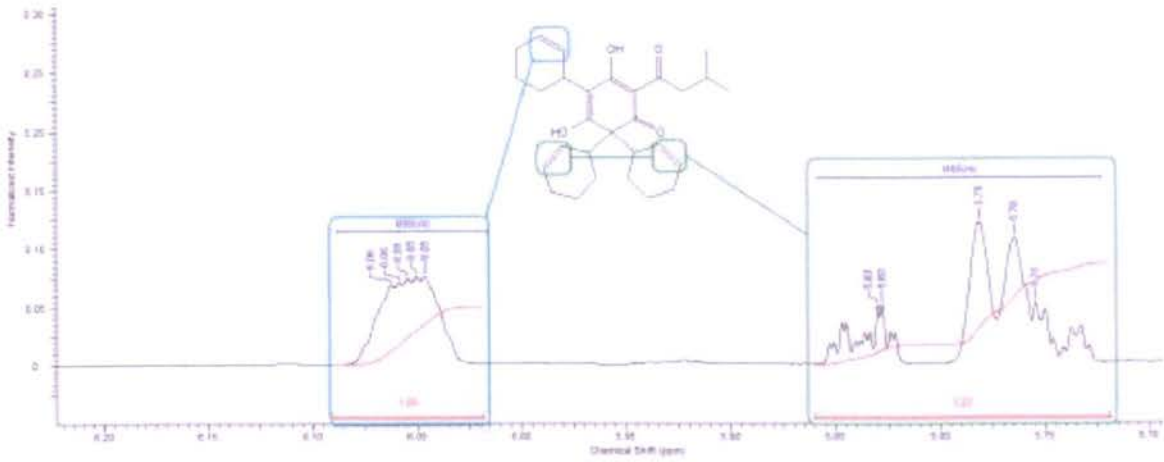

Figure 36b – *Downfield region of of* ^{1}H-NMR *of* **47** *showing characteristic resonances of alkene CH environments fn the cyclohexene moieties.*

The HSQC data highlighted the presence of impurities in the sample, but none the less it was an encouraging experimental result. The same could not be said for the experiment involving the use of 3-bromo-1-phenyl-propene **46** (**Scheme 15**), as no product **48** could be isolated; GC-MS and TLC revealed a multitude of components, none of which could be identified as a potential product lead.

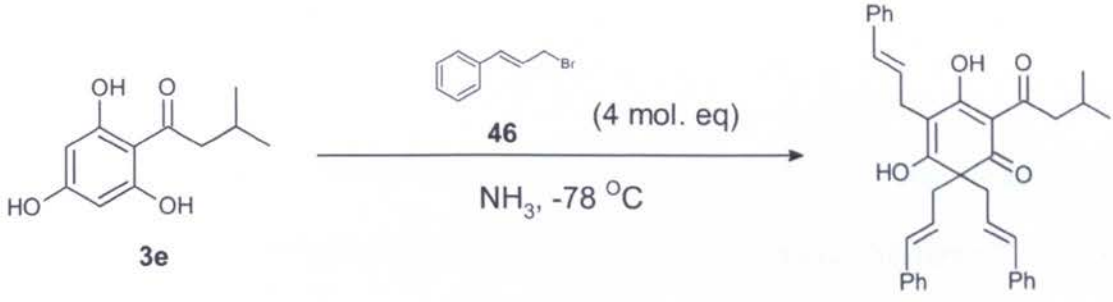

Scheme 15

Further repetitions of the experiment, with particular care paid to ensuring anhydrous conditions and purifying solvents and reagents employed, did not afford the desired product. It would seem, then, that electron-rich allylic bromide do not lend themselves to the C-alkylation reaction under our optimised conditions. Allylic bromides, such as **23**, **41**, **43** and **45** can participate

successfully in the reaction, but purification proved difficult and was hampered by the formation of degradation products; indeed, the formation of compound **47** suggests that steric effects are negligible as the cyclohexene portion is relatively bulky but the reaction proceeds as desired.

2.5 Ring Closing Metathesis and 3rd Generation β-Acid Synthesis

Owing to the successful generation of the 2nd generation β-acid derivatives **42a-g**, it was envisaged that these compounds may lend themselves to ring closure of the geminal allylic moieties through the use of ruthenium-catalysed ring-closing olefin metathesis. Developed by Robert Grubbs and associates in the 1980's[82], ring-closing metathesis (RCM) (**Figure 37**) has proved to be a powerful tool for the formation of closed ring structures that would otherwise be difficult to generate.

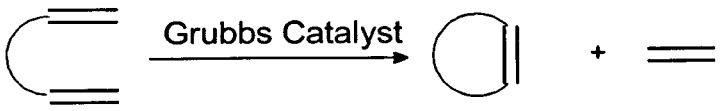

Figure 37

The widely-accepted mechanism for the metathesis reaction was proposed by Chauvin in relation to earlier work involving tungsten-based catalysts[83] and was further found to apply to metathesis reactions where many transition metals, including ruthenium, were present as the catalyst[82, 84]. A key feature of the mechanism is the proposed formation of a metallocyclobutane intermediate, an unstable transition state which promotes the formation of the desired alkene bond[82, 83, 85] (**Figure 38**).

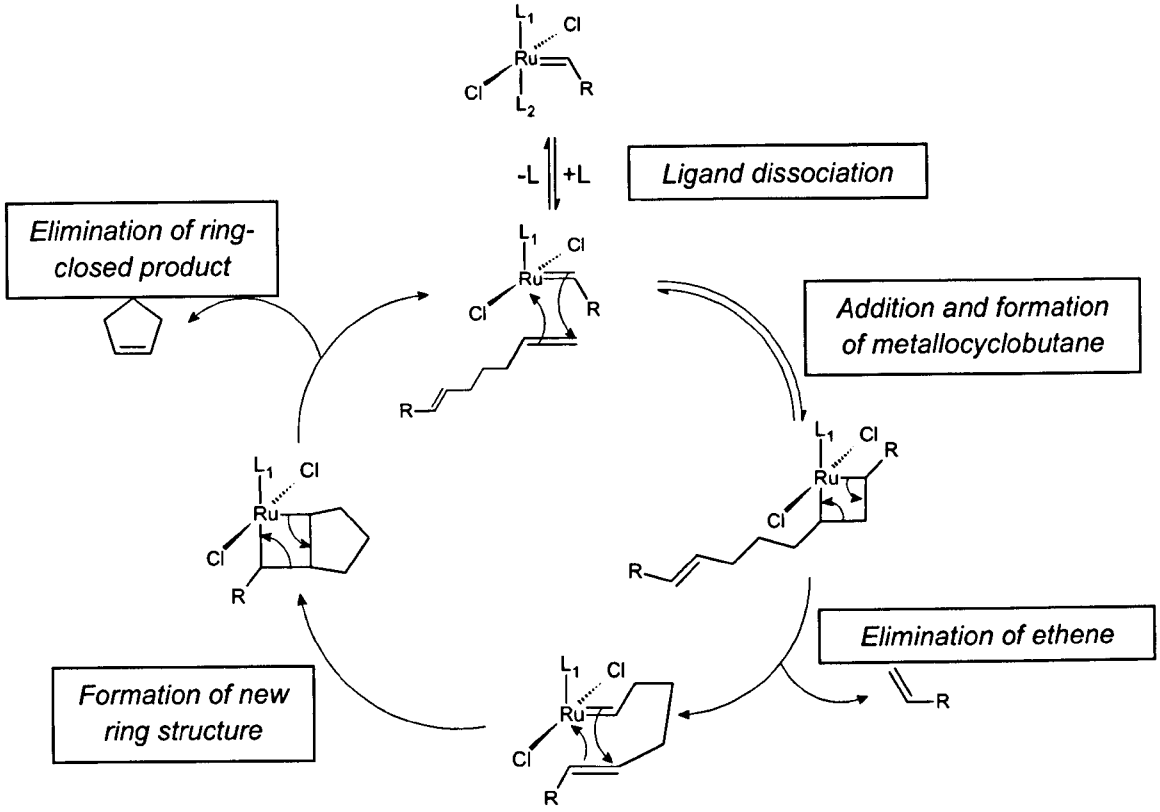

Figure 38: *The widely-accepted Chauvin mechanism depicts the formation of an intermediate metallocyclobutane as a key step in the ruthenium-catalysed ring-closing metathesis reaction.*

The dissociation of a ligand (usually a sigma-electron-donating phosphine ligand) from a stable 18-electron ruthenium complex gives rise to a catalytically active 16-electron species[86]. The re-uptake of the departed ligand is governed by the stability of this 16-e$^-$ complex; the more stable it is, the slower the reuptake of the ligand will occur, hence the probability of the 16-e$^-$ species binding to a pi-electron-donating alkene to initiate the metathesis process is increased[87].

The intention of this line of work was to synthesise novel, spirocyclic compounds; they have the demonstrated capability to give rise to interesting and important physiological responses, including the inhibition of enzymes associated with the onset of Alzheimers disease, type-II diabetes and bipolar disorders[88, 89].

2.5.1 Attempts at Ring Closing Metathesis

We began our investigations using the first generation Grubbs catalyst **49** (**Figure 39**) on compound **42c** using dichloromethane as the solvent, with the intention of generating the spirocyclic compound **50** (**Scheme 16**).

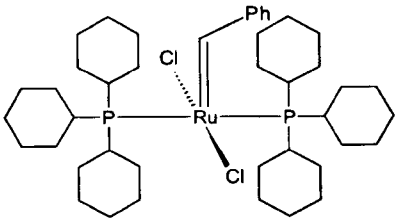

49

Figure 39

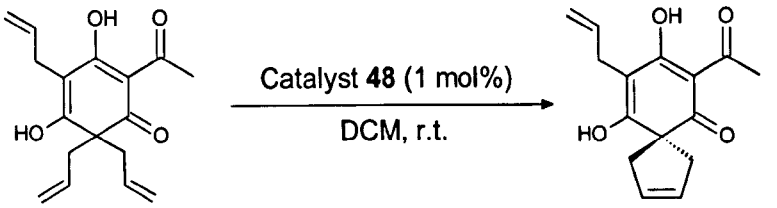

42c **50**

Scheme 16

Much like the C-alkylation reactions that were conducted in liquid ammonia, the set-up of the reaction required much consideration with the most important experimental criteria involving the removal of oxygen from the reaction mixture. It was decided the most practical way to deoxygenate the solvent would be to bubble nitrogen gas through it; this was achieved by fitting the 2-neck reaction flask with a silicone oil bubbler, and passing a needle through a rubber septum with which to bubble nitrogen through the stirring solvent. It was soon realised that the starting material **42c** also contained trapped oxygen within its crystalline matrix, and so this was dissolved in the solvent prior to degassing.

The first attempt was conducted at room temperature, and monitored by GC-MS analysis. Even after extended stirring (+18 hours) no desired product was observed to have formed. Elevating the temperature to 35 °C caused some conversion to **50** as indicated by a GC-MS component with the correct molecular ion peak. However, with extended reaction time further by-products formed, indicating degradation of the starting material. Up to this point, the catalyst loading had been 1 mol%, with a concentration of 0.5 M relative to the starting material. Amending the concentration to a more dilute 0.02 M, and then increasing the catalyst loading to 5 mol%, had no effect on the rate or amount conversion of **42c** to **50**. Understanding that the formation of a potential product was possible, a screening of three other commercially available catalysts was undertaken; Grubbs 2nd Generation **49a**, Hoveyda-Grubbs 1st Generation **49b** and Hoveyda-Grubbs 2nd Generation **49c** (**Figure 40**).

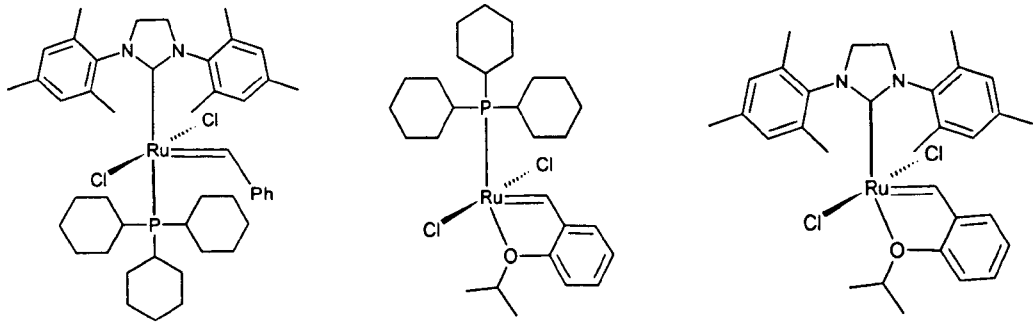

49a **49b** **49c**

Figure 40: *Further commercially-avaliable metathesis catalysts: (from left to right) Grubbs 2nd Generation* **49a**, *Hoveyda-Grubbs 1st Generation* **49b**, *Hoveyda-Grubbs 2nd Generation* **49c**.

The second generation Grubbs catalyst **49a** was expected to form a more stable, catalytically-active 16-e⁻ species on account of the nitrogen-containing heterocyclic carbene ligand (NHC ligand), which discourages binding by the

sigma-donating phosphine ligands and favours the pi-donating properties of an incoming alkene moiety, in this case a terminal alkene unit of **42c**. In contrast the Hoveyda-Grubbs catalysts **49b** and **49c** are thought to be activated to a 16-e$^-$ complex not by dissociation of a phosphine ligand (which is impossible for **49c**) but by the dissociation of the coordinating oxygen atom of the isopropoxystyrene ligand[90]. Whether the dissociation occurs before occupation of the vacant orbital by the incoming alkene substrate, or if there is binding by the alkene as the oxygen leaves is open to debate since it has been calculated that the energies of either process are similar[91].

Our experiments involving **49a-c** revealed that the Hoveyda-Grubbs catalysts were capable of significant conversion of **42c** to **50**, particularly **49c** where the rate of conversion to an observed 1:1 ratio of **42c** : **50** had occurred within 1 hour. Extended stirring did not increase this; however, encouraged by the result the experiment was repeated, resulting in an 80% observed conversion of **42c** to **50** within 2 hours. Conversion to product did not continue despite extended stirring so the reaction was quenched with water and worked up.

Although GC-MS analysis indicated the reaction progressed well, we soon encountered a new problem – isolating the reaction product. Early attempts to isolate the compound by flash column chromatography did not work, and it was considered that residual ruthenium catalyst **49c** may be causing side-reactions during the work-up phase. In order to eliminate this potential pathway of degradation, strategies to remove ruthenium compounds were explored prior to work-up. Attempted adsorption of **49c** onto charcoal gave rise

to a dark brown solution, and GC-MS showed degradation of the mixture components. Stirring with silica gel with the intention of deactivating **49c** returned a much less coloured solution, but both TLC and GC-MS showed degradation of the mixture components.

A search of the literature at this point revealed the use of tris(hydroxymethyl)phosphine **51** (**Figure 41**) as a reagent for removing the ruthenium catalyst[92].

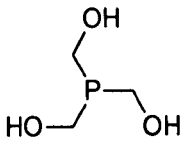

51

Figure 41

Phosphine **51** is thought to bind strongly to the ruthenium metal centre through donation of the lone-pair 3s orbital electrons of the phosphorous atom to the ruthenium, causing degradation of the catalyst. The presence of terminal hydroxyl groups allows the resulting complex to be soluble in the aqueous phase of a liquid-liquid extraction, thereby significantly reducing the chance of side-reactions occurring during the removal of organic solvent under vacuum. This strategy, involving the use of 10 molar equivalents of **51** relative to catalyst **49c** gave rise to a less coloured solution than before the ruthenium complex was removed, but still, isolation of the reaction product proved elusive due to ongoing degradation processes. It was decided then that **49c** was having little to do with product degradation during the work-up process, and that any unwanted reactions were occurring during the reaction phase itself.

It was considered whether the known keto-enol tautomerism of the lupulone derivatives in DCM may be giving rise to complications with the reaction progress and its subsequent work-up. A search of the literature revealed that very few studies had taken place on the use of alternative solvents in ring-closing metathesis; indeed, it would seem that dichloromethane DCM is the default choice, and for higher temperatures toluene is recommended. However, Adjiman *et al*[93] published results showing that of 6 screened solvents (DCM, toluene, cyclohexane, chlorobenzene, acetone and acetic acid), cyclohexane and acetic acid could potentially increase both the rate of reaction and conversion to product. Since **42c** is weakly soluble in hydrocarbons at room temperature, the use of acetic acid as a reaction solvent for ring-closing metathesis was studied, with surprising and pleasing results.

Applying the conditions of 0.02 M concentration and 5 mol% catalyst loading, a degassed solution of **42c** in acetic acid was subjected to ring-closure by the Hoveyda-Grubbs 2nd Generation catalyst **49c**. The reaction progression was monitored by both TLC (every 5 minutes) and GC-MS (every 30 minutes). It was seen that initial observed conversion to product was rapid; after 1 hour, the peak ratio of **42c** to **50** was greater than 90% in favour of **50**. Continued and extended stirring over 18 hours revealed no observed degradation, but no further conversion to product. Isolation was again attempted, but pure product could not be obtained. What was isolated was much a reduced amount of compound relative to that loaded onto the column. With such small amount of material isolated, no analysis beyond ^{1}H-NMR was possible; the reaction was instead repeated on a much larger scale, with the aim of isolating enough material to perform further characterisation. The scaled up reaction allowed the

isolation of a sufficient amount of post-column material to attempt recrystallisation from hexane, achieved successfully in 7% isolated yield of **50a**.

Owing to the success of isolating **50**, the cyclopentane derivative **42f** was also subjected to the same ring-closing metathesis conditions (**Scheme 17**).

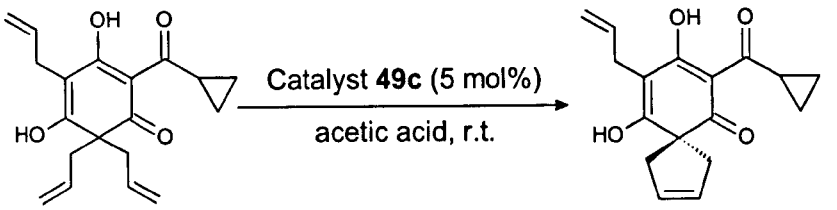

42f **50a**

Scheme 17

This compound was chosen due to positive results from anticancer testing; furthermore, we had observed the apparent stability of a cyclopropane ring in these compounds and wished to investigate that stability further. Again, the reaction was conducted on a gram scale, and isolation of product **50a** was achieved in 11% yield, which was consistent with that of **50a**.

2.5.2 NMR Studies of the 3rd Generation β-acids

The ^{1}H-NMR data of **50** gave rise to several resonances that indicate its successful formation. Comparing the ^{1}H-NMR of the substrate **42c** to that of the product **50**, it is seen that the CH of the two geminal allylic groups on **50** give rise to a resonance upfield to the corresponding 2° allylic CH group present (**Figure 42**). The doublet-doublet-triplet system features resonances for both allylic proton environments, with the geminal allylic protons more upfield at 5.42 – 5.52 ppm. This is not present in the ring-closed product **50**; instead it is

observed that a broad singlet is formed downfield of the original doublet-doublet-triplet at approximately 5.67 ppm (**Figure 43**).

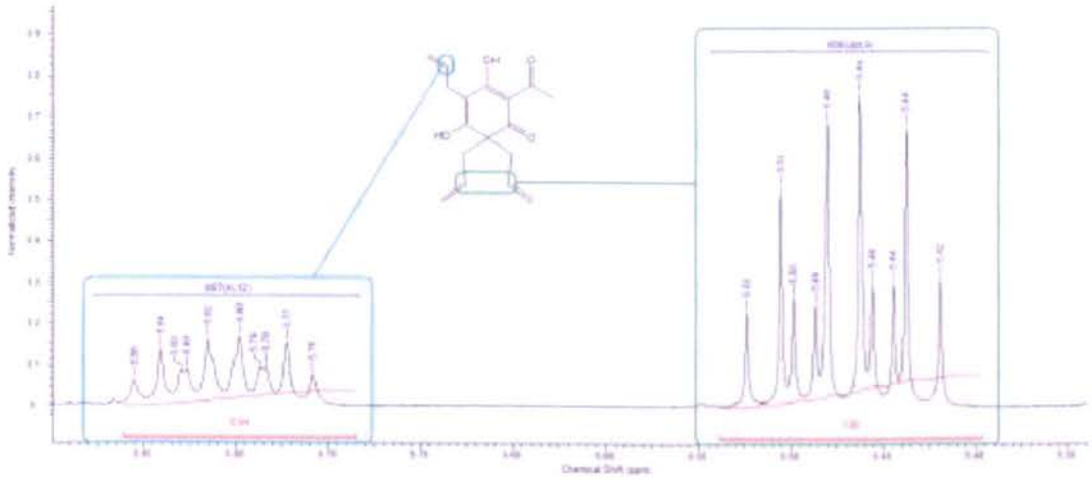

Figure 42: *^{1}H-NMR of* **42c** *- zoomed region showing geminal allylic CH (upfield, green box) and the 2° allylic CH (downfield, blue box).*

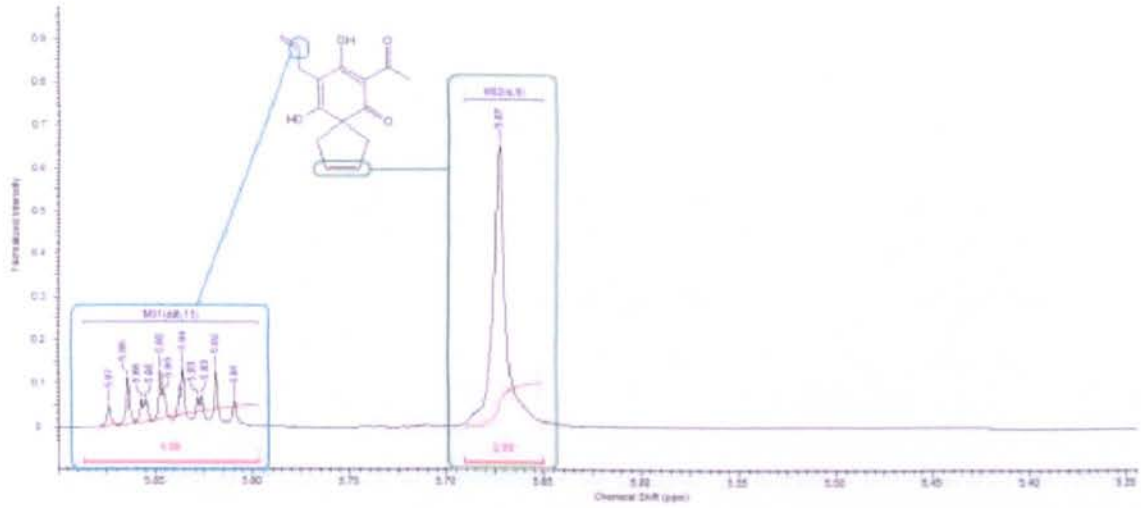

Figure 43: *^{1}H-NMR of* **50** *- zoomed region showing the CH environment of the newly-formed cyclopentene ring (green) and the CH of the remaining allyl group (blue) – there is no peak environment indicative of remaining* **42c**.

2.5.3 Further Discussion of the Ring Closing Metathesis Reaction

The low isolated yield of the reaction is unfortunate but there may be several reasons as to why problems are occurring. As previously discussed, β-acids

can undergo a variety of intramolecular reactions and rearrangements to give alternative products. It is conceivable that the activation of the alkene bond by the catalyst can make it susceptible to attack from the nearby hydroxyl groups, forming a new heterocycle or an isomer of the original structure. Equally possible are intermolecular cross-metathesis reactions leading to polymeric chains of **42c** and **42f**; the highly electron rich nature of the compound serves to activate the allylic groups which would be poised to attack any nearby electrophilic centre. Since the 6-membered ring of **42c / 42f** is planar[18], there is restriction on how close the geminal allyl groups can get, thus it may be more favourable for the remaining allyl group to attack and undergo cross-metathesis (**Figure 44**).

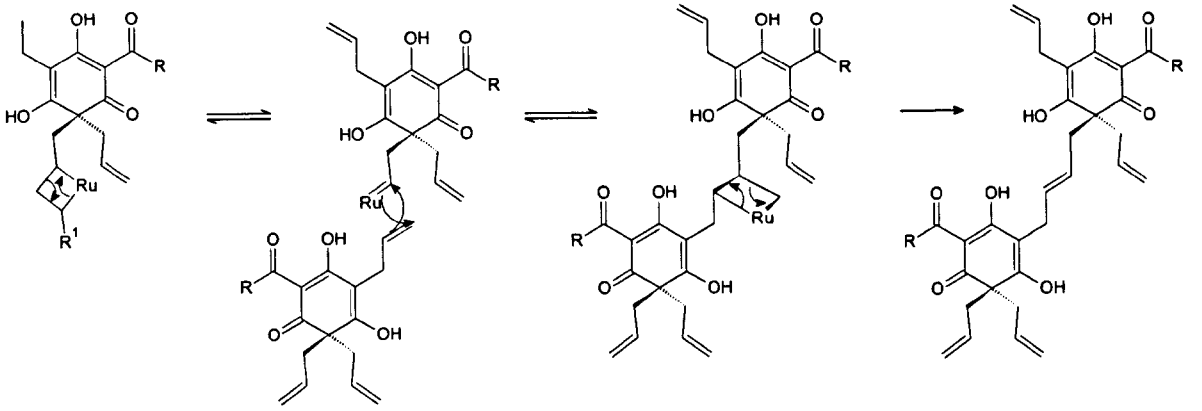

Figure 44: *Potential, undesirable cross-metathesis occurring instead of the desired ring-closing metathesis; the reaction may not stop at the dimer shown.*

Furthermore, there is a small body of evidence[94, 95] suggesting that the Grubbs-type ruthenium catalysts can oxidise alcohols to ketones which may open up pathways for further unwanted reactions.

Considerable thought was given as to why acetic acid appeared to improve the reaction progression and facilitate easier isolation of the desired products **50** and **50a**. There are two major possibilities; firstly, being a polar,

protic solvent only tautomer **42** was present as opposed to tautomer **52** (**Figure 45**), which may form a more stable and thus more reactive intermediate with catalyst **49c**.

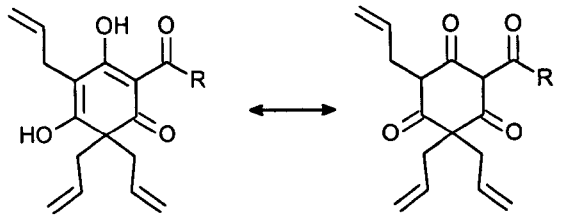

42 **52**

Figure 45

Secondly, the large presence of labile protons from acetic acid may help to form the active 14-electron catalytic species **49c** from the inactive 16-electron species **53**, by protonating the oxygen of the isopropoxy moiety of the isopropoxyphenylmethylene ligand (**Figure 46**).

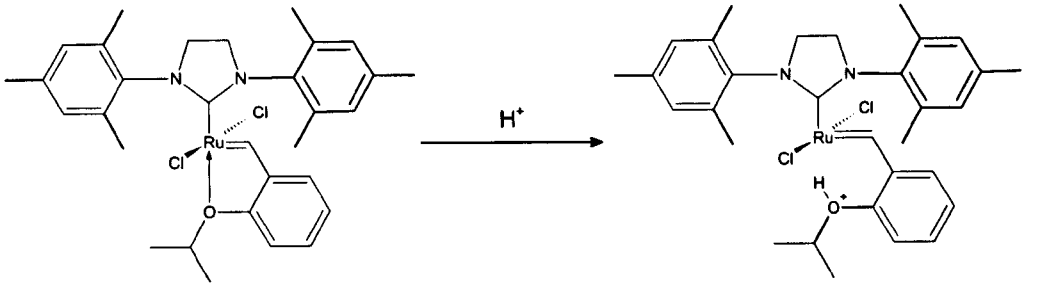

49c **53**

18 e⁻ complex 16 e⁻ complex

Figure 46: *Possible activation of the Hoveyda-Grubb's Second Generation catalyst by protonation of the isopropoxy group.*

Given the long time spent on investigating the ring closing metathesis potential of compounds **42c** and **42f**, we decided that since the reactions gave a poor return on the time and effort invested that no further investigation would be

conducted. Despite this, we are pleased with the results of the experimentation and the exhibition of ring closure on lupulone-type compounds giving rise to a spirocyclic structure.

2.6 An Alternative C-Alkenylation Reaction

We wished to pursue higher generations of the β-acid derivatives, as well as allowing a pathway to the generation of α-acid derivatives in order to further assess the biological activity of hop acids. By considering the biosynthetic pathway, the common compound to both the β-acids and the α-acids are the deoxyhumulones **11**.

Owing to the success of the C-alkenylation reactions in liquid ammonia and the subsequent generation of our 1st generation β-acids lupulone **1**, **1a-n** and the 2nd generation β-acids **42a-g**, we were keen to investigate other methods of C-alkenylation with a view to opening the doors to a well-controlled synthesis of deoxyhumulone derivatives **11**.

2.6.1 Retrosynthetic Analysis of Deoxyhumulone Derivatives

Retrosynthetic analysis of the target compound **54** revealed two possible routes. One may first proceed by performing a Friedel-Crafts acylation of **38**, followed by alkenylation of **39** to give **55** then deprotection of the methoxy groups (**Figure 47a**).

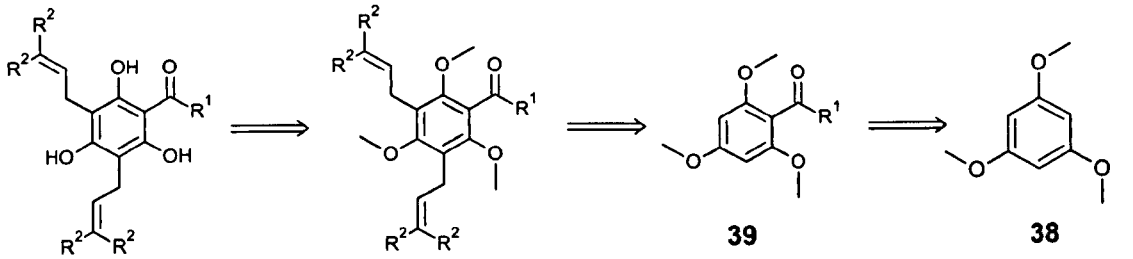

Figure 47a

Conversely, one could begin with the alkenylation of **38**, followed by the Friedel-Crafts acylation of **56** and then deprotection of the methoxy groups (**Figure 47b**). Deprotection as the last step was favourable as the presence of hydroxyl groups may lead to unwanted intramolecular cyclisations, as well as interfering with reaction progression due to switching between tautomeric forms.

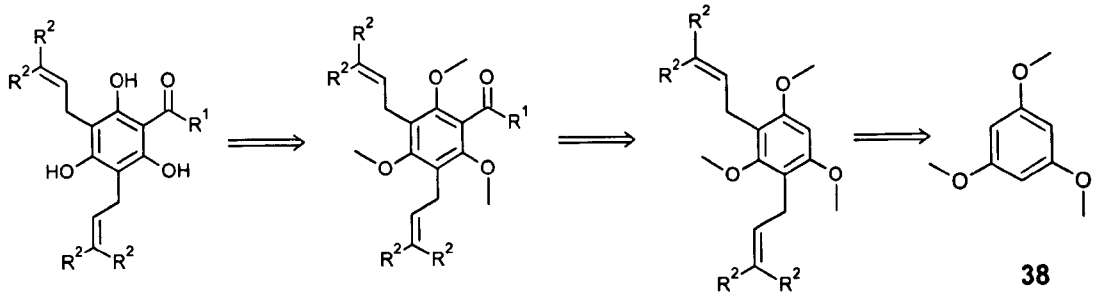

54 **55** **56** **38**

Figure 47b

2.6.2 Attempts to Synthesize the Deoxyhumulones

Since the acylation reaction had been well explored up to this point, we began the synthesis by focussing on the second route, searching for C-alkenylation reaction conditions using ortholithiation as a tool for further coupling. A literature search revealed no published work involving dialkenylation of **38** *via* dilithiation, but Crowther *et al*[96] had published results on the disilylation of **38** *via* a dilithiated intermediate (**Scheme 18**). The important results of that work were that, in comparison to hexanes, diethyl ether resulted in quicker formation of the lithiated species, and that dilithiation had the potential to occur in at least 86% yield as inferred through the reported isolated yield of the disilylated compound **57**.

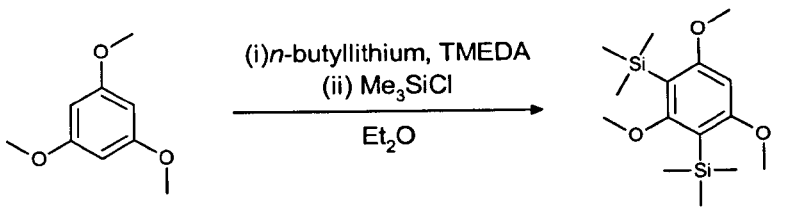

38 57

Scheme 18

Inspired, we set about our first experiment, substituting triethysilyl chloride with allyl bromide **41**. The formation of the dilithiated species required a reported 11 hours at room temperature; we elected to stir for 18 hours overnight under a nitrogen atmosphere to ensure maximum dilithiation occurred. During the lithiation stage, a white suspension formed a few minutes after the addition of *n*-butyllithium, which gradually darkened over the next 18 hours to an eventual tan-yellow suspension. This agreed with the observations reported by Crowther *et al.* Introduction of allyl bromide **41** was completed and the reaction monitored by TLC analysis. Although a faint spot appeared after 1 hour suggesting the formation of a new compound, the majority of the isolated material was unreacted substrate **38**. It was also discovered that dibromination was occurring through bromine-lithium exchange between the formed lithiated species and allyl bromide **41** (**Scheme 19**), to form 2,4-dibromo-1,3,5-trimethoxybenzene **58**.

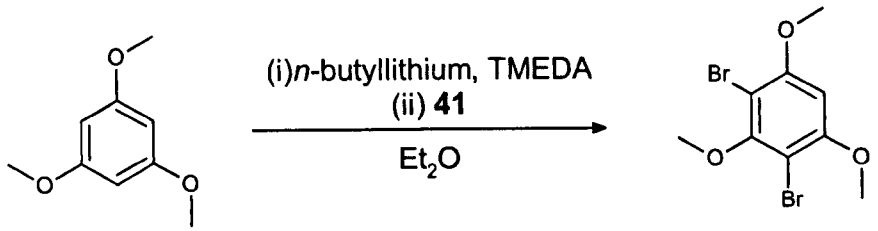

38 58

Scheme 19

We therefore required a method to avoid lithium-bromine exchange. Casas *et al*[97] reported that the addition of an equimolar amount of copper (I) iodide

(relative to *n*-butyllithium) could promote the coupling of **41** to an aromatic amide. Further reading around the subject of the lithio-cuprate coupling brought to our attention Gilman reagents[98]. These are typified by the addition of two equivalents of an organolithium compound **59** to a copper (I) halide, forming a lithium-copper (lithiocuprate) complexed carbanion[99] **60** (**Figure 48**).

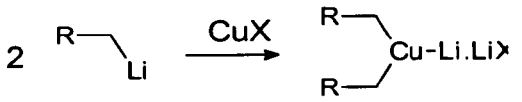

59 **60**

Figure 48

For aromatic compounds, the corresponding mono-lithiocuprate species have been observed to form an 8-membered species[100] **61** where the diethyl ether solvent also plays a role in providing a stable complex (**Figure 49**).

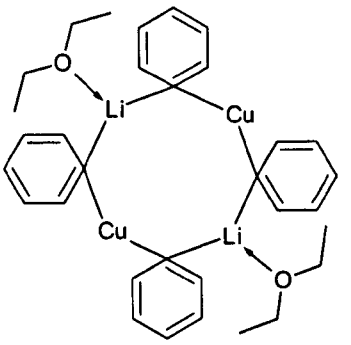

61

Figure 49

For the generated dilithiocuprate species, the structure is harder to predict and is likely to exist as a highly complex structure evolving further from **61**. In any case, the formed lithiocuprate was observed to be less inclined to undergo addition of bromine at the aromatic carbanion. We struck success on the first attempt of the modified reaction conditions, isolating **56a** in 54% isolated yield,

with a subsequent repetition on a larger scale returning an improved 61% isolated yield (**Scheme 20**).

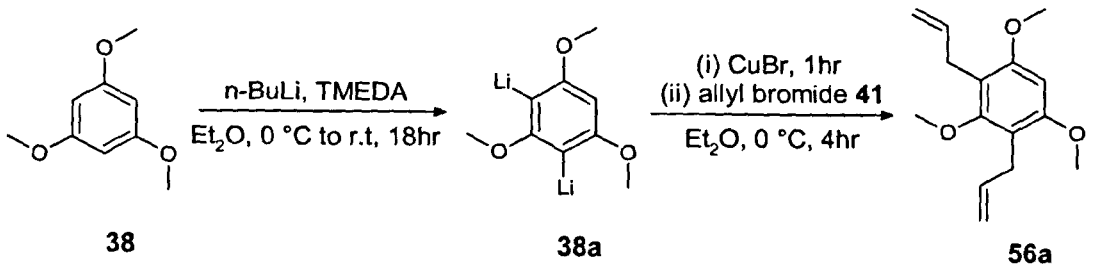

38 **38a** **56a**

Scheme 20

Encouraged by the ease of which we could produce the allyl bromide derivative **56a**, we investigated the use of prenyl bromide **23**, which could reveal by which mechanism the coupling of the allyl group to the aromatic ring was occurring - two routes were theorized; either the direct substitution of the bromine at the sp^3 carbon could occur (**Figure 50a**) as observed in the ammonia-solvated trialkenylation reaction, or attack at the sp^2 carbon could occur, pushing the electrons through to eject the bromide anion (**Figure 50b**).

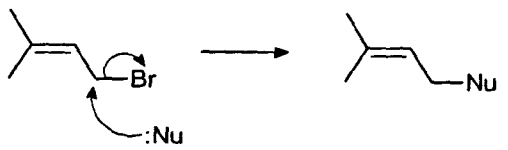

Figure 50a

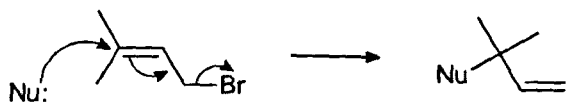

Figure 50b

Using the same reaction conditions as employed in the synthesis of **56a**, it was found that the simpler substitution of bromine through attack on the sp^3 carbon occurred, giving **56b** in 56% yield (**Scheme 20**).

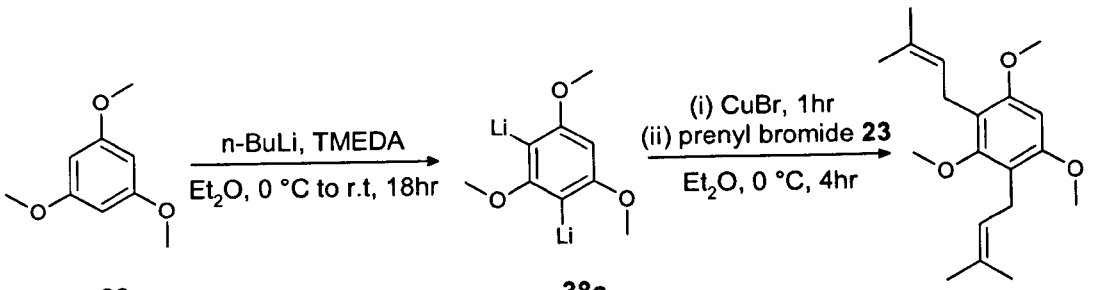

38 38a 56b

Scheme 20

Attention now turned towards acquiring the acylated, deoxyhumulone derivative **55**, which we thought could be generated *via* the Friedel-Crafts acylation which we now had plenty of experience with. We followed the procedure used in the synthesis of compounds **39a-d**, first generating the acylium cation by stirring propionyl chloride **62** with $AlCl_3$ before transferring *via* syringe to a cooled solution of **56a** in DCM, hoping to form **55a** (**scheme 21**).

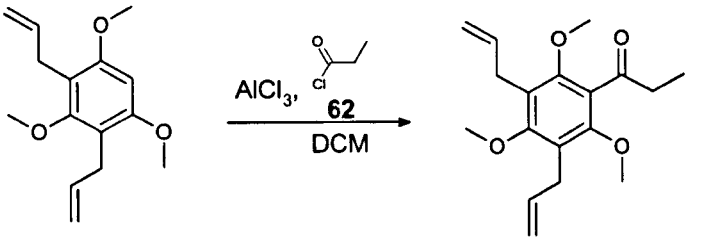

56a 55a

Scheme 21

A strong colour change was observed upon introducing the first drop, and at full addition of the acyl chloride / $AlCl_3$ complex, the solution was almost black in colour – TLC analysis revealed the formation of a new spot, travelling much slower than **56a**; this was expected, since it was previously observed that acylated phloroglucinols **3a-m** and acylated 1,3,5-trimethoxybenzenes **39a-d** produced similar behaviour when compared to **32** and **38** respectively. Purification by flash column chromatography was performed, which returned very little of the expected product – this was surprising, as TLC analysis had

shown the formation of a new product. The experiment was repeated, with the same observations made. The strong colour change, upon addition of the acyl chloride / $AlCl_3$ complex gave cause for concern, so two further experiments were conducted. Firstly, **56a** and **62** were stirred together and no colour change was observed. TLC analysis showed no change of **56a** after 3 hours and again after 18 hours. Aluminium chloride was then introduced in small portions, producing the colour change that had given cause for concern with sub-equimolar amounts present. This prompted the supposition that the Lewis acid was giving rise to an unwanted process, confirmed by the addition of aluminium chloride to separate stirred solutions of both **56a** and **62**. TLC analysis now revealed degradation of the starting material in the presence of the Lewis acid. We also investigated the use of other Lewis acids titanium tetrachloride, boron tribromide and iron (III) chloride on both **56a** and **56b**, all producing the black solution and similar degradation as observed by TLC analysis when aluminium chloride was used. The results of this also meant that the desired deprotection step, generating a trihydroxy derivative from the trimethoxy compound, would also be met with degradation of the allylated compound. Never having encountered such a reaction before, it was found in the literature that Lewis acids are infact well known to strongly promote cationic polymerization of allylic compounds[101-103] (**Figure 51**).

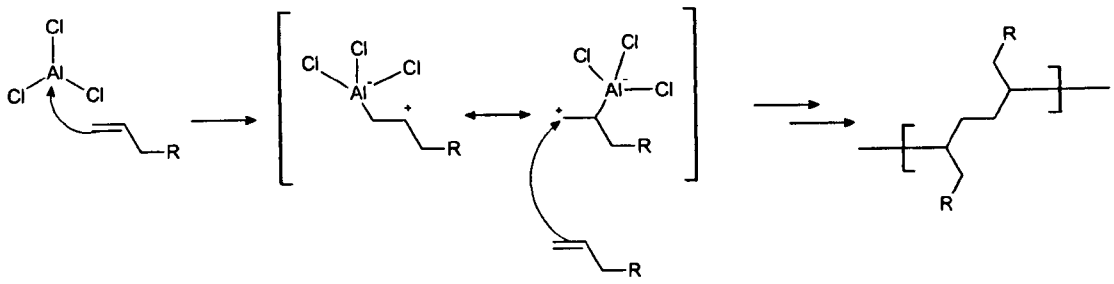

Figure 51: *Cationic polymerisation of an allylic compound initiated by the Lewis acid $AlCl_3$.*

This explained several observations; firstly, the strong colour change could have been the generation of the cationic species, which as the reaction became more concentrated with the Lewis acid initiator, became darker and darker in colour. The yield of crude product isolated after the work-up but before attempted purification by column chromatography was almost quantitative, however most, if not all, remained on top of the silica column (i.e. baseline residue) which is indicative of high molecular weight compounds unable to pass through the silica gel, even when ethyl acetate alone was used as the eluent. Satisfied with the explanation and the fitting observations, this route to deoxyhumulones was to be pursued no longer. Before abandoning completely, ortholithiation was attempted, since a site remained on the aromatic ring where lithiation could occur. It was found that lithiation did not occur, hence no coupling to propionyl chloride **62** occurred. It was at this point, we looked towards investigating the alternative route, first generating an acylated product then performing the dialkenylation *via* dilithiation.

The alternative route derived from the retrosynthesis (**Figure 47b**) showed that it may be possible to first acylate **38** *via* the Friedel-Crafts reaction and then perform the lithio-cuprate coupling reaction. Since we had a good amount of **39a** available to us, we attempted the coupling reaction to generate **63** (**Scheme 23**).

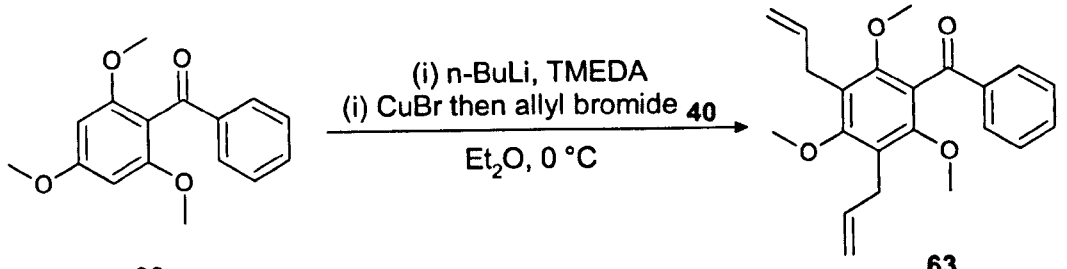

39a **63**

Scheme 23

Lithiation of **39a** was conducted under the same conditions as before, with an orange solution formed in contrast to the previously encountered tan suspension of the lithium species **38a**. Upon transfer to stirred CuBr, a dark purple solution was formed, not dissimilar to that observed in the previous alkenylation reactions involving **38**. Following addition of allyl bromide **41**, the reaction was monitored by TLC revealing several new products, all travelling further than the starting material. A component of the crude mixture was isolated by column chromatography, albeit in low yield (7%).

2.6.2 NMR Studies of a Novel Monoallyated Compound

Further analysis by ^{1}H-NMR of isolated product obtained during the reaction of substrate **39a** with allyl bromide **41** by ^{1}H-NMR revealed a contaminated sample; however, some peaks could be assigned (**Figure 52a-b**), and it was deduced that monoalkenylation may have occurred, producing **64** (**Scheme 24**).

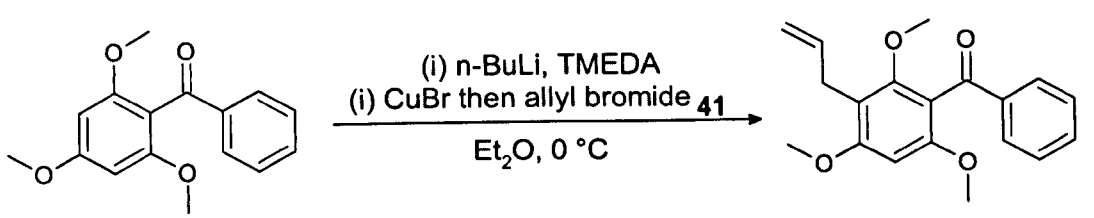

39a **64**

Scheme 24

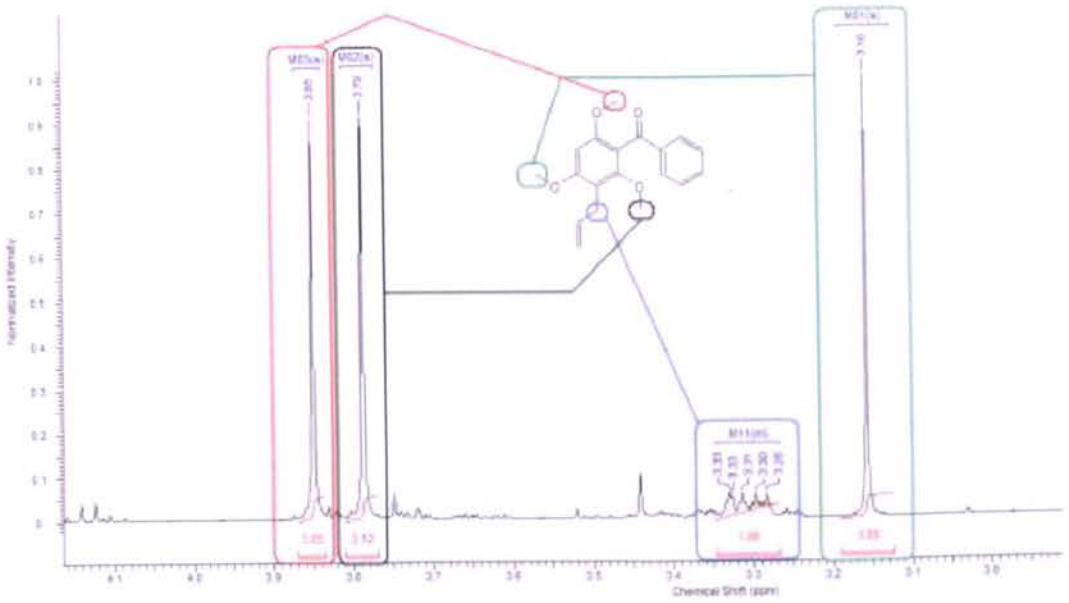

Figure 52a: *^{1}H-NMR upfield region of* **64** *showing the three distinct CH_3 environments of the non-equivalent methoxy groups (green, black and red boxes), and the CH_2 environment of the allyl side-chain (blue box).*

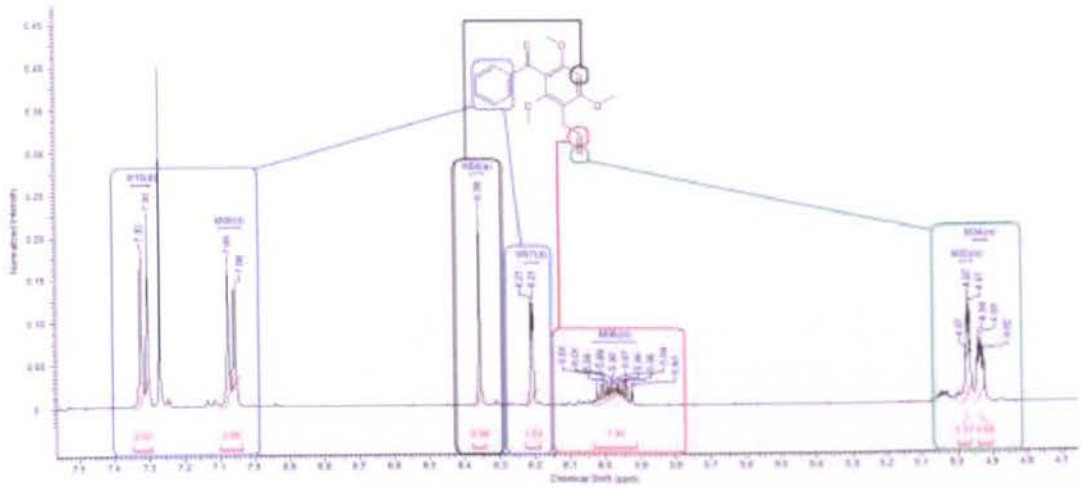

Figure 52b: *^{1}H-NMR dpwnfield region of* **64** *showing the terminal allylic CH_2 environment (green box), the allylic CH environment (red box), the phenyl ring CH environments (blue boxes) and the lone CH group of the trimethoxybenzene ring (black box).*

Our search of the literature revealed only one example[104] of a similar compound, prepared *via* a Claisen rearrangement of ether **65**, followed by methylation to give the alkenylated compound **66** (**Scheme 25**).

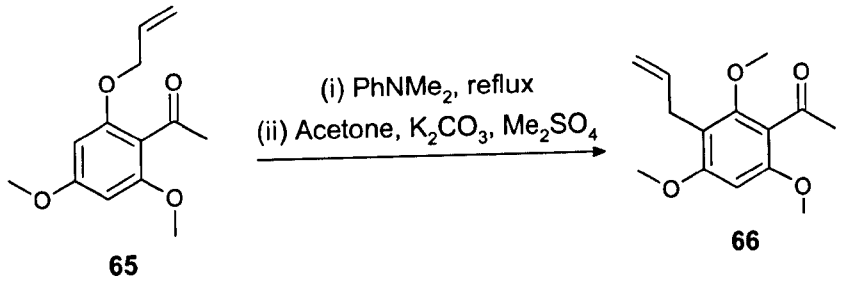

65 66

Scheme 25

Further repetitions of the reaction could not boost the yield or improve the purity of this curious product, hence no further insight into its structure and composition could be gained. We concluded that it was found that dialkenylation of **38a** could not be accomplished, and that since even monoalkenylation was proving unsuccessful by this method that we would cease our efforts towards a synthesis of derivatives of deoxyhumulone **11**.

Chapter Three:

Antibacterial Studies

Results and Discussion

3.1 Summary of Methodology

Given the known activity of naturally occurring lupulone **1** and natural congeners **1a-d** to inhibit antibacterial growth in Gram-positive bacteria, we set about investigating the antibacterial potential of some of our first-generation β-acids **1** and **1a-m**, and also assess the activity of the second generation β-acids **41a-g**, using a disc-diffusion assay. The British Society for Antimicrobial Chemotherapy (BSAC) publishes a frequently updated procedure[105] for a standardised assay which we followed in our investigations. In summary, we observed the following practices in our methodology:

- Bacteria were subcultured from a stock stored at -80 °C onto a nutrient-agar plate, incubated at 37 °C for 18 hours, then subcultured once more and incubated again at 37 °C for 18 hours before use in the assay.
- All suspensions of bacteria prepared prior to disc inoculation were suspended in Ringers solution and the turbidity matched to that of a 0.5 McFarland solution.
- All suspensions of bacteria were used to inoculate Meuller-Hinton agar plates for the disc diffusion experiment within 10 minutes of their creation
- The depth of each Meuller-Hinton agar used was 4-5 mm
- Each test was repeated in triplicate over successive days; at the end of each day, new subcultures of bacteria were prepared and incubated 37 °C for 18 hours before use in the next experiment.
- Each disc was 6 mm in diameter.

Each inoculated Meuller-Hinton agar plate had placed upon it four discs; two infused with 10 μL of compounds **1**, **1a-b** and **1e-g** taken from a 50 mM stock of each compound, a commercial antibiotic disc as a positive control and a blank disc as a negative control (**Figure 53**).

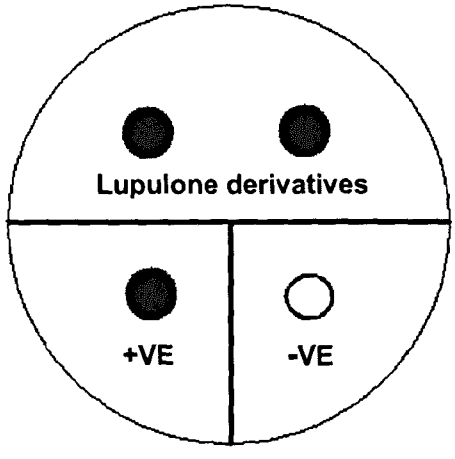

Figure 53: *Each inoculated agar plate had placed upon it two samples of lupulone derivative (top), a positive (+VE) control (commercially available antibiotic disc i.e. ciprofloxacin or vancomycin, bottom left) and a negative (-VE) control (blank disc, bottom right)*

We assessed the antibacterial potential of the compounds by measuring the diameter of the circular zone where no bacterial growth was observed to have taken place; this is the Zone of Inhibition (ZoI).

3.2 Initial Investigations

We began our investigations by seeking to confirm those observations reported in the literature i.e. that β-acids are effective as antibacterial agents only against Gram-positive species, and have no action against Gram-negative. For this, we used compounds **1**, **1a-b** and **1e-g**, and 5 bacterial strains:

- Gram-positive bacteria: *Bacillus subtilis* and *Staphylococcus epidermidis*
- Gram-negative bacteria: *Pseudomonas, Escherichia coli* and *Proteus*

The load-weight of each compound **1a-c** and **1e-g** per disc was calculated to allow for direct comparison with the positive controls used (**Table 9**).

Compound Number	Mass deposited per disc/ ug
1	207
1a	200
1b	192
1e	200
1f	189
1g	197

Table 9; *The positive control was either ciprofloxacin (5 ug) or vancomycin (5 ug). Vancomycin was only used in the experiments involving MRSA.*

In agreement with the literature, we observed no action against the Gram-negative bacteria, however good activity was observed against both Gram-positive bacteria (**Figure 54**).

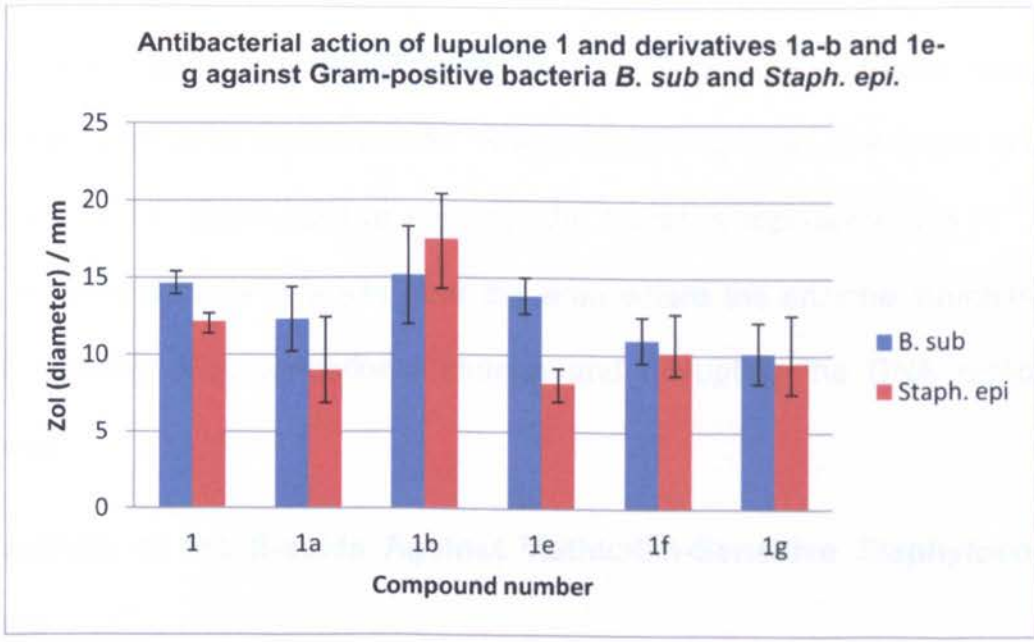

Figure 54: *Disc diffusion assay results of compounds 1a-1c and 1f-1h against Bacillus subtilis (blue) and Staphylococcus aureus (red) (n = 3).*

With these results, we confirmed to ourselves the action of lupulone derivatives against gram positive bacteria, and went on to assess their activity against five strains of methicillin-sensitive *Staphylococcus aureus* (MSSA 1-5). Our control for these experiments was a disc infused with 5 µg ciprofloxacin **67** (**Figure 55**), a commercially available fluoroquinolone antibacterial compound active against many bacterial species, and is recommended for the control of *Bacillus anthracis* infections contracted through inhalation which otherwise gives rise to the anthrax disease[106, 107].

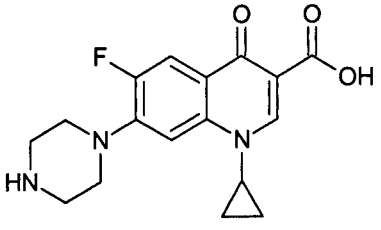

67

Figure 55

Fluoroquinolones such as **67** work by targeting topoisomerase enzymes responsible for DNA replication; for Gram-negative species, the target is DNA-gyrase, and for Gram-positive species, the target is topoisomerase IV[108, 109]. The compound binds to a site near the area where the enzyme interacts with DNA, causing a conformational change and disrupting the DNA replication process.

3.3 Activity of the β-acids Against Methicillin-Sensitive *Staphylococcus aureus*

We continued to observe antibacterial activity of β-acids against all five strains of MSSA (**Figure 56**).

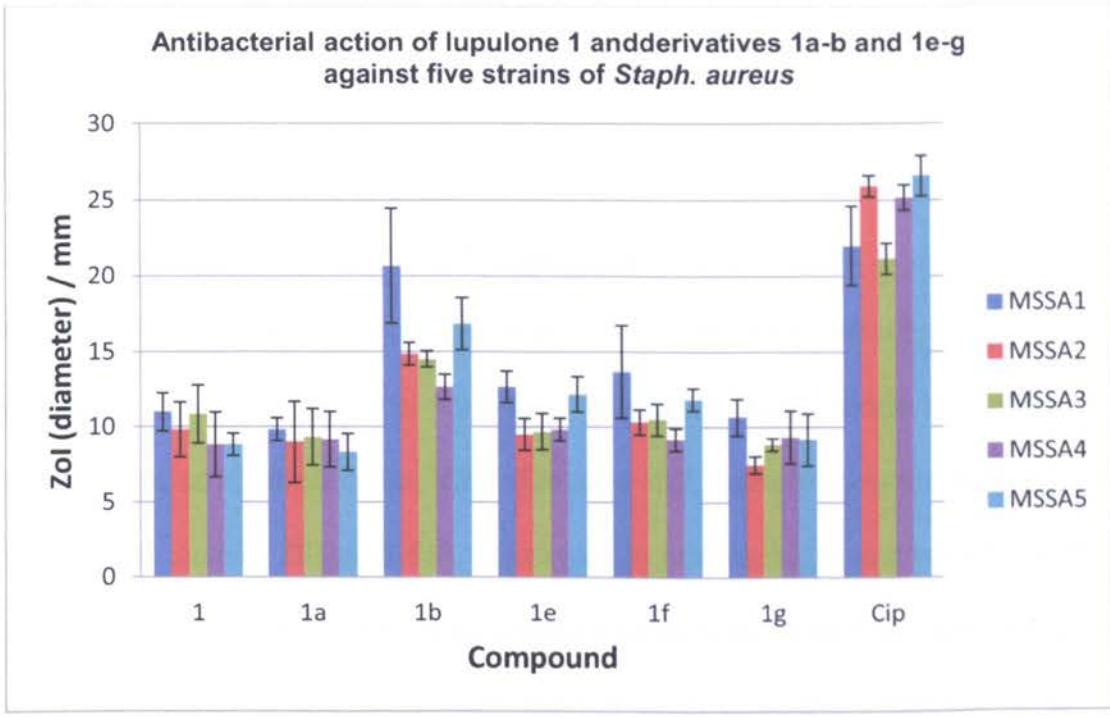

Figure 56: *Antibacterial activity of compounds* **1, 1a-b** *and* **1e-g** *against five strains of methicillin-sensitive Staphylococcus aureus. Ciprofloxacin (Cip) was the positive control (n = 3).*

It was observed that inoculated plates exposed to postlupulone **1b** consistently exhibited the largest zone of inhibition across all five MSSA strains, which was also observed where *B. sub* and *Staph. epi* where exposed to **1**, **1a-b** and **1e-g**. There is some reasoning behind this; postlupulone **1b** has a relatively small acyl side chain ($-CH_2CH_3$), reducing the steric hindrance as it traverses the bacterial wall. The reduced steric hindrance will also lower the energy of formation of a dimer or higher-order chelate around a metal atom, as it seeks to bind to metal ions and leave the bacteria cell. The CH_2CH_3 acyl side-chain may well have the correct lipophilic properties as it was observed that for compound **1f**, where the side-chain is a smaller methyl group ($-CH_3$), the zone of inhibition was statistically comparable to the bulkier compounds **1**, **1a**, **1e** and **1g** with respective acyl side chains of $CH_2CH(CH_3)_2$, $CH(CH_3)_2$, $CH_2CH_2CH_3$ and a cyclopropyl ring.

We also wished to also investigate the effects of a change in the allyl groups, from a prenyl ($CH_2CHC(CH_3)_2$) chain to an propenyl (CH_2CHCH_2) chain, i.e. our 2nd generation β-acids. Compounds **42a-f** were chosen as their acyl side-chains could allow comparisons with compounds **1**, **1a-b** and **1e-g**. We used MSSA strain 1 since the largest zones of inhibition were observed for this strain where compounds **1a-c** and **1f-h** were used. Moderate action was observed for compounds **42a**, **42c**, **42e** and **42f**, but compounds **42b** and **42d** showed little activity (**Figure 57**). This was an interesting result which is difficult to explain in terms of the structure-activity relationship, given the similarity of the structures overall – one would not predict such dramatic changes in activity between branched and straight-chain compounds, and it would seem that arguing the steric hindrance could be responsible is incorrect as **42d** (R = propyl) has a potentially less hindered side chain compared to **42e** (R = isopropyl).

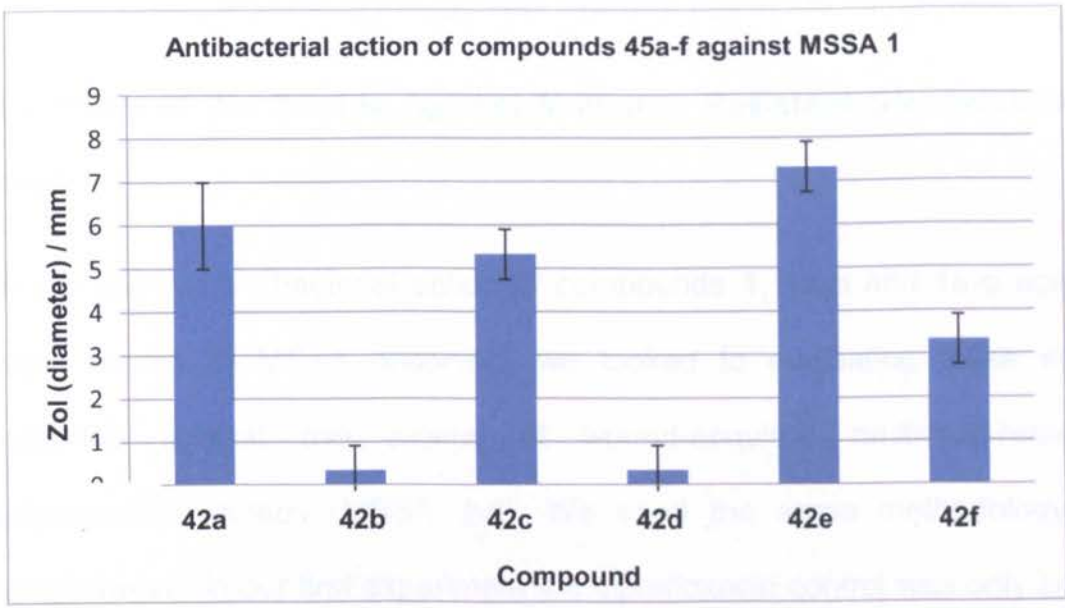

Figure 57: *Antibacterial activity of compounds* **42a-f** *against MSSA 1 (n = 3)*

The observed difference between compounds with matching acyl side-chains was found to be that the 1st generation β-acids (with a prenyl side-chain) performed better than the 2nd generation β-acids (with a propenyl sidechain) overall as antibacterial agents against MSSA; for example, compound **1** and compound **42a** have the same acyl side-chain (R = $CH_2CH(CH_3)_2$, but **1** was marginally better performing, a trend that was continually observed for other, matching derivatives. This is highly likely to be due to a reduction in the lipophilicity of the 2nd generation β-acids **42a-f** compared to the 1st generation compounds **1**, **1a-b** and **1e-g**. The reason for the assumed drop in lipophilicity is the absence of the dimethyl groups on allylic side chains, resulting in weaker Van der Waals interactions with the cell componentry. This is not a surprising result, since it has been previously reported[29, 30] that the increased potency of naturally occurring β-acids, when compared to humulones and iso-humulones, is due to the increase lipophilicity of the β-acids due to the presence of the third prenyl side chain, in place of the geminal hydroxyl unit of the humulones.

3.4 Activity of the β-acids Against Multidrug Resistant *Staphylococcus aureus*

With the positive antibacterial action of compounds **1**, **1a-b** and **1e-g** against multiple strains of MSSA observed, we looked to evaluating these same compounds against five strains of wound-acquired multidrug-resistant *Staphylococcus aureus* (MRSA 1-5). We used the same methodology as before, however in our first experiment the ciprofloxacin control was only active against one of the five MRSA strains, whereas compounds **1**, **1a-b** and **1e-g** exhibited inhibition of growth against all five MRSA strains (**Figure 58**). Fluoroquinolone resistance can be acquired by both MSSA and MRSA[110],

however there is precedence for its treatment against infections by these bacterial species[111] hence our initial decision to employ it as our positive control. In fluoroquinolone-resistant strains, the amino-acid sequence of the topoisomerase target enzyme are different. This means that those residues to which the fluoroquinolone would intereact with and bind to are not present, hence no binding and therefore no inhibition of the enzyme's function can occur[108, 109]. Some Gram-positive species of bacteria have been observed to incorporate membrane-bound pumps (efflux pumps) which can, at the expense of ATP, actively remove fluoroquinolones from the intracellular space[109]. In light of the observations made, we changed the positive control to 5 µg vancomycin, which we observed to be active against all five MRSA strains.

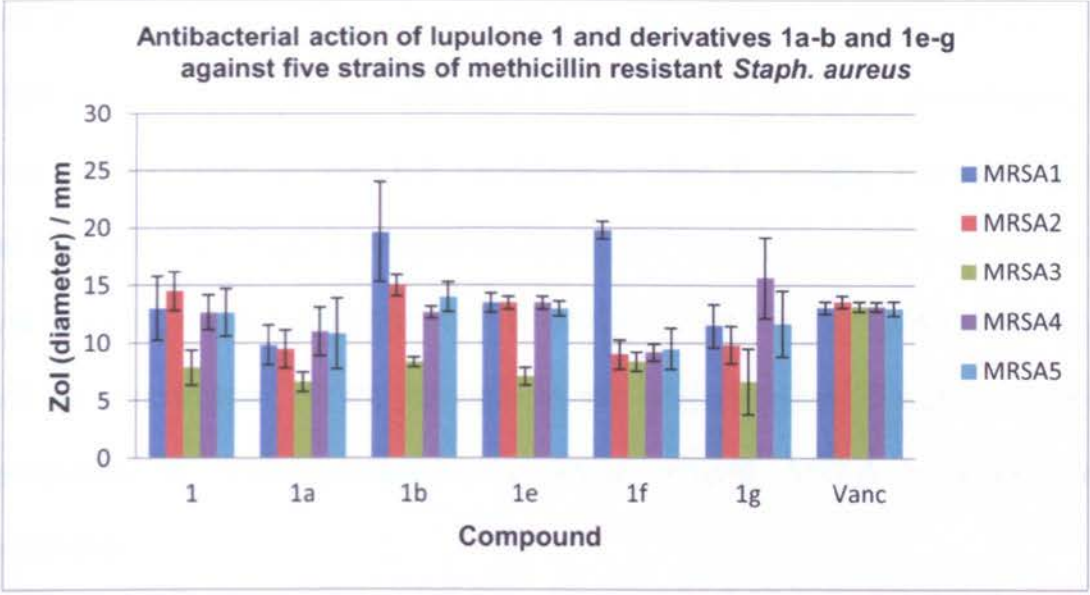

Figure 58: *Antibacterial activity of compounds* **1**, **1a-b** *and* **1e-g** *against five strains of multidrug-sensitive Staphylococcus aureus. Vancomycin (Vanc) was the positive control (n = 3).*

The observed difference in activity between each compound against MRSA is not as clear-cut as observed for MSSA, however for a given strain, postlupulone **1b** and synthetic derivative **1e** give rise to comparable zones of inhibition for MRSA strains 2-5, and for MRSA strain 1 postlupulone **1b** and synthetic

derivative **1f** have comparable activity. This observation suggests that depending on a particular MRSA strain, a given lupulone derivative may prove more effective over another.

The results obtained from the microbiological studies are encouraging on several levels. Firstly, it is seen that natural derivatives **1** and **1a-b** have comparable activity to synthetic derivatives **1e-g**, suggesting that the other synthetic derivatives **1h-m** would also possess antibacterial activity. Secondly, the observation of activity across five MRSA strains where the commercial antibiotic ciprofloxacin was only active against one suggests that β-acids have a potentially wider spectrum of activity, and that their mode of action may be one which *Stapholycoccus aureus* has not yet acquired wide-spread resistance towards. Furthermore, at the weight-loadings involved in this study, antibacterial action was similar to that of vancomycin, despite the lupulone discs having 40 times more compound than the vancomycin discs by weight. However, given that hop acids are regularly ingested during the consumption of beer, the toxic level is much, much higher than that encountered for regularly prescribed drugs such as vancomycin; on the strength of this attribute alone β-acids may lend themselves to chemotherapeutic practices where MRSA infections are concerned.

We had hoped to investigate and determine the minimum inhibitory concentrations (MIC's) of the lupulone derivatives; however their insolubility in aqueous systems thwarted plans to measure the growth inhibition using an appropriate assay. There is also the very real possibility that strains of MRSA that are sensitive to β-acids may quickly develop resistance, in much the same

way as observed for *Lactobacillus* species encountered in the beer brewing process[2, 32, 112].

Chapter Four:

Anticancer Studies

Results and Discussion

4.1 Anticancer Studies – Summary of Methodology

During our previous collaboration with the Colston group, based at St Georges Hospital[18], we observed that lupulone **1** gave rise to anti-proliferative action against the MDA-MB-231 breast cancer cell line. We now wished to continue this line of collaborative research by further investigating the anticancer properties of lupulone **1** and **1a-m** with a view to establishing if the synthetic modification of the acyl side-chain gave rise to any difference in activity. If this was found to be so, we wished to further establish the extent that changing the acyl group has on the anti-proliferative potential of these compounds. The results presented in this section were provided to the author by the Coulston group[113, 114], who carried out the anticancer testing independently at St Georges Hospital using the provided compounds synthesised by the author of this thesis.

For each assay, the total cell count (cell viability) was determined using an MTT assay; this is a colorimetric evaluation that quantifies the metabolic activity of a given population of cells and involves the mitrochondrial reduction of the tetrazolium salt (3-(4,5-dimethylthiazol-2-yl)-2,5-diphenyltetrazolium bromide (MTT **68**) by a mitrochondrial reductase enzyme to give the corresponding formazan **69** (**Scheme 25**).

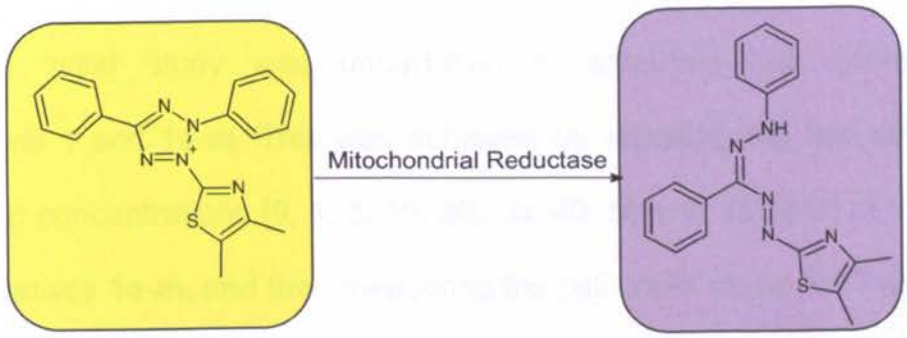

68 **69**

Scheme 25

Once reduction has taken place, the yellow colour of MTT **68** changes to the purple colour of **69**, and spectrometric analysis was conducted using a plate reader with a 550 nm wavelength light source. The intensity of this purple colour enabled a quantitative measurement of the living cells; comparison with a negative control (where no cytotoxic drug was present) thus enabled the percentage of living (viable) cells to be determined.

4.2 Breast Cancer Studies

4.2.1 Cyctoxicity against MCF-7 and MDA-MB-231 Cell Lines

The cell lines MCF-7 and MDA-MB-231 were used for the anticancer studies. MCF-7 cells are non-metastatic and estrogen-sensitive; they are considered to be representative of low-aggression breast cancer due to their poor invasive characteristics[113-115]. MDA-MB-231 cells are used as a model for high-aggression, non-hormone dependent breast cancer, and are characteristically invasive with the ability to metastasise[113, 114]. In selecting these cell lines, it was possible to compare and evaluate the activity of lupulone **1** and derivatives **1a-m** for their ability to inhibit cell proliferation where different cellular mechanisms exist. We could also investigate if the most active compound against one cell line was also the most active compound against the other cell line.

An initial study was undertaken to ascertain the cytotoxicity of compounds **1** and **1a-m**. This was achieved by exposing the two cell lines to increasing concentrations (0, 1, 5, 10, 20, 30, 40, 50 and 100 μM) of lupulone **1** and derivatives **1a-m**, and then measuring the cell count *via* an MTT assay after 48 hours and 72 hours. A representative curve of cell proliferation inhibition by lupulone **1** for both cell lines (**Figure 59a-b**) illustrates both time and

concentration dependent activity, observed for all derivatives; indeed, cell viability after 72 hours was less than that observed after 48 hours.

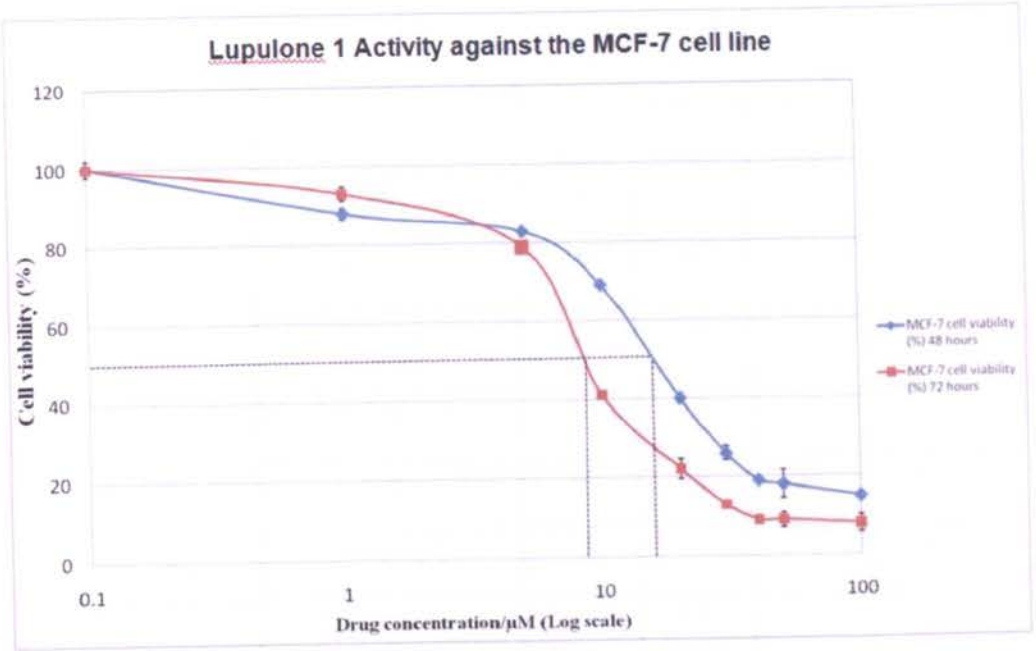

Figure 59a

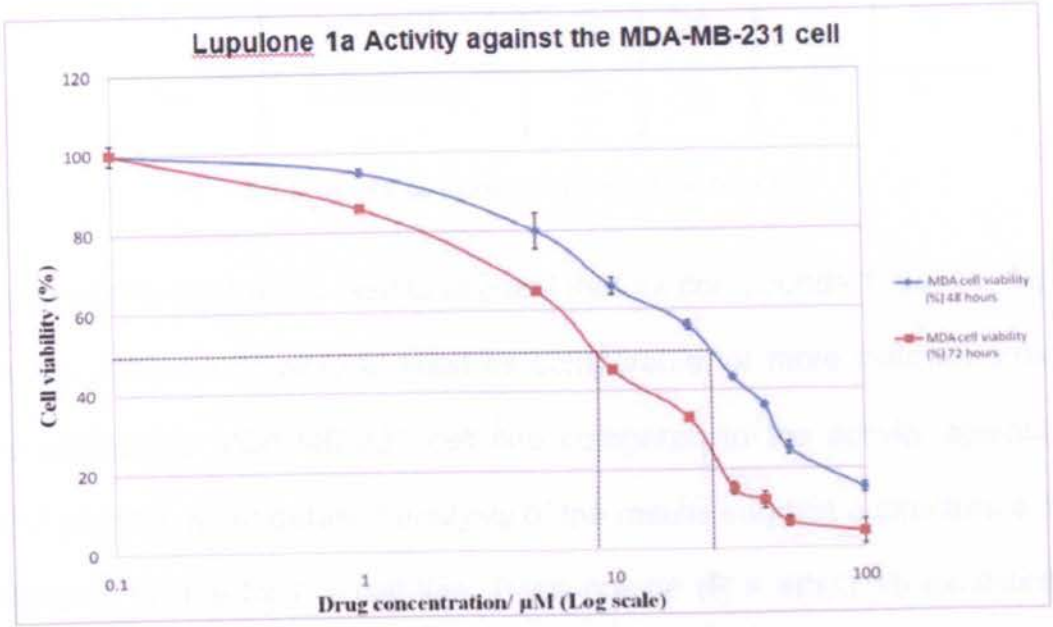

Figure 59b

The effects of change in the acyl side-chain produced some very interesting results when the IC_{50} (the concentration of compound required to kill 50% of the

total population of viable cells) of each compound was calculated from the respective curves of each compound against the given cell line (**Table 10**).

Compound	Acyl side chain	MCF-7 Cells IC_{50} / μM		MDA-MB-231 Cells IC_{50} / μM	
		48 hours	72 hours	48 hours	72 hours
1	$CH_2CH(CH_3)_2$	20	9.0	40	9.5
1a	$CH(CH_3)_2$	44	40	50	35
1b	CH_2CH_3	6.0	8.0	38	22
1e	$CH_2CH_2CH_3$	9.2	9.0	25	8.8
1f	CH_3	40	35	55	55
1g	cyclopropyl	20	10	10	4.5
1i	cyclopentyl	16	5.5	18	13
1j	cyclohexyl	22	17	18	9.5
1k	phenyl	21	18	25	8.5
1l	*p*-methoxyphenyl	36	36	15	10
1m	*p*-nitrophenyl	30	18	33	4.5

Table 10; *for all cytotoxicity experiments, n = 3*

Analysis of the cytotoxicity results suggest that for compounds **1**, **1a**, **1e**, **1g** and **1l-m**, the compounds were at least as comparable, or more toxic towards the more aggressive MDA-MB-231 cell line compared to the activity against the MCF-7 cell line. More detailed analysis of the results suggest a structure activity relationship for the MCF-7 cell line. Postlupulone (R = ethyl) **1b** exhibited the highest cytotoxicity after 48 hours with an IC_{50} of 6.0 μM, whereas the methyl derivative **1f** had a relatively high IC_{50} of 40 μM (**Figure 60**).

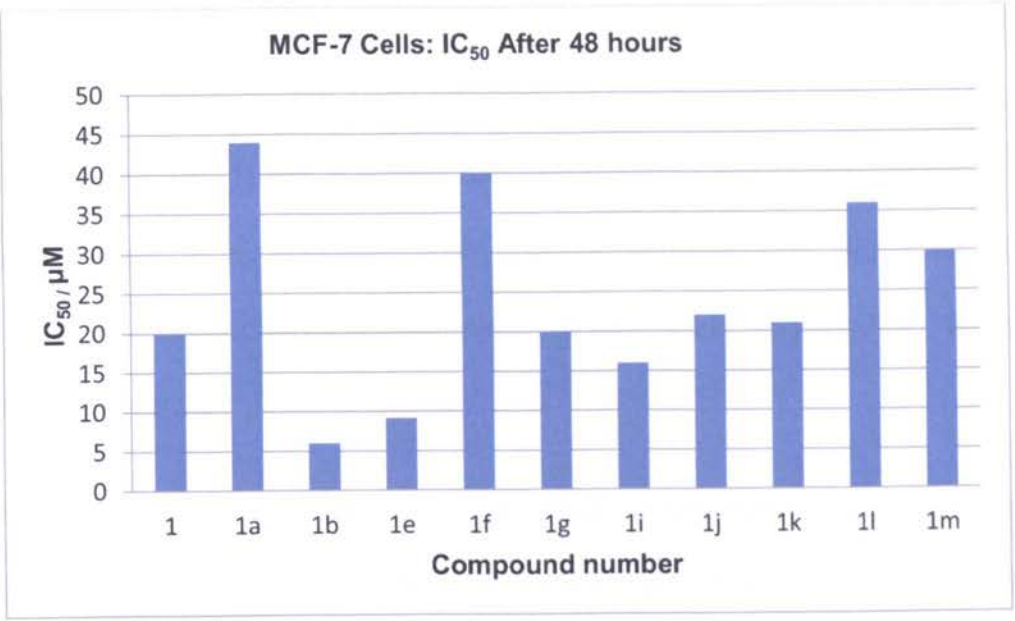

Figure 60

After 72 hours exposure, however, it was observed that the cyclopentyl derivative **1i** had the lowest IC_{50} of 5.5 µM. A similar activity was observed with **1**, **1b**, **1f** and **1i** where the IC_{50} values were all under 10 µM (**Figure 61**).

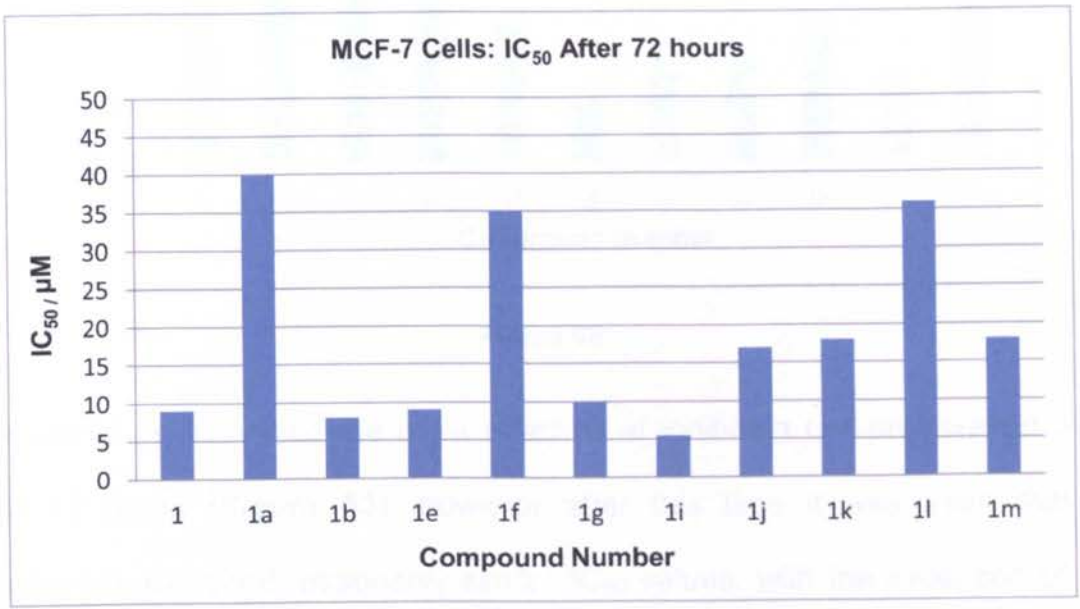

Figure 61

A further observation was made that while compounds **1e** and **1i** both have a similar carbon chain length (-$CH_2CH_2CH_3$ and cyclopentyl respectively, i.e. 3 carbon atoms long), **1i** has a significantly enhanced antiproliferative effect upon the MCF-7 cells. It is proposed, then, that an aliphatic ring allows for greater stability in the optimised conformation, which could explain the enhanced activity of **1i** over **1e**.

The MDA-MB-231 cell line results revealed a far more elaborate structure-activity relationship; it was observed that the most cytotoxic compound after 48 hours was the cyclopropyl derivative **1g** with an IC_{50} of 10 μM (**Figure 62**).

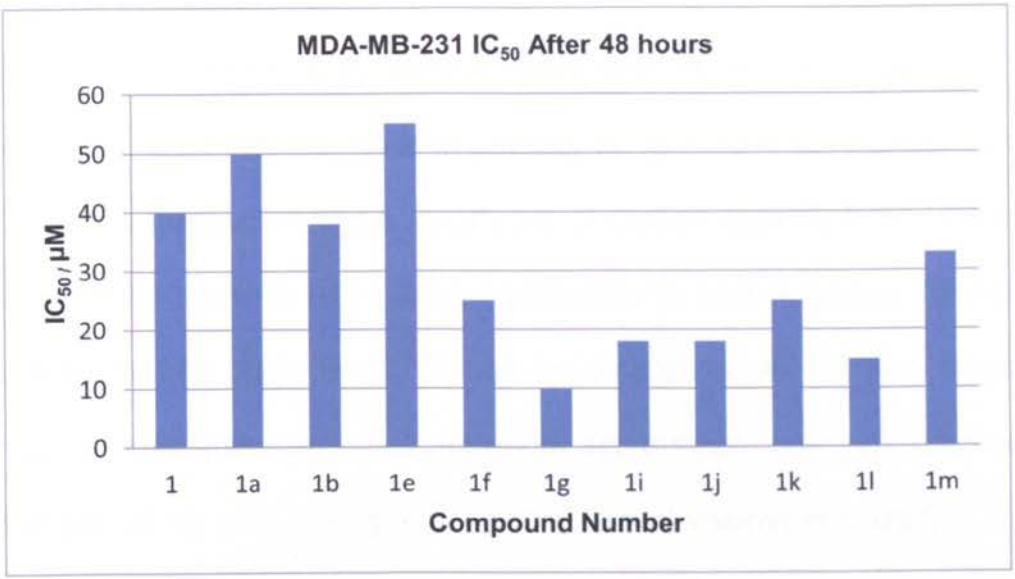

Figure 62

Compound **1g** remained the most effective at inhibiting cell proliferation even after 72 hours (**Figure 63**), however after this time it was seen that all compounds exhibited reasonably similar IC_{50} values, with the exception of **1a**, **1b** and **1e**.

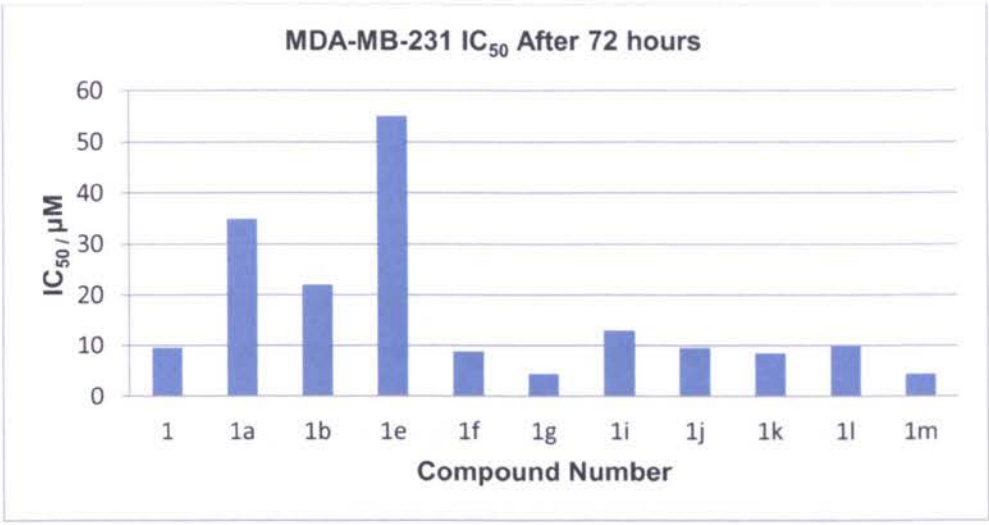

Figure 63

We found it interesting that **1g** (R = cyclopropyl) had consistent cytotoxic activity over time compared to the other analogues investigated. If one compares the activity of **1g** to its isomeric congeners colupulone **1a** (R = isopropyl) and **1e** (R = propyl), it is seen that the order of potency is **1g** > **1e** > **1a**. Further to this, if one considers the carbon chain length (i.e. 2 carbon atoms), then comparison between postlupulone **1b** ($-CH_2CH_3$), colupulone **1a** and derivative **1g** indicates that optimal carbon chain length cannot be considered as the sole reason for the much greater antiproliferative activity of **1g**. Instead, one may consider the "cone angle" of the acyl side group, i.e. the spatial volume occupied in a given environment. **1b** has increased activity over **1a**. Assuming the compounds interact with a binding site, then **1g** may be considered to form a more energetically favourable structure with the binding site in comparison to either of its isomeric analogues **1e** and **1a**. The isopropyl group has a carbon-carbon bond angle of approximately 109°, which is commonly encountered in sp^3-hybridised carbon bonding systems. However, despite being sp^3 hybridised, the carbon-carbon bond angle of cyclopropane is strained at 60° (**Figure 64**), which results in an overall reduced cone angle.

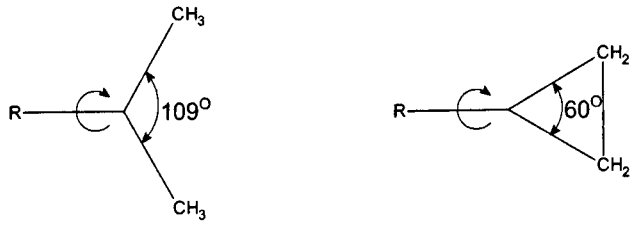

Figure 64: *Illustration of the "cone angle" as a function of the static bond angle for the isopropyl group (left) and the cyclopropyl group (right).*

Both groups can undergo rotation about the C(O)-CH bond; the volume of the space in which the group rotates is less for the cyclopropyl ring when compared with the isopropyl group, on account of the reduced cone angle. One can therefore interpret that more favourable Van der Waals interactions occur at the target as a result of this, resulting in the increased antiproliferative potential of the cyclopropyl group over its isomeric congeners.

4.2.2 Mechanistic Insights of the Action of β-acids against Breast Cancer Cell Lines

As well as investigating the cytotoxicity of lupulone **1** and derivatives **1a-1m**, we also wished to investigate the mechanism of cellular death. The scientific literature on this topic suggests that hop acids induce apoptosis[18, 54], which we sought to provide further supporting evidence by investigating the cleavage of PARP (poly(ADP-ribose)polymerase) by **1a**, **1b**, **1g** and **1i**. The detection of PARP is used as a marker for cellular death, and the relative concentration of cleaved PARP enzymes compared to an actin control can be used to quantify the extent of cellular death for a given population of cells[116] (i.e. the PARP:actin ratio). For both cell lines (MCF-7 and MDA-MB-231), it was shown that after 24 hours there was some cleavage by the more active compounds, but after 48

hours all 4 compounds caused cleavage of PARP. This is indicative of an apoptotic pathway to cellular death being activated.

In the individual cell-line cases, it was observed that for MCF-7 cells, both compound **1g** and **1i** gave strong PARP:actin ratios after western blotting experiments after 24 hours, where **1i** had the higher PARP:actin ratio, indicating increased apoptotic activity. After 48 hours, **1i** remained correlated with the highest amount of PARP cleavage, whilst **1a** and **1b** had increased activity to match that of the cyclopropyl derivative **1g** (**Figure 65**).

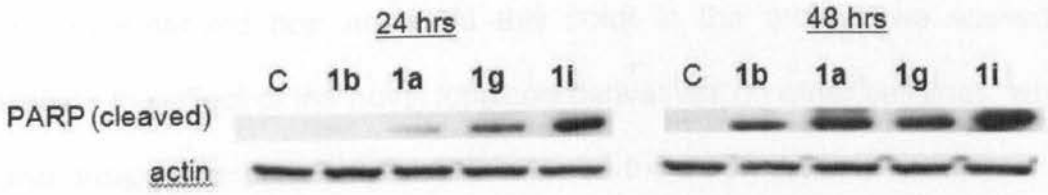

Figure 65: *MCF-7 Western blot results. PARP (cleaved):actin ratios for cells after 24 and 48 hours incubation with compounds **1a**, **1b**, **1g** and **1i**. 'C' is a negative control.*

In the case of the MDA-MB-231 cell line, it was observed that a similar trend followed to the MCF-7 cells, in that after 24 hours two compounds exhibited PARP cleavage, although in this case compounds **1a** and **1g** were the most potent which also agrees with the observed IC_{50} values for these compounds after the same amount of time. After 48 hours, **1g** gave rise to increased PARP cleavage, and while **1a** appeared to not have caused any increase, compound **1b** did have a dramatic increase, ending up with a greater correlation to PARP cleavage than **1a**. Furthermore, **1i** gave rise to PARP cleavage after 48 hours as well (**Figure 66**).

Figure 66: *MDA-MB-231 Western blot results. PARP (cleaved):actin ratios for cells after 24 and 48 hours incubation with compounds **1a**, **1b**, **1g** and **1i**. 'C' is a negative control.*

The evidence gained demonstrating PARP cleavage is suggestive of the involvement and activation of the caspase pathway to apoptosis, since caspase-3 is known to be involved in PARP cleavage[57]. Furthermore, we have provided further evidence that a caspase pathway is undergoing activation by the lupulone-derived hop acids. At this point in the project, we wished to investigate the effect of the novel lupulone derivatives on other cell lines, where we also designed experiments to further probe the mechanism of action.

4.3 Prostate Cancer Studies

4.3.1 Cyctoxicity against PC3 and DU145 Cell Lines

We investigated the antiproliferative potential of all 13 synthesised lupulone **1** and derivatives **1a-m** against the prostate cancer cell lines PC3 and DU145, again using an MT assay to quantify the cellular population. Both cell lines were exposed to a given compound for 72 hours exhibiting concentration-dependent activity (**Table 11**), as previously observed for the breast cancer cell lines.

Compound Number	R =	PC3 IC_{50} / μM	DU145 IC_{50} / μM
1	$CH_2CH(CH_3)_2$	8.8	8.7
1a	$CH(CH_3)_2$	8.0	5.8
1b	CH_2CH_3	32	33
1c	$CH_2CH_2CH(CH_3)_2$	50	50
1e	$CH_2CH_2CH_3$	7.0	10
1f	CH_3	41	33
1g	cyclopropyl	40	30
1h	cyclobutyl	50	50
1i	cyclopentyl	3.5	4.5
1j	cyclohexyl	3.1	2.7
1k	phenyl	35	18
1l	*p*-methoxyphenyl	38	38
1m	*p*-nitrophenyl	20	18

Table 11 (*n = 3)*

For the both cell lines, it was observed that compounds **1**, **1a**, **1e**, **1i** and **1j** were very active (IC_{50} < 10 μM) (**Figure 67a** and **Figure 67b**), in the order **1j** > **1i** > **1a** > **1a** > **1e**; again, much as was observed with the breast cancer cell lines, the aliphatic, cyclic, non-naturally occurring compounds were found to be most effective. Several structure-activity relationships were identified that provided explanation for the observed results.

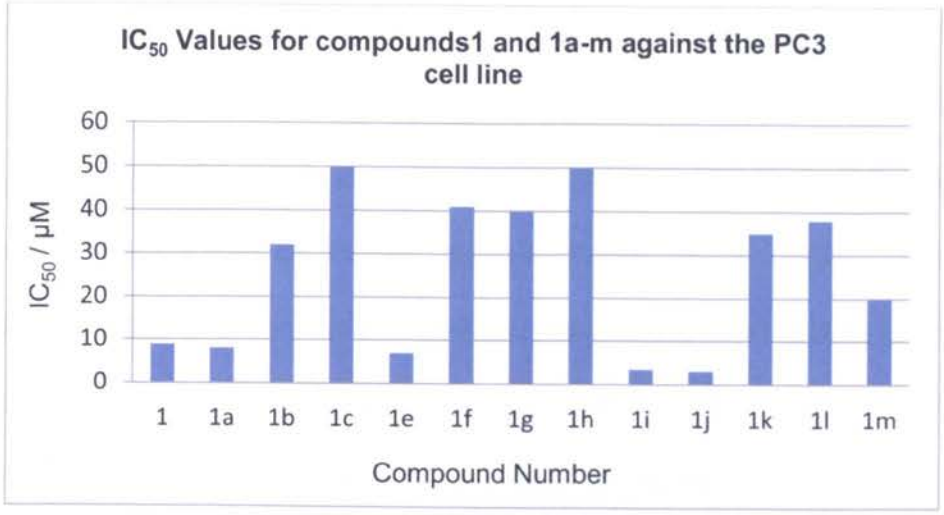

Figure 67a

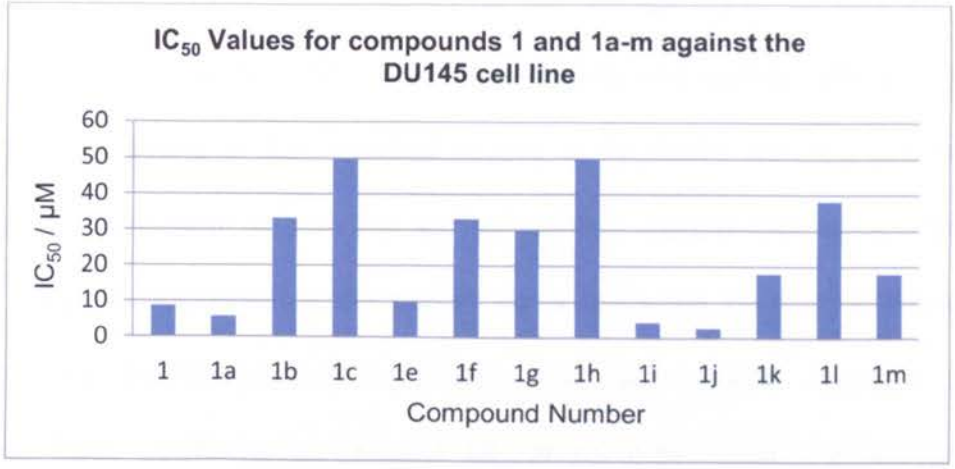

Figure 67b

The evidence that **1**, **1a** and **1e** had strong activity whilst **1b** and **1f** did not suggests that for straight-chain and branched-chain derivatives, there is an optimal chain length i.e. isopropyl > $CH_2CH(CH_3)_2$ > $CH_2CH_2CH_3$ >> CH_2CH_3 / CH_3. The presence of a branched methyl group also appears to enhance the activity, indicative of greater inter-molecular bonding (e.g. hydrophobic Van der Waals) forces between the compound and the active site of the cell target entity, as the volume of that active site is filled more efficiently by a bulkier group. This theory is supported when one considers the relative activity of the

aliphatic cyclic derivatives **1g–1j**; **1g** (R = cyclopropyl) and **1h** (R = cyclobutyl) perform relatively poorly compared to **1i** (R = cyclopentyl) and **1j** (R = cyclohexyl). The cyclopropyl and cyclobutyl group occupy less physical space than the cyclopentyl and cyclohexyl groups, therefore the strength of bonding interactions within a given target pocket are weaker for those smaller ring systems, since they are further away from the active-site binding moieties and thus the strength of the hydrophobic interaction is reduced.

It was also observed that when comparing the most potent cyclohexyl derivative **1j** against the phenyl derivative **1k**, the activity of **1k** was an order of magnitude lower, despite both rings being formed of 6 carbon atoms. There are two possible reasons for the reduced activity of **1k**; firstly, the ring is confined to a planar conformation due to the sp^2-hybridized carbon atoms, and therefore cannot adopt a puckered conformation as is favoured by the cyclohexyl ring, formed of sp^3-hybridized carbon atoms. The cyclohexane ring can adopt a "chair" or "boat" conformation (**Figure 68**), which may result in a stronger inter-molecular bond as the ring and portions of the active site are in closer proximity to each other.

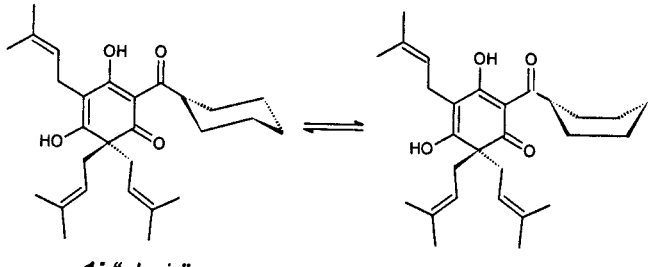

1j "chair" *1j "boat"*

Figure 68

It is not possible to say, however, which conformation is favoured at the active site; while the "chair" conformation is typically the lowest energy conformation

(due to minimal steric interference), it may be the "boat" conformation results in the lowest overall system energy when the compound is bound to the target active site. This reasoning can also explain the similarly high activity of the cyclopentyl derivative **1i**, which can also adopt a puckered conformation (**Figure 69**).

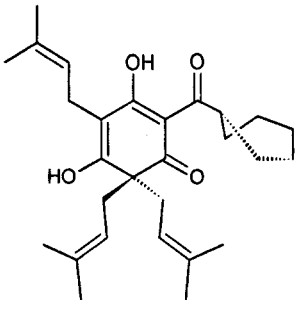

Figure 69: *1j "puckered" structure*

The second possible reason for the phenyl derivative having relatively low activity may be the lack of π-bonding partners at the active site to enable π–stacking between a site-bound phenyl group and the phenyl group of **1k**.

Further to the relative activities of the aliphatic derivatives **1** and **1-j**, it was seen that for phenyl derivatives **1k-m**, the presence of an activating methoxy (-OMe) group at the para-position on the phenyl ring lowered the activity against both PC3 and DU145 cells. Further to this, in the case of the PC3 cell line, the presence of a deactivating nitro ($-NO_2$) group on the para position of the phenyl ring increased the activity of the compound. As well as observing steric effects, we also have evidence to suggest electronic effects play a role in determining the potential of a lupulone derivative to inhibit cell proliferation and promote cell death; an electron-rich ring has decreased activity, whilst an electron poor-ring can have increased activity.

4.3.2 Mechanistic Insights of the action of β-acids against Prostate Cancer Cell Lines

Further to our previous studies into the mode of action of cell death induced by compounds **1** and **1a-m**, we wished to probe further and confirm that apoptosis does indeed occur, and by which pathway apoptosis is being induced. Continuing this investigation with the prostate cancer cell lines PC3 and DU145, we investigated the apoptotic induction using 10 μM solutions of lupulone **1**, colupulone **1a** and the cyclohexyl derivative **1j**, chosen since it exhibited the lowest IC_{50} value against both cell lines. The initial experiment confirmed apoptosis in PC3 and DU145 cells by measurement of PARP cleavage, mirroring the results of the previous experiments with breast cancer cell lines (**Figure 70**)

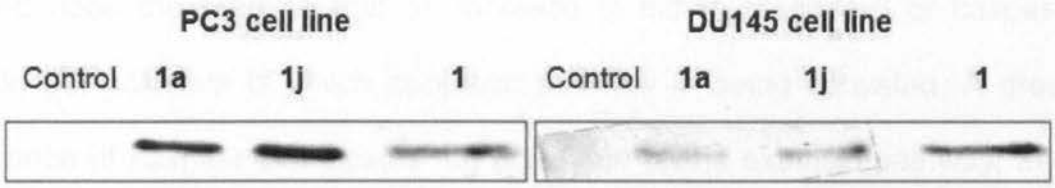

Figure 70: *PARP cleavage induced by compounds **1**, **1a** and **1j** against prostate cancer cell lines PC3 and DU145. The control was* 10 μM *DMSO.*

We sought further indication of apoptosis by measuring the concentration of nucleosomes in the cytoplasm. Nucleosomes are associasted with genetic (DNA) material in the cell nucleus, and an increased concentration of nucleosomes in the cyctoplasm indicates the induction of the apoptotic process as the cell dies. For cells exposed to compounds **1, 1a** and **1j**, an increase in cytoplasmic nucleosomes was observed (**Figure 71**), indicating the induction of apoptosis.

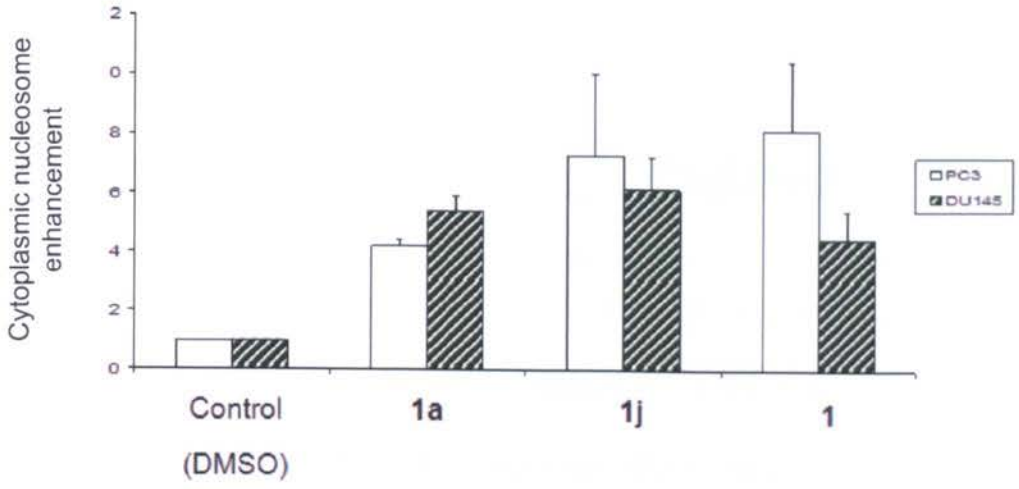

Figure 71; *(n = 3)*

These experiments confirmed that apoptosis was occurring and so we focused on measuring the concentration of cleaved caspases -3, -8 and -9. This was based upon the premise that an increase in either caspase-8 or caspase-9 would be indicative of which apoptotic pathway is being activated. A greater presence of caspase-8 indicates the activation of the extrinsic pathway, and a greater presence of caspase-9 would indicate the activation of the intrinsic pathway. Analysis by Western blotting showed a relatively greater presence of caspase-8 over caspase-9 (**Figure 72**) for all cells exposed to compounds **1**, **1a** and **1j**.

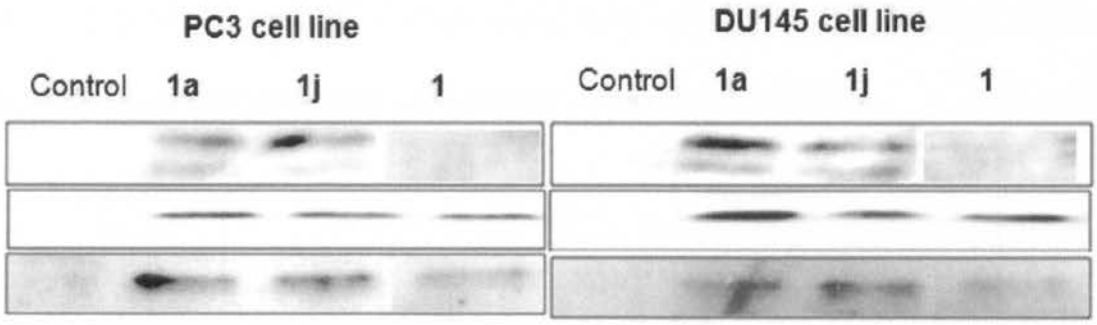

Figure 72: *Western blot analysis of caspase-3 (top), caspase-8 (middle) and caspase-9 (bottom) after treatment of PC3 and DU145 cell lines with compounds **1**, **1a** and **1j**.*

The activation of caspase-3 was also detected for cells exposed to **1a** and **1j**, however as observed for the PARP-cleavage band, cells exposed to **1** did not exhibit a band for caspase-3. This does not imply that lupulone **1** doesn't induce apoptosis, as the evidence previously presented (**Figure 71**) shows indicators of apoptosis when the cells are exposed to compound **1**. Overall, the results here suggested to us that as caspase-8 was in greater abundance, the extrinsic apoptotic pathway was being activated. In order to confirm this, an experiment was designed in which each cell line would be exposed to compound **1** and **1j**, plus one of three caspase inhibitors - Z-VAD, Z-IETD and Z-LEHD. Z-VAD inhibits the action of all caspases, whilst Z-IETD inhibits the action of caspase-8 and Z-LEHD inhibits the action of caspase-9. Our group has had previous experience[18] of introducing Z-VAD into the experimental procedure, showing that SK-MES lung cancer cells exposed to lupulone and Z-VAD together ceases apoptosis, whereas exposure to lupulone alone resulted in reduced cell viability; we were confident we would observe the same trend with both PC3 and DU145 prostate cancer cell lines.

Exposure to both cell lines to either compound **1** or **1j** confirmed the increased presence of nucleosomes in the cytoplasm, and as hypothesised,

introducing Z-VAD into the system along with either **1** or **1j** drastically reduced the cytoplasmic concentration of nucleosomes (**Figure 73**).

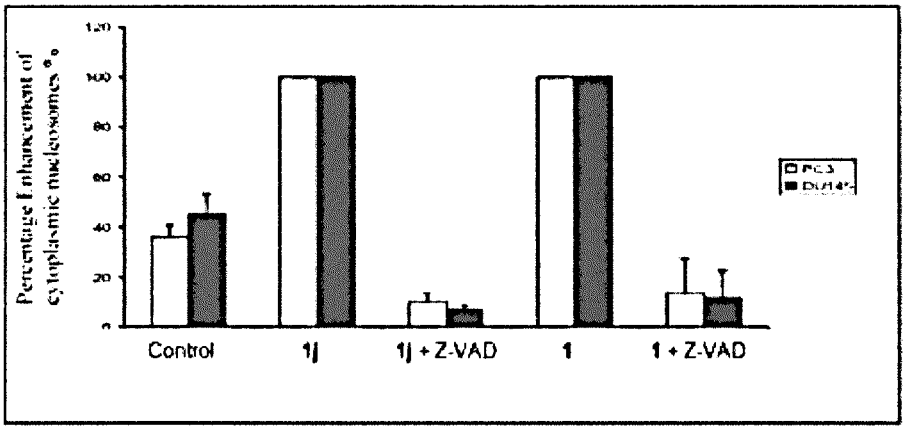

Figure 73: *PC3 and DU145 cells exposed to **1**, **1**+ Z-VAD, **1j**, **1j**+Z-VAD and the control (DMSO).*

When the cells were exposed to either **1** + Z-IETD or **1j** + Z-IETD, a reduction in the concentration of nucleosomes in the cytoplasm was still observed (**Figure 74**), although to a lesser extent than where Z-VAD was present.

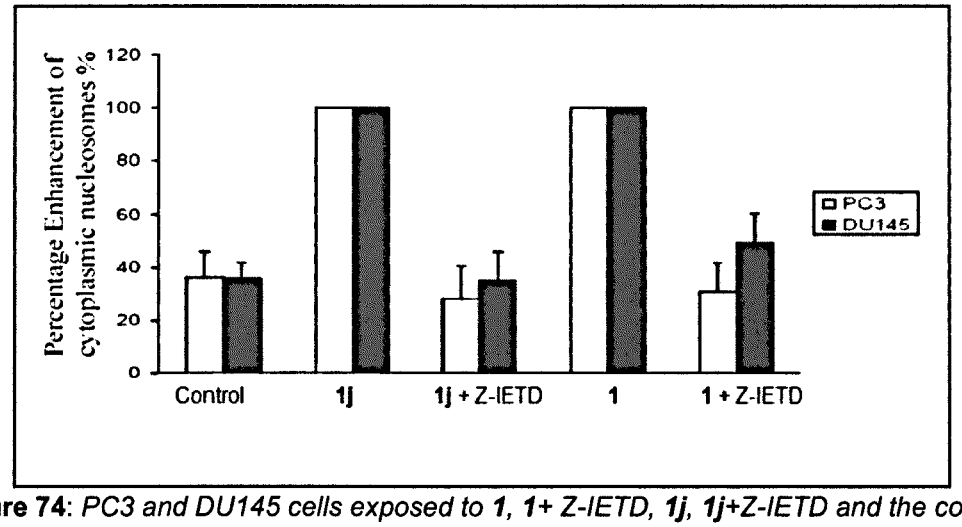

Figure 74: *PC3 and DU145 cells exposed to **1**, **1**+ Z-IETD, **1j**, **1j**+Z-IETD and the control (DMSO).*

In contrast, where the cells were exposed to **1a** + Z-LEHD or **1k** + Z-LEHD, the reduction in cytoplasmic nucleosomes was not ultimately significant compared to the experiments involving either compound alone (**Figure 75**).

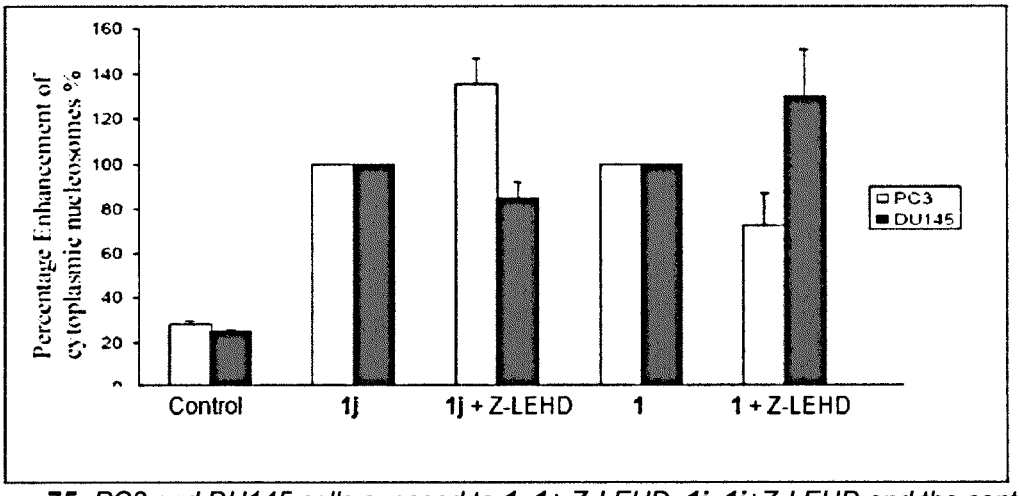

Figure 75: *PC3 and DU145 cells exposed to **1**, **1**+ Z-LEHD, **1j**, **1j**+Z-LEHD and the control (DMSO).*

These results provided us with strong evidence that lupulone-derived compounds **1** and **1a-m** activate the extrinsic apoptotic pathway, a result that has far-reaching implications in the future research direction of the anticancer action of hop-acid derived compounds. The evidence presented here further adds to that published by Lamy *et al*[58], and also shows that the mechanism of action is consistent across different cell types.

At this point, we did not have the time to further explore the mechanism, and so we are left with further questions - we could not ascertain the exact cellular target; the compounds may enter the cell, cause an effect which then causes external changes triggering the extrinsic apoptotic pathway. Conversely, the compounds may be interacting with cellular componentry on the cell wall surface or within the cell wall. It is desirable to explore this in future work, which may require the synthesis of labelled compounds, either radioisotope-labelled, or with a fluorescent moiety. In any case, at this time in the research project we had completed one of our main research aims; to evaluate the effects of lupulone derivatives on cancer cells, and to investigate the mechanism of action.

Chapter Five:

Conclusions and Future Work

In this research, the main aims were to synthesise individual, naturally and non-naturally occurring hop acids and assess the anticancer and antibacterial potential. Our aim was to extend the chemistry of these compounds which resulted in the synthesis of two novel spirocyclic compounds **50** and **50a**. Due to time constraints, these were not screened for their biological activity but there is scope to improve our methodology in order to optimise the yields. We have also developed one potential reaction that could be useful in a future synthesis of deoxyhumulones **11**, which could then be used to generate humulone **2** and novel derivatives not just of humulone but of hop bitter acids in general.

Although it has not been discussed in this thesis, we envisaged synthesis and use of weinreb amide **70** (**Scheme 26**) from 2,4,6-trimethoxybenzoic acid **71** and *N*,*O*-dimethylhydroxylamine hydrochloride **72**, applying the use of the coupling reagent COMU **73** which has been shown to allow the facile synthesis of amides[117].

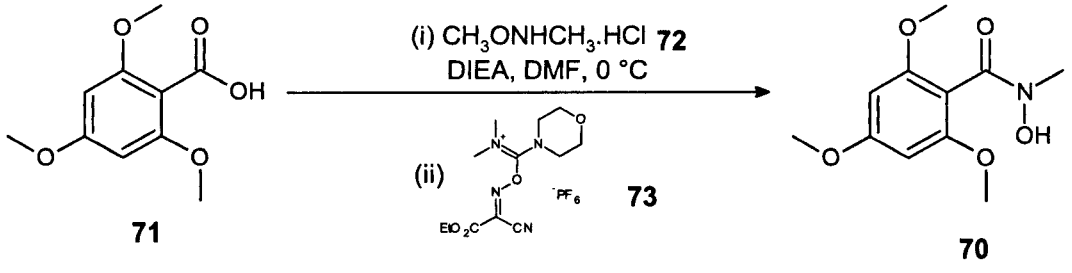

Scheme 26

The rationale for this synthesis is that the $N(CH_3)(OH)$ moiety may be readily displaced by an organometallic species[118, 119] and phosphonium salts[120], thus allowing for the syntheses of more complex side-groups at the acyl site, including fluorescent tags and radiolabelled compounds for in-depth biological studies.

We have demonstrated that the β-acids have multipotent biological activity; against bacteria, we have shown that they are effective against Gram-positive species, including MRSA. Further to this, we have demonstrated that against MRSA, these compounds have a potentially broader spectrum of activity than the commercially available antibiotic ciprofloxacin **60** and could be a viable alternative. However, we have not established the mechanism of antibacterial action, and so future studies in this area would need to first establish if the β-acids are bactericidal (kill bacteria) or bacteriostatic (halt the growth of bacteria but do not actively kill it), followed by investigations into the mechanism by which the compounds work against MRSA.

Against cancer cell lines, we have demonstrated activity against breast cancer and prostate cancer. For the breast cancer cell lines used, we observed greater anticancer activity against the MDA-MB-231 cell line, representative of an aggressive breast cancer. We also observed that the most active compound was the non-natural derivative **1g** featuring a cyclopropyl acyl group, which we explained in terms of the optimal occupation of space in the as-yet unknown cellular target compared with its isomeric congeners **1a** and **1e**. For the prostate cancer cell lines, we observed that the most active compound was the cyclohexyl derivative **1j,** again a non-natural β-acid. Comparison of its activity compared with the other β-acids lead us to conclude that in the cellular target, the resulting conformation of the cyclohexyl group was key to its enhanced activity. Furthermore, we observed similar activity by the cyclopentyl derivative **1i**, which we explained in similar terms.

The prostate cancer studies also allowed us to investigate the mechanism by which cell death was occurring; we knew from the breast cancer studies that activation of apoptosis was likely. We confirmed this was true again against the prostate cancer cell lines, and we also found evidence to suggest the activation of the extrinsic apoptotic pathway. Future work in this area should concentrate on discovering the cellular target of the β-acids, as this has not yet been elucidated and remains a gap in scientific knowledge.

Chapter Six:

Experimental

6.1 Chemical Synthesis

6.1.1 Reagents, Solvents and Reaction Conditions

All chemicals were purchased form Sigma Aldrich chemical company, and used as purchased unless otherwise stated. All reaction solvents were anhydrous, either purchased from Sigma Aldrich chemical company or dried as required. All reactions were performed under a dry nitrogen atmosphere, and all glassware used was either dried for 48 hours in a vacuum oven at 120 $^{\circ}$C or flame-dried under high vacuum prior to use. Bench grade solvents used for the work-up procedures and column chromatography were purchased from Fisher chemical company. Foil-backed silica gel thin layer chromatography (TLC) plates were purchased from Sigma Aldrich chemical company. Powdered silica gel for column chromatography was purchased from Fisher chemical company.

6.1.2 Analytical Equipment Used

Melting points were obtained using a Stuart Scientific SMP3 melting point apparatus. ^{1}H and ^{13}C NMR spectra were recorded using a Bruker AvanceIII 400 two channel FT-NMR spectrometer equipped with a 5 mm PABBO BB-1H/D Z-GRD probehead. The nominal frequency is 400 MHz for ^{1}H and 100 MHz for ^{13}C, and the collected raw data was processed using ACD/labs NMR processing software. The reference used was the residual non-deuterated solvent peak. Infra-red spectra were recorded using a Nicolet iS5 FT-IR spectrometer with an iD5 ATR accessory, with OMNIC Version 8.2 control and processing software. Mass spectra were recorded using an Agilient Technologies Gas Chromatography Mass Spectrometry instrument consisting of a 6890N Network GC system and a 5973 Network Mass Selective Detector.

Data was processed using Agilent Technologies Enhanced Chemstation software. High-resolution mass spectrometry was performed by the EPSRC National Mass Spectrometry Service Centre, based at Swansea University.

6.1.3 Friedel-Crafts Acylation of Phloroglucinol

The general reaction scheme is as follows:

The synthesis of 1-(2,4,6-trihydroxyphenyl)ethanone **(3a)**

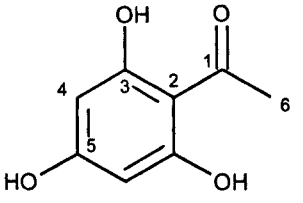

To a 2-necked round bottom flask fitted with a reflux condenser were added phloroglucinol **32** (2.08 g, 16.5 mmol, 1 eq) and aluminium chloride (3.37 g, 25.3 mmol, 1.5 eq) in DCM (20 ml) and stirred. Nitromethane (1.4 ml, 26.1 mmol, 1.5eq) was added dropwise *via* syringe to produce a homogenous solution. Acetyl chloride (1.2 ml, 16.5 mmol, 1eq) was added *via* syringe and the reaction mixture stirred for 15 minutes at 35 °C. The reaction mixture was then poured onto ice, and the crude product extracted with diethyl ether (3 x 50 ml). The combined organic layers were then washed successively with 10% HCl solution (2 x 50 ml), water (2 x 50 ml), brine (2 x 50 ml), and then dried over anhydrous sodium sulphate. The mixture was filtered and the solvent was removed *in vacuo* to give a solid which was recrystallised from water, yielding

yellow crystals (2.51 g, 9.65 mmol, 53%). Mpt = 217.4–218.6 °C (lit.[71] = 218 °C) ν_{max} (neat)/cm^{-1} = 3528 (O-H), 3113 (Ar-H), 2923 (C-H), 2853, 1629 (C=O), 1532 (C=C), 1281 (C-O), 1167, 1065, 1021, 962, 829; δ_H (400 MHz, CD_3OD) = 2.59 (s, 3H, C*H*$_3$ **6**), 5.79 (s, 2H, Ar-*H* **4**); δ_C (100 MHz, CD_3OD) = 32.9 (CH_3 **6**), 95.7 (CH **4**), 105.7 (C **5**), 166.1 (C **3**), 166.5 (C **2**), 204.7 (C **1**); *m/z*: = 168 (M^+), 153, 139, 124, 111, 84, 69.

The synthesis of 1-(2,4,6-trihydroxyphenyl)propan-1-one **(3b)**

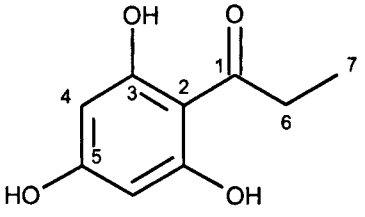

This was carried out as detailed for the synthesis of 1-(2,4,6-trihydroxyphenyl)ethanone **3a**, with the following reagents and quantities:

- Phloroglucinol **32** (6.44 g, 51 mmol, 1 eq)
- Aluminium chloride (13.7 g, 102 mmol, 2 eq)
- DCM (50 ml)
- Nitromethane (5.5 ml, 102 mmol, 2 eq)
- Propionyl chloride (4.5 ml, 51.8 mmol, 1 eq)

The title compound **3b** was obtained as a white powder (4.79 g, 26.3 mmol, 51%). Mpt = 173.8-174.6 °C (Lit.[71] = 174 °C); ν_{max} (neat)/cm^{-1} = 3341 (O-H), 2923 (C-H), 2853, 1629 (C=O), 1517 (C=C), 1222 (C-O), 1075, 1011; δ_H (400 MHz, CD_3OD) = 1.12 (t, *J* = 7.30 Hz, 3H, C*H*$_3$ **7**), 3.05 (q, *J* = 7.30 Hz, 2H, C*H*$_2$ **6**), 5.80 (s, 2H, Ar-*H* **4**); δ_C (100 MHz, CD_3OD) = 9.22 (CH_3 **7**), 38.0 (CH_2 **6**), 95.7 (CH **4**), 105.3 (C **5**), 165.9 (C **3**), 166.0 (C **2**), 207.9 (C **1**); *m/z*: = 182

(M^+), 153, 111, 77, 69, 55. *Accurate Mass* ($[M+H]^+$, calculated for $[C_9H_{11}O_4]^+$ = 183.0648): Found 183.0652.

The synthesis of 1-(2,4,6-trihydroxyphenyl)butan-1-one **(3c)**

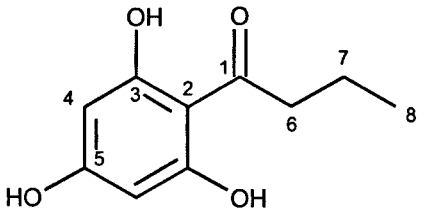

This was carried out as detailed for the synthesis of 1-(2,4,6-trihydroxyphenyl)ethanone **3a**, with the following reagents and quantities:

- Phloroglucinol **32** (4.24 g, 33.6 mmol, 1 eq)
- Aluminium chloride (8.95 g, 67.1 mmol, 2 eq)
- DCM (30 ml)
- Nitromethane (3.6 ml, 67.1 mmol, 2 eq)
- Butyryl chloride (3.5 ml, 33.4 mmol, 1 eq)

The title compound **3c** was obtained as a light yellow powder (2.05 g, 10.4 mmol, 54%). Mpt = 191.6–193.0 °C (Lit.[71] = 141 °C). ν_{max} (neat)/cm^{-1} = 3511 (O-H), 3187 (Ar-H), 2924 (C-H), 2853, 1640 (C=O), 1515 (C=C), 1291, 1207 (C-O); δ_H (400 MHz, CD_3OD) = 0.96 (t, *J* = 7.41, 3H, CH_3 **8**), 1.67 (sext, *J* = 7.40, 2H, CH_2 **7**), 3.00 (t, *J* = 7.37, 2H, CH_2 **6**), 5.80 (s, 2H, Ar-H **4**); δ_C (100 MHz, CD_3OD) = 14.5 (CH_3 **8**), 19.6 (CH_2 **7**), 46.9 (CH_2 **6**), 95.8 (CH **4**), 105.5 (C-OH **5**), 166.0 (C-OH **3**), 166.1 (C **2**), 207.4 (C **1**); *m/z*: = 196 (M^+); 181, 168, 153, 139, 126, 55. *Accurate Mass* ($[M+H]^+$, calculated for $[C_{10}H_{13}O_4]^+$ = 197.0808): Found 197.0809.

The synthesis of 2-methyl-1-(2,4,6-trihydroxyphenyl)propan-1-one **(3d)**

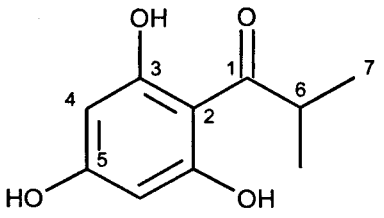

This was carried out as detailed for the synthesis of 1-(2,4,6-trihydroxyphenyl)ethanone **3a**, with the following reagents and quantities:

- Phloroglucinol **32** (2.36 g, 18.7 mmol, 1 eq)
- Aluminium chloride (4.97 g, 37.3 mmol, 2 eq)
- DCM (30 ml)
- Nitromethane (2.0 ml, 37.3 mmol, 2 eq)
- Isobutyryl chloride (2.0 ml, 19.1 mmol, 1 eq)

The title compound **3d** was obtained as a white crystalline solid (1.69 g, 8.60 mmol, 46%). Mpt = 140.7-141.4 °C (Lit.[71] = 141 °C); ν_{max} (neat)/cm^{-1} = 3498 (O-H), 3269 (Ar-H), 2992 (C-H), 2937, 1626 (C=O), 1525 (C=C), 1299, 1224 (C-O), 973, 816; δ_H (400 MHz, CD_3OD) = 1.13 (t, *J* = 6.78, 6H, CH_3 **7**), 4.00 (sept, *J* = 6.78, 1H, CH **6**), 5.80 (s, 2H, Ar-H **4**); δ_C (100 MHz, CD_3OD) = 19.7 (CH_3 **7**), 40.0 (CH **6**); 95.9 (CH **4**), 104.6 (C-OH **5**), 165.9 (C-OH **3**), 165.8 (C **2**), 211.3 (C **1**); *m/z*: = 196 (M^+), 179, 163, 153, 139, 124, 111, 96, 69, 55. *Accurate Mass* ($[M+H]^+$, calculated for $[C_{10}H_{13}O_4]^+$ = 197.0808): Found 197.0807.

The synthesis of 3-methyl-1-(2,4,6-trihydroxyphenyl)butan-1-one **(3e)**

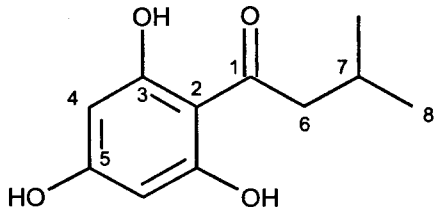

This was carried out as detailed for the synthesis of 1-(2,4,6-trihydroxyphenyl)ethanone **3a**, with the following reagents and quantities:

- Phloroglucinol **32** (3.29 g, 26.1 mmol, 1eq)
- Aluminium chloride (7.00 g, 52.5 mmol, 2 eq)
- DCM (30 ml)
- Nitromethane (2.9 ml, 54.0 mmol, 2 eq)
- Isovaleryl chloride (3.2 ml, 26.2 mmol, 1 eq)

The title compound **3e** was obtained as a light yellow powder (4.08 g, 19.4 mmol, 74%). Mpt = 145.5 – 146.9 °C (Lit.[71] = 145 °C); ν_{max} (neat)/cm^{-1} = 3515 (O-H), 3276 (Ar-H), 2923 (C-H), 2853, 1604 (C=O), 1517 (C=C), 1203 (C-O), 1159; δ_H (400 MHz, CD_3OD) = 0.97 (d, *J* = 6.50, 6H, $(CH_3)_2$ **8**), 2.22 (dt, *J* = 13.49, 6.68, 1H, C*H* **7**), 2.92 (d, *J* = 7.03, 2H, CH_2 **6**), 5.83 (s, 2H, CH **4**); δ_C (100 MHz, CD_3OD) = 23.2 (CH_3 **8**), 26.8 (CH **7**), 53.7 CH_2 **6**); 95.8 (CH **4**), 105.7 (C-OH **5**), 165.9 (C-OH **3**), 166.0 (C **2**), 207.1 (C=O **1**); *m/z*: = 210 (M^+), 195, 153, 126, 69, 55.

The synthesis of 4-methyl-1-(2,4,6-trihydroxyphenyl)pentan-1-one **(3f)**

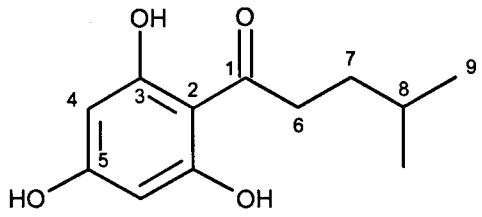

4-methylvaleryl chloride was prepared by the following method; a 2-necked round bottom flask (100 ml) was charged with 4-methylvaleric acid (1.85 g, 15.9 mmol, 1eq) and DCM (10 ml). With cooling in an ice bath, oxalyl chloride (1.4 ml, 16.0 mmol, 1 eq) was added dropwise, followed by DMF (1 drop). After the initial effervescence had ceased, the reaction mixture was stirred at room temperature for 1 hour. This was then used in the Friedel-Crafts acylation following the procedure for the synthesis of **3a**, with the following quantities of reagents and materials:

- Phloroglucinol **32** (2.03 g, 16.0 mmol, 1 eq)
- Aluminium chloride (4.18 g, 31.3 mmol, 2 eq)
- DCM (20 ml)
- Nitromethane (1.7 ml, 31.7 mmol, 2 eq)

The title compound **3f** was obtained as a white powder (2.00 g, 8.90 mmol, 56%). Mpt = 157.2-158.6 °C; ν_{max} (neat)/cm^{-1} = 3270 (broad O-H), 2953, 2869 (C-H), 1637 (C=O), 1595, 1518 (C=C), 1274 (C-O), 1189, 1069, 986, 931; δ_H (400 MHz, CD_3OD) = 0.93 (d, *J* = 6.40 Hz, 6H, $(CH_3)_2$ **9**), 1.49-1.56 (m, 2H, CH_2 **8**), 1.57-1.65 (1H, C*H* **7**), 2.96-3.08 (m, 2H, CH_2 **6**), 5.80 (s, 2H, CH **4**); δ_C (100 MHz, CD_3OD) = 23.0 (CH_3 **9**), 29.4 (CH **8**), 35.5 (CH_2 **7**), 43.0 (CH_2 **6**), 95.8 (CH **4**), 105.4 (C-OH **5**), 165.9 (C-OH **3**), 166.1 (C **2**), 207.9 (C=O **1**); *m/z*: = 224

(M^+), 204, 181, 168, 153, 135, 111, 97, 83, 69, 55; *Accurate Mass* (calculated for $[C_{12}H_{16}O_4]^+$ = 224.1043): Found 224.1044.

The synthesis of Cyclopentyl(2,4,6-trihydroxyphenyl)methanone **(3g)**

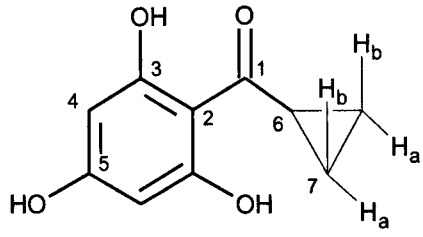

This was carried out as detailed for the synthesis of 1-(2,4,6-trihydroxyphenyl)ethanone **3a**, with the following reagents and quantities:

- Phloroglucinol **32** (2.09 g, 16.6 mmol, 1 eq)
- Aluminium chloride (4.40 g, 32.9 mmol, 2 eq)
- DCM (30 ml)
- Nitromethane (1.8 ml, 33.5 mmol, 2 eq)
- Cyclopropanecarbonyl chloride (1.5 ml, 16.3 mmol, 1 eq)

The title compound **3g** was obtained as a white powder (2.13 g, 11.0 mmol, 66 %). Mpt = 226.8 – 228.1 °C. ν_{max} (neat)/cm^{-1} = 3364 (O-H), 3244 (Ar-H), 2923 (C-H), 2853, 1607 (C=O), 1569 (C=C), 1256 (C-O), 1184, 1110; δ_H (400 MHz, CD_3OD) = 0.92-1.05 (m, 2H, **7** $\mathbf{H_A}$), 1.07-1.22 (m, 2H, **7** $\mathbf{H_B}$), 3.46 (tt, *J* = 7.97, 4.71, 1H, C*H* **6**), 5.85 (s, 2H, Ar-H **4**); δ_C (100 MHz, CD_3OD) = 12.4 (CH_2 **7**), 20.9 (CH **6**), 95.1 (CH **4**), 106.1 (C **5**), 165.5 (C **3**), 165.7 (C **2**), 206.5 (C **1**); *m/z*: = 194 (M^+), 179, 166, 153, 137, 124, 69. *Accurate Mass* (calculated for $[C_{10}H_{10}O_4]^+$ = 194.0574): Found 194.0573.

The synthesis of Cyclobutyl(2,4,6-trihydroxyphenyl)methanone **(3h)**

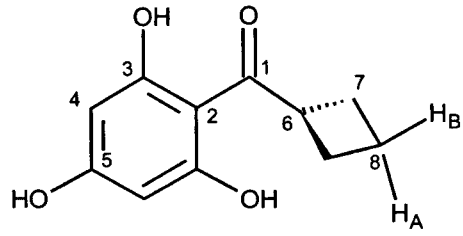

This was carried out as detailed for the synthesis of 1-(2,4,6-trihydroxyphenyl)ethanone **3a**, with the following reagents and quantities:

- Phloroglucinol **32** (3.12 g, 24.7 mmol, 1 eq)
- Aluminium chloride (6.61 g, 49.6 mmol, 2 eq)
- DCM (30 ml)
- Nitromethane (2.7 ml, 50.3 mmol, 2 eq)
- Cyclobutanecarbonyl chloride (2.8 ml, 24.5 mmol, 1 eq)

The title compound **3h** was obtained as a white powder (2.38 g, 11.5 mmol, 46%). Mpt = 166.4–167.9 °C. ν_{max} (neat)/cm^{-1} = 3375 (O-H), 3267 (Ar-H), 2982 (C-H), 2848, 1629 (C=O), 1603, 1524 (C=C), 1250 (C-O), 1171, 1095, 830; δ_H (400 MHz, CD_3OD) = 1.83 (td, *J* = 9.41, 4.52, 1H, CH **8** $\mathbf{H_A}$), 1.91–2.06 (m, 1H, CH **8** $\mathbf{H_B}$), 2.20–2.40 (m, 4H, CH_2 **7**), 4.26 (quin, *J* = 8.34, 1H **6**), 5.81 (s, 2H, CH **4**); δ_C (100 MHz, CD_3OD) = 18.5 (CH_2 **8**), 25.8 (CH_2 **7**), 47.4 (CH **6**), 95.7 (CH **4**), 105.3 (C **5**), 165.8 (C **3**), 166.7 (C **2**), 207.4 (C **1**), *m/z*: = 208 (M^+), 191, 179, 153, 137, 124, 69, 55; *Accurate Mass* (calculated for $[C_{11}H_{12}O_4]^+$ = 208.0730): Found 208.0732.

The synthesis of Cyclopentyl(2,4,6-trihydroxyphenyl)methanone **(3i)**

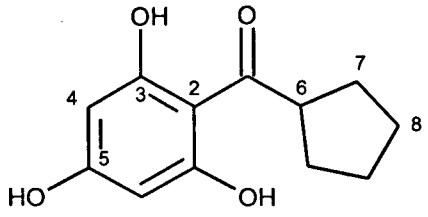

This was carried out as detailed for the synthesis of 1-(2,4,6-trihydroxyphenyl)ethanone **3a**, with the following reagents and quantities:

- Phloroglucinol **32** (5.19 g, 41.2 mmol, 1 eq)
- Aluminium chloride (11.0 g, 82.3 mmol, 2 eq)
- DCM (30 ml)
- Nitromethane (4.4 ml, 82.0 mmol, 2 eq)
- Cyclopentanecarbonyl chloride (5 ml, 41.1 mmol, 1 eq)

The title compound **3i** was obtained as a white powder (5.58 g, 25.1 mmol, 61%). Mpt = 98.9–99.7 °C; ν_{max} (neat)/cm^{-1} = 3471 (O-H), 3249 (Ar-H), 2923 (C-H), 2853, 1607 (C=O), 1579 (C=C), 1298, 1221 (C-O), 1169, 1075. δ_H (400 MHz, CD_3OD) = 1.57–1.75 (m, 4H, C*H*$_2$ **8**), 1.68–1.85 (m, 4H, C*H*$_2$ **7**), 4.11-4.20 (m, 1H, C*H* **6**), 5.80 (s, 2H, Ar-*H* **4**); δ_C (100 MHz, CD_3OD) = 27.2 (CH_2 **8**), 31.1 (CH_2 **7**), 51.5 (CH **6**), 95.9 (CH **4**), 105.2 (C **5**), 165.8 (C **3**), 165.9 (C **2**), 210.2 (**1**); *m/z*: = 222 (M^+); 207, 176, 153, 124, 97, 69. *Accurate Mass* (calculated for $[C_{12}H_{14}O_4]^+$ = 222.1046): Found 222.1049.

The synthesis of Cyclohexyl(2,4,6-trihydroxyphenyl)methanone **(3j)**

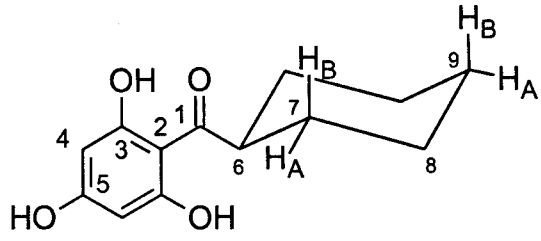

This was carried out as detailed for the synthesis of 1-(2,4,6-trihydroxyphenyl)ethanone **3a**, with the following reagents and quantities:

- Phloroglucinol **32** (1.90 g, 15.1 mmol, 1 eq)
- Aluminium chloride (4.02 g, 30.1 mmol, 2 eq)
- DCM (30 ml)
- Nitromethane (1.6 ml, 29.8 mmol, 2 eq)
- Cyclohexanecarbonyl chloride (2.0 ml, 14.7 mmol, 1 eq)

The title compound **3i** was obtained as a light yellow powder (1.26 g, 5.31 mmol, 36%). Mpt = 101.2 - 103.1 $^{\circ}$C; ν_{max} (neat)/cm^{-1} = 3270 (Broad O-H), 2923, 2851 (C-H), 1627 (C=O), 1594, 1557 (C=C), 1249, 1209 (C-O), 1155, 1134, 1072, 971; δ_H (400 MHz, CD_3OD) = 1.18-1.31 (m, 1H, CH_A **9**), 1.31-1.47 (CH, 4H, CH_2 **8**), 1.71 (d, *J* = 12.3 Hz, 1H, CH_B **9**), 1.75-1.84 (m, 2H, CH_A **7**), 1.85-1.97 (m, 2H, CH_B **7**), 3.62-3.76 (m, 1H, CH **6**), 5.80 (s, 2H, CH **4**); δ_C (100 MHz, CD_3OD) = 27.3 (CH_2 **9**), 27.4 (CH_2 **8**), 30.7 (CH_2 **7**), 50.6 (CH **6**), 95.9 (CH **4**), 104.8 (C **5**), 165.8 (C **3**), 165.9 (C **2**), 210.7 (**1**); *m/z*: = 236 (M^+), 191, 181, 153, 147, 135, 121, 97, 81, 69, 55. *Accurate Mass* (calculated for $[C_{13}H_{16}O_4]^+$ = 236.1043): Found 236.1042.

The synthesis of phenyl(2,4,6-trihydroxyphenyl)methanone **(3k)**

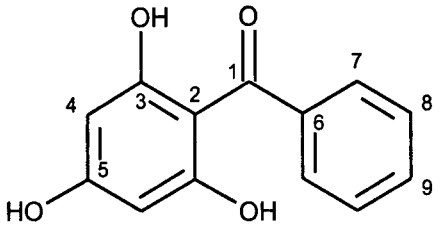

Aluminium chloride (1.49 g, 11.2 mmol, 1.5eq) and DCM (20 ml) where placed in a round-bottomed flask (100 ml) and cooled in an ice-bath. Nitromethane (0.75 ml, 14.0 mmol, 2eq) was added *via* syringe, followed by benzoyl chloride (0.85 ml, 7.32 mmol, 1eq), and stirred for 15 minutes at 0 °C then allowed to warm to room temperature over 45 minutes. The formed aluminium chloride-benzoyl chloride complex was then transferred dropwise *via* syringe to a 2-necked round bottomed flask (100 ml), equipped with a nitrogen inlet and rubber septum, containing phloroglucinol **32** (0.927 g, 7.35 mmol, 1 eq) and DCM (20 ml). The reaction mixture was stirred for 18 hours before pouring onto ice. The product was extracted into diethyl ether (3 x 50 ml). The combined organic layers were then washed successively with 10% HCl solution (2 x 50 ml), water (2 x 50 ml), brine (2 x 50 ml), and then dried over anhydrous sodium sulphate. The mixture was filtered and the solvent was removed *in vacuo* to give a solid which was purified by flash chromatography (45% ethyl acetate : 55% 40-60 petroleum ether). Removal of the solvent *in vacuo* followed by recrystallisation from water yielded yellow needles (0.422 g, 1.84 mmol, 25 %). Mpt = 163.6-164.2 °C (Lit.[71] = 164 °C); ν_{max} (neat)/cm^{-1} = 3567 (O-H), 3295 (Ar-H), 2923 (C-H), 2853, 1642 (C=O), 1604, 1298 (C-O), 1174, 1070. *m/z*: = 230 (M^+), 229, 153, 105, 77, 69, 51; δ_H (400 MHz, CD_3OD) = 5.85 (s, 2H, Ar-*H* **4**), 7.35-7.39 (m, 2H, Ar-*H* **8**), 7.44-7.47 (m, 1H, Ar-*H* **9**), 7.57 (d, *J* = 7.41, 2H, Ar-*H*

8); δ_C (100 MHz, CD_3OD) = 94.5 (Ar CH **4**), 104.5 (C **5**), 127.3 (Ar CH **9**), 128.0 (Ar CH **8**), 130.8 (Ar CH **7**), 141.6 (C **3**), 162.5 (C **6**), 164.6 (C **2**), 199.3 (C **1**); *Accurate Mass* (Negative ion mode, calculated for $[C_{13}H_{10}O_4]^+$ =230.0574): Found 230.0571.

The synthesis of (4-methoxyphenyl)(2,4,6-trihydroxyphenyl)methanone **(3l)**

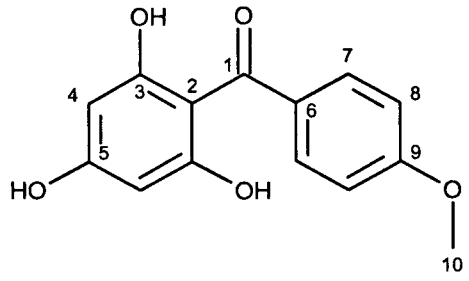

This was carried out as detailed for the synthesis of phenyl(2,4,6-trihydroxyphenyl)methanone **3k**, with the following reagents and quantities:

- 4-methoxybenzoyl chloride (3.5 ml, 25.4 mmol, 1 eq)
- Aluminium chloride (6.82 g, 51.1 mmol, 2 eq)
- Nitromethane (2.8 ml, 52.2 mmol, 2 eq)
- Phloroglucinol **32** (3.27 g, 25.9 mmol, 1 eq)

The crude product was purified by flash column chromatography (45% ethyl acetate : 55% 40-60 petroleum ether). Removal of the solvent *in vacuo* isolated the title compound **3l** as a yellow powder (3.35 g, 12.9 mmol, 50%). Mpt = 172.1 - 174.3 °C. ν_{max} (neat)/cm^{-1} = 3578 (O-H), 3295 (Ar-H), 2923 (C-H), 2853, 1642 (C=O), 1604, 1298 (C-O), 1174, 1070; δ_H (400 MHz, CD_3OD) = 3.87 (s, 3H, CH_3 **10**), 5.90 (s, 2H, CH **4**), 6.95 (d, *J* = 9.0 Hz 2H, Ar-*H* **8**), 7.68 (d, *J* = 9.0 Hz, 2H, Ar-*H* **7**); δ_C (100 MHz, CD_3OD) = 54.5 (CH_3 **10**), 94.4 (CH **4**), 105.1 (C-OH **5**), 112.6 (CH **8**), 131.0 (CH **7**), 133.2 (C **9**), 161.1 (C **6**), 162.9 (C **3**), 163.4 (C

2), 197.6 (C **1**); *m/z*: = 260 (M^+), 245, 229, 217, 207, 152, 135, 124, 108, 92, 77, 69, 51; *Accurate Mass* (Negative ion mode, calculated for $[C_{14}H_{11}O_5]^-$ = 259.0612): Found 259.0606.

The synthesis of (4-nitrophenyl)(2,4,6-trihydroxyphenyl)methanone **(3m)**

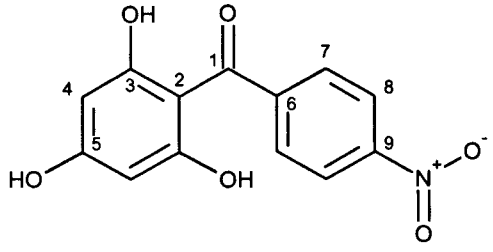

4-nitrobenzoyl chloride was prepared by the following method; a 2-necked round bottom flask (100 ml) was charged with 4-nitrobenzoic acid (4.17 g, 24.9 mmol, 1 eq) and DCM (10 ml). With cooling in an ice bath, oxalyl chloride (2.3 ml, 26.4 mmol, 1 eq) was added dropwise, followed by DMF (1 drop). After the initial effervescence had ceased, the reaction mixture was stirred at room temperature for 2 hours. This was then used in the Friedel-Crafts acylation following the procedure for the synthesis of **3k**, with the following quantities of reagents and materials:

- Aluminium chloride (6.62 g, 49.6 mmol, 2 eq)
- Nitromethane (2.6 ml, 48.4 mmol, 2 eq)
- Phloroglucinol **32** (3.17 g, 25.1 mmol, 1 eq)

The crude product was purified by flash column chromatography (45% ethyl acetate : 55% 40-60 petroleum ether). Removal of the solvent *in vacuo* isolated the title compound **3l** as yellow needles (2.23g, 8.10 mmol, 33%). Mpt = 244.1 °C (decomposed). ν_{max} (neat)/cm^{-1} = 3436 (O-H), 3115 (Ar-H), 1692 (C=O) 1606, 1294, (C-O), 1164, 717; δ_H (400 MHz, CD_3OD) = 5.85 (s, 2H, CH **4**), 7.69 (d, *J*

= 8.91, 2H, CH **7**), 8.25 (d, *J* = 8.78, 2H, CH **8**); δ_C (100 MHz, CD_3OD) = 96.1 (CH **4**), 105.3 (C-OH **5**), 124.0 (CH **8**), 129.7 (CH **7**); *Accurate Mass* (Negative ion mode, calculated for $[C_{13}H_8NO_6]^-$ =274.0357): Found 274.0351.

6.1.4 Friedel-Crafts Acylation of 1,3,5-trimethoxybenzene

The general reaction scheme is as follows:

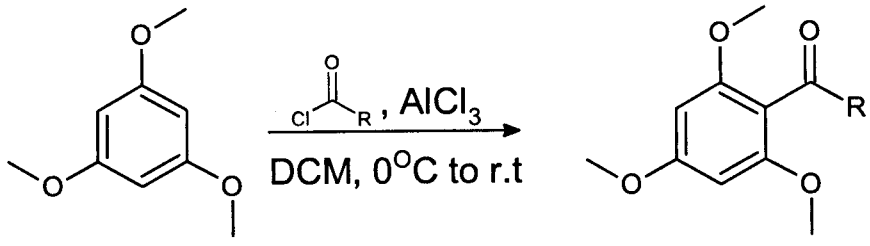

The synthesis of 1-phenyl(2,4,6-trimethoxyphenyl)methanone **(39a)**

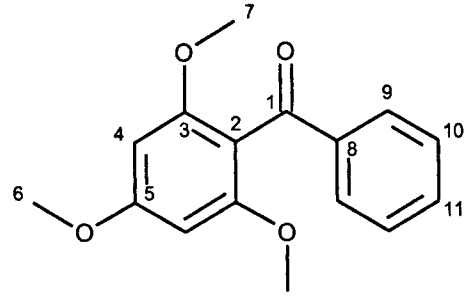

To a 2-necked round-bottomed flask was added aluminium chloride (1.74 g, 13.0 mmol, 1.5 eq) and DCM (50 ml). With cooling in an ice-bath, benzoyl chloride **35** (1.0 ml, 8.61 mmol, 1 eq) was added dropwise *via* syringe, and the resulting mixture stirred for 1hr at 0 °C. This was then transferred *via* syringe to a stirred solution of 1,3,5-trimethoxybenzene **38** (1.45 g, 8.63 mmol, 1 eq) at 0 °C. Upon complete transfer of the aluminium chloride-benzoyl chloride complex, the reaction mixture was allowed to reach room temperature and stirred for a further 18 hours. The reaction mixture was then poured onto ice and the product extracted into DCM (3 x20 ml). The organic layer was then washed

successively with 10% HCl solution (2 x 30 ml), 15% sodium hydrogen carbonate solution (2 x 30 ml), brine (2 x 30 ml) and dried over anhydrous sodium sulphate. The mixture was filtered and the solvent was removed *in vacuo*. The crude mixture purified by flash column chromatography (2:8 ethyl acetate / 40-60 petroleum ether) to afford **39a** as white crystals (1.26 g, 4.65 mmol, 54%). Mpt = 114.7-115.7 °C (lit.[77] = 113-115 °C) ν_{max} (neat)/cm^{-1} = 3303 (Ar-H), 2950, 2843 (C-H), 1658 (C=O), 1583 (C=C), 1408 (C-H), 1122 (C-O), 1032, 953, 753. δ_H (400 MHz, $CDCl_3$) = 3.69 (s, 6H, CH_3 **7**), 3.87 (s, 3H, CH_3 **6**), 6.18 (s, 2H, CH **4**), 7.39-7.45 (m, 2H, CH **10**), 7.50-7.57 (m, 1H, CH **11**), 7.83-7.88 (m, 2H, CH **9**); δ_C (100 MHz, $CDCl_3$) = 55.5 (CH_3 **6**), 55.8 (CH_3 **7**), 90.6 (CH **4**), 110.9 (C **5**), 128.3 (CH **10**), 129.4 (CH **9**), 132.9 (CH **11**), 138.1 (C **3**), 158.7 (C **2**), 162.4 (C **8**), 195.0 (C **1**); *m/z*: = 272 (M^+), 255, 195, 180, 152, 137, 105, 91, 77, 51.

The synthesis of (4-methoxyphenyl)(2,4,6-trimethoxyphenyl)methanone **(39b)**

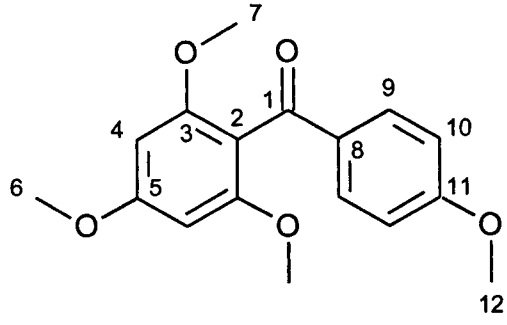

This was carried out as detailed for the synthesis of 1-phenyl(2,4,6-trimethoxyphenyl)methanone **39a**, with the following reagents and quantities:

- Aluminium chloride (1.45 g, 10.9 mmol, 1.5 eq)
- *p*-Methoxybenzoyl chloride (1.0 ml, 7.26 mmol, 1 eq)
- 1,3,5-trimethoxybenzene **38** (1.22 g, 7.25 mmol, 1 eq)

The crude mixture was purified by flash column chromatography (2:8 ethyl acetate / 40-60 petroleum ether) to afford the title compound **39b** as a white crystalline solid. (1.18 g, 3.92 mmol, 54 %). Mpt = 136.4-137.6 °C; ν_{max} (neat)/cm^{-1} = 3201 (Ar-H), 2939, 2841 (C-H), 1648 (C=O), 1595, 1574 (C=C), 1421 (C-H), 1254, 1157, 1105 (C-O), 1028, 917, 773; δ_H (400 MHz, $CDCl_3$) = 3.69 (s, 6H, CH_3 **7**), 3.85 (s, 3H, CH_3 **6**), 3.86 (s, 3H, CH_3 **12**), 6.17 (s, 2H, CH **4**), 6.89 (d, *J* = 9.0, 2H, CH **10**), 7.82 (d, *J* = 9.0, 2H, CH **9**); δ_C (100 MHz, $CDCl_3$) = 30.9 (CH_3 **12**), 55.4 (CH_3 **6**), 55.8 (CH_3 **7**), 90.6 (CH **4**), 111.2 (C **5**), 131.4 (CH **10**), 131.7 (CH **9**), 132.2 (CH **11**), 158.5 (C **3**), 162.1 (C **2**), 163.5 (C **8**), 193.6 (C **1**); *m/z*: = 302 (M^+), 285, 257, 195, 181, 135 ,121, 92, 77, 63; *Accurate Mass* (calculated for $[C_{17}H_{18}O_5]^+$ = 302.1149): Found 302.1147.

The synthesis of 1-(4-methylphenyl)(2,4,6-trimethoxyphenyl)methanone **(39d)**

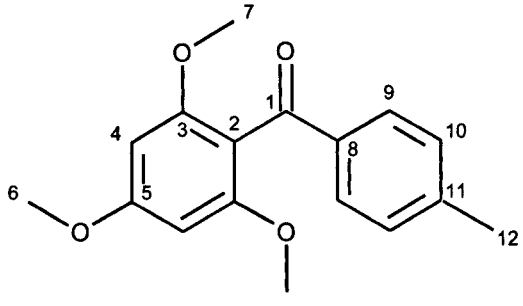

This was carried out as detailed for the synthesis of 1-phenyl(2,4,6-trimethoxyphenyl)methanone **39a**, with the following reagents and quantities:

- Aluminium chloride (1.51 g, 11.3 mmol, 1.5eq)
- *p*-Toluoyl chloride **35d** (1.0 ml, 7.56 mmol, 1 eq)
- 1,3,5-trimethoxybenzene **38** (1.29 g, 7.68 mmol, 1 eq)

The crude mixture was purified by flash column chromatography (2:8 ethyl acetate / 40-60 petroleum ether) to afford the title compound **39d** as a white

crystalline solid (0.697 g, 2.44 mmol, 32%). Mpt = 119.2-120.4 °C. ν_{max} (neat)/cm^{-1} = 3005 (Ar-H), 2964, 2835 (C-H), 1663 (C=O), 1603 (C=C), 1451, 1409 (C-H), 1123 (C-O), 1057, 1032, 953, 760; δ_H (400 MHz, $CDCl_3$) = 2.41 (s, 3H, CH_3 **12**), 3.69 (s, 6H, CH_3 **7**), 3.87 (s, 3H, CH_3 **6**), 6.18 (s, 2H, CH **4**), 7.22 (d, *J* = 7.9, 2H, CH **10**), 7.75 (d, *J* = 8.2, 2H, CH **9**); δ_C (100 MHz, $CDCl_3$) = 21.7 (CH_3 **12**), 55.5 (CH_3 **6**), 55.8 (CH_3 **7**), 90.6 (CH **4**), 111.2 (C **5**), 129.2 (CH **10**), 129.6 (CH **9**), 135.7 (CH **11**), 143.7 (C **3**), 158.6 (C **2**), 162.2 (C **8**), 194.6 (C **1**); *m/z*: = 286 (M^+), 269, 195, 180, 152, 137, 119, 105, 91, 77, 65, 51.

6.1.5 Deprotection of Aromatic Methoxy Groups

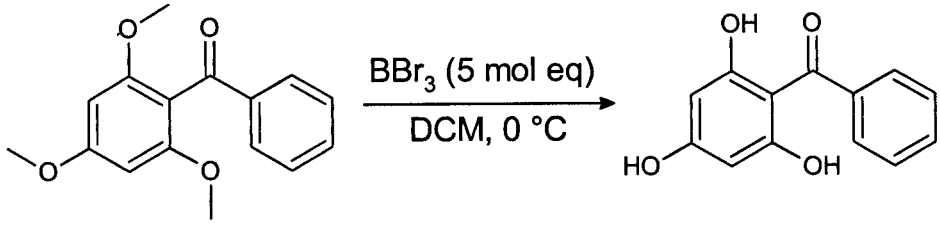

1-phenyl(2,4,6-trimethoxyphenyl)methanone **39a** (0.842 g, 3.10 mmol, 1 eq) and a magnetic stirrer bar were added to a 2-neck round bottom flask (100 ml) equipped with a nitrogen inlet and a rubber septum. Anhydrous DCM (20 ml) was introduced dropwise *via* syringe, and the solution cooled in an ice bath to 0 °C. Boron tribromide (1.5 ml, 3.88 g, 15.5 mmol, 5 eq) was added in one portion *via* syringe, and the reaction mixture allowed to warm to room temperature and stirred for 24 hours. Water (20 ml) was then carefully added to the reaction to quench the boron tribromide, and the crude product extracted into ethyl acetate (2 x 20 ml). The combined organic layers were washed with 1M HCl (2 x 20 ml), water (2 x 20 ml), brine (2 x 20 ml) and dried over anhydrous sodium sulphate. The crude was concentrated *in vacuo* and purified by flash column

chromatography (45% ethyl acetate : 55% petroleum ether as the eluent). The desired fractions were pooled and the solvent removed *in vacuo* to give a yellow powder, recrystallised from water yielding the title compound **3k** as yellow needles (0.584 g, 2.54 mmol, 82%). *Analytical data of this reaction product was the same as previously reported for phenyl(2,4,6-trihydroxyphenyl)methanone **3k** generated from the Freidel-Crafts acylation.*

6.1.6 Synthesis of 1st Generation β-Acids

The general reaction scheme is as follows:

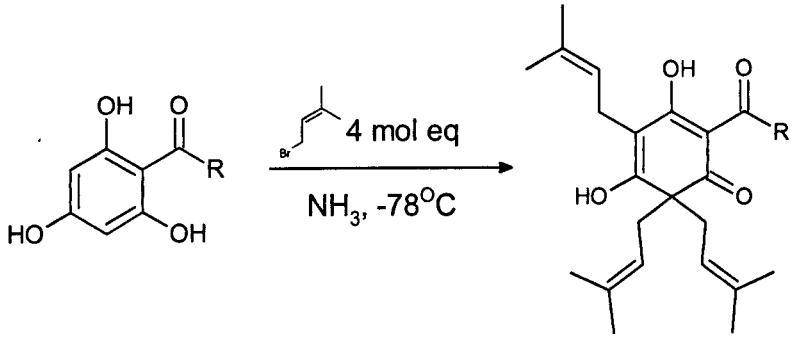

The synthesis of 3,5-Dihydroxy-4,6,6-tris-(3-methyl-but-2-enyl)-2-(3-methylbutyryl)-cyclohexa-2,4-dienone **(Lupulone, 1)**

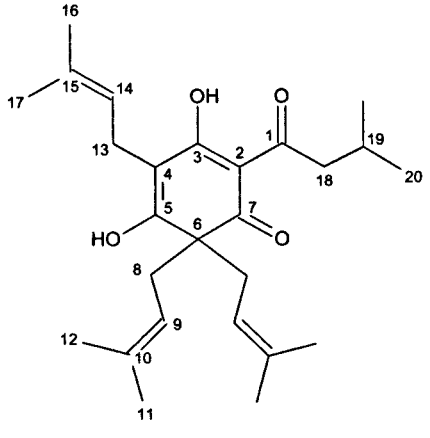

A round bottomed flask (500 ml) was charged with sodium-dried ammonia (200 ml) at -78 °C. With stirring, 3-methyl-1-(2,4,6-trihydroxyphenyl)butan-1-one **3e**

(3.81 g, 18.1 mmol, 1 eq) in diethyl ether (30 ml) was added dropwise *via* syringe, and the solution allowed to stir for 15 minutes. 3,3-dimethylallyl bromide **23** (8.4 ml, 72.1 mmol, 4 eq) in diethyl ether (30 ml) was added dropwise *via* syringe and the reaction mixture was stirred at -78 °C for 5 hours before the reaction mixture was warmed to room temperature to allow the ammonia to evaporate. The semi-solid was diluted in diethyl ether (100 ml), and washed successively with 10% HCl solution, water, brine and the organic layer dried over anhydrous sodium sulphate. The mixture was filtered and the solvent was removed *in vacuo*. The crude was recrystallised first from hexane, then from acetonitrile to afford white crystals (3.99 g, 9.65 mmol, 53%). Mpt = 92.1–93.1 °C (Lit[65]. = 93 °C). ν_{max} (neat)/cm^{-1} = 3157 (O-H), 2924 (C-H), 2854, 1654 (C=O), 1586 (C=C), 1519, 1367, 1227 (C-O), 1172, 1103. δ_H (400 MHz, CD_3OD) = 0.94 (d, *J* = 6.72, 6H, (C*H*$_3$ **20**), 1.53 (s, 6H, C*H*$_3$ **12**), 1.56 (d, *J* = 0.34, 6H, C*H*$_3$ **11**), 1.66 (s, 3H, C*H*$_3$ **17**), 1.73 (s, 3H, C*H*$_3$ **16**), 2.06 (sept, *J* = 6.78, 1H, C*H* **19**), 2.58 (m, 4H, C*H*$_2$ **8**), 2.82 (d, *J* = 6.92, 2H, C*H*$_2$ **18**), 3.08 (d, *J* = 6.92, 2H, C*H*$_2$ **13**), 4.75 (t, *J* = 7.52, 2H, allylic C*H* **9**), 5.00 (t, *J* = 6.85, 1H, CH_2 **14**); δ_C (100 MHz, CD_3OD) = 18.1 (**16**), 18.2 (**11**), 21.8 (**13**), 23.3 (**20**), 26.2 (**12**, **17** (HSQC indicates overlapping ^{13}C resonances for the separate carbon environments)), 27.2 (**19**), 38.9 (**8**), 50.2 (**18**), 58.9 (**6**), 109.5 (**4**), 112.6 (**2**), 119.4 (**9**), 123.4 (**14**), 132.7 (**10**), 135.8 (**15**), 174.5 (**5**), 191.2 (**3**), 198.3 (**7**), 204.1 (**1**); *m/z*: = 414 (M^+), 345, 289, 277, 261, 247, 235, 219, 205, 189, 177, 165, 135, 109, 69, 57; *Accurate Mass* (positive ion mode, calculated for $[C_{27}H_{39}O_4]^+$ = 415.2843): Found 415.2845.

The synthesis of 3,5-Dihydroxy-4,6,6-tris-(3-methyl-but-2-enyl)-2-(isopropyl)-cyclohexa-2,4-dienone **(Colupulone, 1a)**

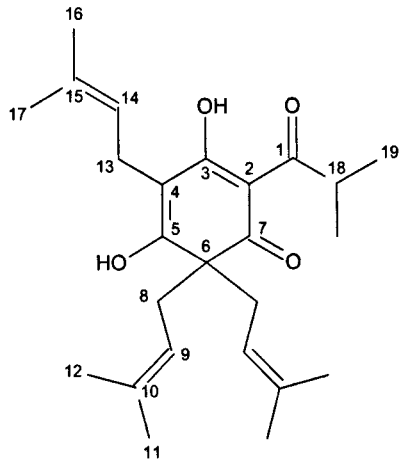

This was carried out as detailed for the synthesis of 3,5-Dihydroxy-4,6,6-tris-(3-methyl-but-2-enyl)-2-(3-methylbutyryl)-cyclohexa-2,4-dienone (lupulone) **1** with the following reagents and quantities:

- 2-methyl-1-(2,4,6-trihydroxyphenyl)propan-1-one **3d** (0.711 g, 3.63 mmol, 1 eq)
- 3,3-dimethylallyl bromide **23** (1.7 ml, 14.6 mmol, 4 eq)
- Ammonia (50 ml)

The title compound **1a** was obtained as white crystals (0.571 g, 1.43 mmol, 47%). Mpt = 93.2–94.1 °C (Lit[61]. = 94 °C). ν_{max} (neat)/cm^{-1} = 3401 (O-H), 2965 (C-H), 2914, 1655 (C=O), 1584 (C=C), 1436, 1372, 1227 (C-O), 1196, 1099; δ_H (400 MHz, CD_3OD) = 1.09 (d, *J* = 6.78, 6H, C*H*$_3$ **19**), 1.55 (s, 6H, C*H*$_3$ **12**), 1.57 (s, 6H, C*H*$_3$ **11**), 1.67 (s, 3H, C*H*$_3$ **17**), 1.73 (s, 3H, C*H*$_3$ **16**), 2.53-2.66 (m, 4H, C*H*$_2$ **8**), 3.10 (d, *J* = 6.67, 2H, C*H*$_2$ **13**), 3.98 (pent, *J* = 6.84, 1H, CH **18**), 4.77 (t, *J* = 7.40, 2H, C*H* **9**), 5.02 (t, *J* 1H, C*H* **14**); δ_C (100 MHz, CD_3OD) = 18.1 (CH_3 **16**), 18.2 (CH_3 **11**), 19.4 (CH_3 **19**), 21.8 (CH_2 **13**), 26.2 (CH_3 **12**), 37.3 (CH **18**), 39.0 (CH_2 **8**), 59.1 (C **6**), 108.2 (C **2**), 112.4 (C **4**), 119.4 (CH **9**), 123.4 (CH **14**), 132.7 (C **10**), 135.8 (C **15**), 174.6 (C **5**), 191.2 (C **3**), 198.1 (C **7**), 209.0 (C **1**);

m/z: = 400 (M^+-2), 331, 289, 275, 263, 245, 233, 177, 69, *Accurate Mass* (calculated for $[C_{25}H_{36}O_4]^+$ = 400.2608): Found 400.2607.

The synthesis of 3,5-Dihydroxy-4,6,6-tris-(3-methyl-but-2-enyl)-2-(3-propionyl)-cyclohexa-2,4-dienone **(Postlupulone, 1b)**

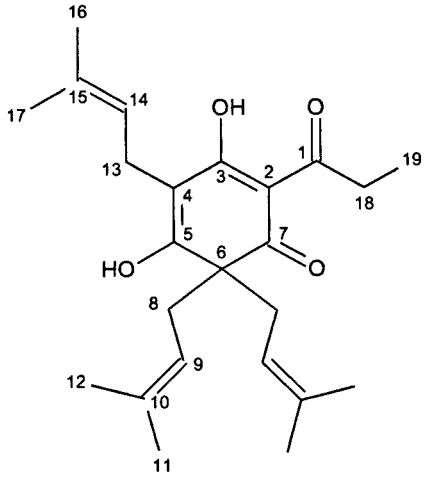

This was carried out as detailed for the synthesis of 3,5-Dihydroxy-4,6,6-tris-(3-methyl-but-2-enyl)-2-(3-methylbutyryl)-cyclohexa-2,4-dienone (lupulone) **1** with the following reagents and quantities:

- 1-(2,4,6-trihydroxyphenyl)propan-1-one **3b** (0.891 g, 4.90 mmol, 1 eq)
- 3,3-dimethylallyl bromide **23** (2.2 ml, 18.9 mmol, 4 eq)
- Ammonia (50 ml)

The title compound **1b** was obtained as white crystals (1.19 g, 3.11 mmol, 63%). Mpt = 102.4-103.4 °C (Lit[61]. = 103 °C). ν_{max} (neat)/cm^{-1} = 3161 (O-H), 2923 C-H), 2854, 1653 (C=O), 1584 (C=C), 1519, 1358, 1230 (C-O), 1172, 1106; δ_H (400 MHz, CD_3OD) = 1.09 (t, *J* = 7.32, 3H, C*H*$_3$ **19**), 1.53 (s, 6H, C*H*$_3$ **12**), 1.56 (s, 6H, C*H*$_3$ **11**), 1.66 (s, 3H, C*H*$_3$ **17**), 1.72 (s, 3H, C*H*$_3$ **16**), 2.59 (m, 4H, C*H*$_2$ **8**), 2.96 (q, *J* = 7.23, 2H, CH_3 **18**), 3.08 (d, *J* = 6.77, 2H, C*H*$_2$ **13**), 4.75 (t, *J* = 7.60, 2H, C*H* **9**), 5.00 (t, *J* = 6.50, 1H, C*H* **14**); δ_C (100 MHz, CD_3OD) =

16.8 (CH_3 **12**), 20.3 (CH_2 **13**), 22.9 (CH_3 **19**), 24.7 (CH_3 **11**), 33.9 (CH_2 **18**), 37.5 (CH_2 **8**), 57.5 (C **6**), 110.7 (C **4**), 117.9 (C **9**), 121.9 (CH **14**), 131.2 (C **10**), 134.3 (C **15**, 173.2 (C **5**), 189.3 (C **3**), 196.9 (C **7**), 204.1 (C **1**); *m/z*: = 386 (M^+); 317; 261; 249; 233; 219; 207; 189; 177; 109; 69; 57; *Accurate Mass* (calculated for $[C_{24}H_{34}O_4]^+$ = 386.2452): Found 386.2450.

The synthesis of 3,5-Dihydroxy-4,6,6-tris-(3-methyl-but-2-enyl)-2-(4-methylpentryl)-cyclohexa-2,4-dienone **(Prelupulone, 1c)**

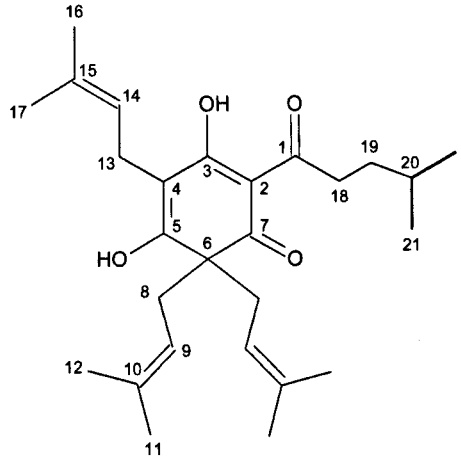

This was carried out as detailed for the synthesis of 3,5-Dihydroxy-4,6,6-tris-(3-methyl-but-2-enyl)-2-(3-methylbutyryl)-cyclohexa-2,4-dienone (lupulone) **1** with the following reagents and quantities:

- 4-methyl-1-(2,4,6-trihydroxyphenyl)pentan-1-one **3f** (1.62 g, 7.25 mmol, 1 eq)
- 3,3-dimethylallyl bromide **23** (3.4 ml, 29.2 mmol, 4 eq)
- Ammonia (100 ml)

The title compound **1c** was obtained as white crystals (1.72 g, 4.01 mmol, 55%). Mpt = 94.8-95.7 °C. ν_{max} (neat)/cm^{-1} = 3251 (O-H), 2957, 2920 (C-H), 1649 (C=O), 1584 (C=C), 1456, 1196 (-O), 1101; δ_H (400 MHz, CD_3OD) = 0.94

(d, J = 6.59 Hz, 6H, CH_3 **21**), 1.43-1.50 (m, 2H, CH_2 **19**), 1.55 (s, 6H, CH_3 **12**), 1.58 (s, 6H, CH_3 **11**), 1.62 (m, 1H, CH **20**), 1.67 (s, 3H, CH_3 **17**), 1.73 (s, 3H, CH_3 **16**), 2.53-2.66 (m, 4H, CH_2 **8**), 2.92-3.00 (m, 2H, CH_2 **18**), 3.10 (d, J = 6.78 Hz, 2H, CH_2 **13**), 4.76 (t, J = 7.54, 2H, CH **9**), 5.02 (t, J = 6.88, 1H, CH_2 **14**); δ_C (100 MHz, CD_3OD) = 18.1 (**16**), 18.3 (**11**), 21.8 (**13**), 23.0 (**21**), 26.18 (**17**), 26.19 (**12**), 29.5 (**20**), 35.5 (**19**), 38.9 (**8**), 39.8 (**18**), 58.9 (**6**), 109.1 (**4**), 112.4 (**2**), 119.4 (**9**), 123.4 (**14**), 132.7 (**10**), 135.8 (**15**), 174.6 (**5**), 191.0 (**3**), 198.2 (**7**), 205.0 (**1**); *m/z*: = 428 (M^+), 359, 303, 291, 261, 205, 177, 109, 69, 55; *Accurate Mass* (negative ion mode, calculated for $[C_{27}H_{39}O_4]^+$ = 427.2854): Found 427.2844.

The synthesis of 3,5-Dihydroxy-4,6,6-tris-(3-methyl-but-2-enyl)-2-(butyryl)-cyclohexa-2,4-dienone **(1e)**

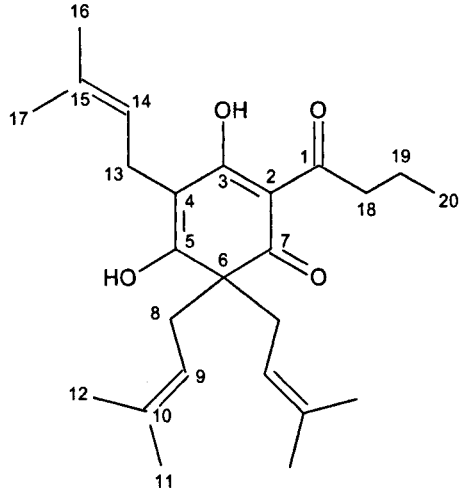

This was carried out as detailed for the synthesis of 3,5-Dihydroxy-4,6,6-tris-(3-methyl-but-2-enyl)-2-(3-methylbutyryl)-cyclohexa-2,4-dienone (lupulone) **1** with the following reagents and quantities:

- 1-(2,4,6-trihydroxyphenyl)butan-1-one **3c** (0.711 g, 3.63 mmol, 1 eq)
- 3,3-dimethylallyl bromide **23** (1.7 ml, 14.6 mmol, 4 eq)

- Ammonia (50 ml)

The title compound **1e** was obtained as white crystals (0.544 g, 1.35 mmol, 37%). Mpt = 110.2–111.2 °C (Lit[60]. = 110 °C); ν_{max} (neat)/cm^{-1} = 2924 (C-H), 2854, 1652 (C=O), 1584 (C=C), 1375, 1217 (C-O), 1160, 1107; δ_H (400 MHz, CD_3OD) = 0.96 (t, *J* = 7.37, 3H, C*H*$_3$ **20**), 1.54 (s, 6H, C*H*$_3$ **12**), 1.56 (s, 6H, C*H*$_3$ **11**), 1.58-1.64 (m, 2H, CH_3 **18**), 1.66 (s, 3H, C*H*$_3$ **17**), 1.72 (s, 3H, C*H*$_3$ **16**), 2.58 (sept, *J* = 7.58, 3H, C*H*$_2$ **8**), 2.91 (t, *J* = 7.42, 2H, C*H*$_2$ **19**), 3.08 (d, *J* = 6.87, 2H, C*H*$_2$ **13**), 4.75 (tt, J_1 = 1.01, J_2 = 7.85, 2H, C*H* **9**), 4.99-5.02 (m, 1H, C*H* **14**); δ_C (100 MHz, CD_3OD) = 13.1 (*C*H$_3$ **20**), 16.8 (*C*H$_3$ **12**), 18.4 (CH_2 **19**), 20.3 (*C*H$_2$ **13**), 22.9 (*C*H$_3$ **16**), 24.7 (*C*H$_3$ **11**), 29.4 (*C*H$_3$ **17**), 37.5 (*C*H$_2$ **8**), 42.2 (*C*H$_2$ **18**), 57.5 (C **6**), 99.9 (C **5**), 110.9 (*C* **4**), 117.9 (C **9**), 121.9 (*C*H **14**), 131.3 (C **10**), 134.4 (C **15**), 173.2 (*C*-OH **3**), 208.7. (C **1**); *m/z*: = 400 (M^+), 357, 331, 275, 263, 233, 221, 205, 177, 109, 69; *Accurate Mass* (calculated for $[C_{25}H_{36}O_4]^+$ = 400.2608): Found 400.2602.

The synthesis of 3,5-Dihydroxy-4,6,6-tris-(3-methyl-but-2-enyl)-2-(3-acetyl)-cyclohexa-2,4-dienone **(1f)**

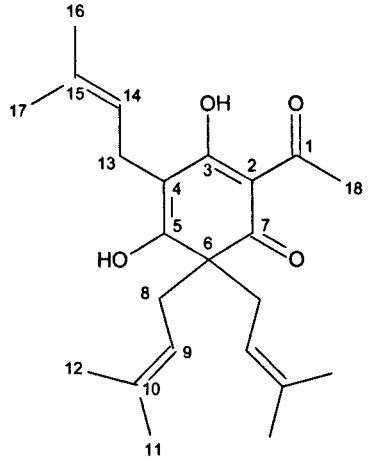

This was carried out as detailed for the synthesis of 3,5-Dihydroxy-4,6,6-tris-(3-methyl-but-2-enyl)-2-(3-methylbutyryl)-cyclohexa-2,4-dienone (lupulone) **1** with the following reagents and quantities:

- 1-(2,4,6-trihydroxyphenyl)ethanone **3a** (0.299 g, 1.78 mmol, 1 eq)
- 3,3-dimethylallyl bromide **23** (0.83 ml, 7.13 mmol, 4 eq)
- Ammonia (25 ml)

The title compound **1f** was obtained as white crystals (0.1857 g, 0.499 mmol, 28%). Mpt = 122.9–123.8 °C (Lit[61]. = 123 °C). ν_{max} (neat)/cm^{-1} = 3259 (O-H), 2971 (C-H), 2919, 1650 (C=O), 1590, 1530 (C=C), 1454, 1240 (C-O), 1101, 983; δ_H (400 MHz, CD_3OD) = 1.55 (s, 6H, CH_3, **12**), 1.57 (s, 6H, CH_3, **11**), 1.67 (s, 3H, CH_3, **17**), 1.73 (s, 3H, CH_3, **16**), 2.51 (s, 3H, CH_3, **18**), 2.60 (spt, *J* = 7.50, 4H, CH_2, **8**), 3.09 (d, *J* = 6.77, 2H, CH_2, **13**), 4.76 (tt, *J* = 7.60, 1.28, 2H, CH, **9**), 5.01 (t, *J* = 6.27, 1H, CH, **14**); δ_C (100 MHz, CD_3OD) = 18.1 (CH_3 **16**), 18.2 (CH_3 **11**), 21.7 (CH_2 **13**), 26.2 (CH_3 **12** and **17** (HSQC indicates overlapping ^{13}C resonances for the separate carbon environments)); 29.3 (CH_3 **18**), 38.9 (CH_2 **8**), 59.0 (C **6**), 109.6 (C **4**), 112.3 (C **2**), 119.3 (CH **9**), 123.4 (CH **14**), 132.7 (C **10**), 135.9 (C **15**), 174.9 (C **5**), 190.7 (C **3**), 198.6 (C **7**), 201.6 (C **1**); *m/z*: = 371 (M^+-1), 302, 247, 233, 193, 165, 114, 91, 69; Accurate Mass (calculated for $[C_{23}H_{32}O_4]^+$ = 371.2220): Found 371.2228.

The synthesis of 3,5-Dihydroxy-4,6,6-tris-(3-methyl-but-2-enyl)-2-(3-cyclopropyl)-cyclohexa-2,4-dienone **(1g)**

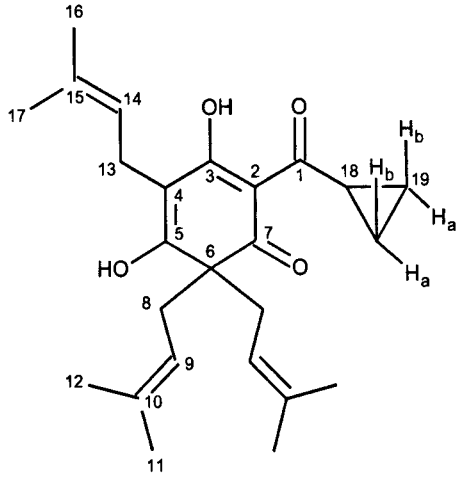

This was carried out as detailed for the synthesis of 3,5-Dihydroxy-4,6,6-tris-(3-methyl-but-2-enyl)-2-(3-methylbutyryl)-cyclohexa-2,4-dienone (lupulone) **1** with the following reagents and quantities:

- cyclopropyl(2,4,6-trihydroxyphenyl)methanone **3g** (4.67 g, 24.1 mmol, 1 eq)
- 3,3-dimethylallyl bromide **23** (11.2 ml, 96.2 mmol, 4 eq)
- Ammonia (250 ml)

The title compound **1g** was obtained as white crystals (4.10 g, 10.3 mmol, 43 %). Mpt = 98.2–99.1 °C. ν_{max} (neat)/cm^{-1} = 3583, 3271 (O-H), 2923 (C-H), 1645 (C=O), 1578 (C=C), 1517, 1443, 1365, 1218 (C-O), 1160, 1106, 921, 826; δ_H (400 MHz, CD_3OD) = 0.99 – 1.07 (m, 2H, C*H* 19 **Hb**), 1.16 - 1.23 (m, 2H, C*H* **19 Ha**), 1.59 (s, 6H, CH_3 **12**), 1.61 (d, *J* = 0.34, 6H, CH_3 **11**), 1.69 (s, 3H, CH_3 **17**), 1.75 (s, 3H, CH_3 **16**), 2.54 – 2.76 (m, 4H, CH_2 **8**), 3.11 (d, *J* = 7.03, 2H, CH_2 **13**), 3.57 – 3.68 (m, CH **18**), 4.83 (t, *J* = 7.47, 2H, C*H* **9**), 5.03 (t, *J* = 6.78, 1H, CH **14**); δ_C (100 MHz, CD_3OD) = 11.1 (CH_2 **19**), 16.6 (CH_3 **16**), 16.7 (CH_3 **12**), 20.2 (CH_2 **13**), 22.9 (CH **18**), 24.6 (CH_3 **17**), 24.7 (CH_3 **11**), 37.4 (CH_2 **8**), 56.6 (C, **6**),

108.16 (C **4**), 110.45 (C **2**), 117.9 (CH **9**), 121.9 (CH **14**), 131.1 (C **10**), 134.3 (C **15**), 172.6 (C **5**), 188.6 (C **3**), 197.3 (C **7**), 202.6 (C **1**); *m/z*: = 398 (M^+), 329, 273, 261, 231, 219, 205, 189, 177, 165, 135, 109, 69, 57; *Accurate Mass* (calculated for $[C_{25}H_{34}O_4]^+$ = 398.2452): Found 398.2450.

The synthesis of 3,5-Dihydroxy-4,6,6-tris-(3-methyl-but-2-enyl)-2-(cyclobutanecarbonyl)-cyclohexa-2,4-dienone **(1h)**

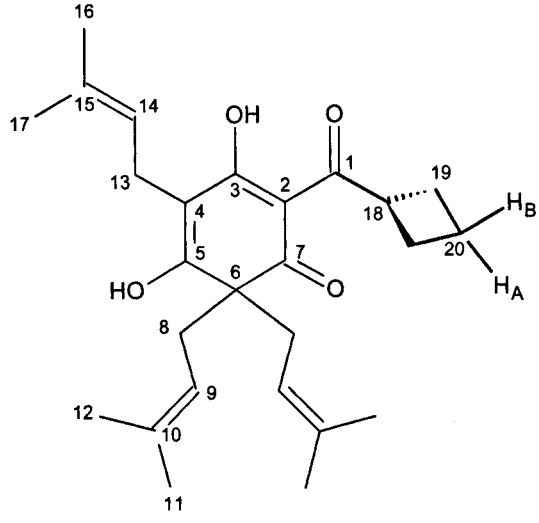

This was carried out as detailed for the synthesis of 3,5-Dihydroxy-4,6,6-tris-(3-methyl-but-2-enyl)-2-(3-methylbutyryl)-cyclohexa-2,4-dienone (lupulone) **1** with the following reagents and quantities:

- cyclobutyl(2,4,6-trihydroxyphenyl)methanone **3h** (1.11 g, 5.32 mmol, 1 eq)
- 3,3-dimethylallyl bromide **23** (2.2 ml, 18.9 mmol, 3.6 eq)
- Ammonia (100 ml)

The title compound **1h** was obtained as white crystals (0.610 g, 1.48 mmol, 28%). Mpt = 98.2–99.1 °C. ν_{max} (neat)/cm^{-1} = 3384 (O-H), 2924 (C-H), 1644 (C=O), 1584 (C=C), 1517, 1457, 1376, 1212 (C-O), 1164, 925, 827; δ_H (400 MHz, CD_3OD) = 1.54 (s, 6H, C*H*$_3$ **12**), 1.56 (s, 6H, C*H*$_3$ **11**), 1.67 (s, 3H, C*H*$_3$

11), 1.73 (s, 3H, C*H*$_3$ **16**), 1.76-1.87 (m, 1H, **20 H$_A$**), 1.98 (sxt, 1H, *J* = 9.14 Hz, **20 H$_B$**), 2.17-2.28 (m, 4H, **19**), 2.49-2.65 (m, 4H, C*H*$_2$ **8**), 3.09 (d, *J* = 6.90, 2H, C*H*$_2$ **13**), 4.24 (quin, *J* = 8.31, 1H **18**), 4.74 (t, *J* = 7.47, 2H, C*H* **9**), 5.02 (t, *J* = 6.65, 1H, CH **14**); δ_C (100 MHz, CD_3OD) = 18.1 (**16**), 18.2 (**11**), 18.8 (**20**), 21.8 (**13**), 25.7 (**19**), 26.2 (**11**, **16** (HSQC indicates overlapping ^{13}C resonances for the separate carbon environments)), 39.0 (**8**), 45.2 (**18**), 56.0 (**6**), 107.8 (**4**), 112.1 (**2**), 119.4 (**9**), 123.5 (**14**), 132.6 (**10**), 135.7 (**15**), 175.0 (**5**), 190.6 (**3**), 197.8 (**7**), 204.9 (**1**); *m/z*: = 412 (M^+), 343, 287, 275, 233, 205, 189, 177, 165, 135, 109, 69, 55; *Accurate Mass* (Positive ion mode, calculated for $[C_{26}H_{37}O_4][H]^+$ = 413.2686): Found 413.2688.

The synthesis of 3,5-Dihydroxy-4,6,6-tris-(3-methyl-but-2-enyl)-2-(cyclopentanecarbonyl)-cyclohexa-2,4-dienone **(1i)**

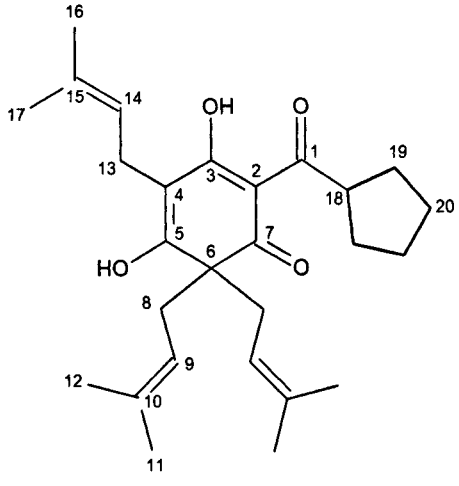

This was carried out as detailed for the synthesis of 3,5-Dihydroxy-4,6,6-tris-(3-methyl-but-2-enyl)-2-(3-methylbutyryl)-cyclohexa-2,4-dienone (lupulone) **1** with the following reagents and quantities:

- cyclopentyl(2,4,6-trihydroxyphenyl)methanone **3i** (1.03 g, 4.66 mmol, 1 eq)
- 3,3-dimethylallyl bromide **23** (1.9 ml, 16.3 mmol, 4 eq)
- Ammonia (100 ml)

The title compound **1i** was obtained as white crystals (0.349 g, 0.819 mmol, 18%). Mpt = 76.5–78.1 °C. ν_{max} (neat)/cm^{-1} = 3160 (O-H), 2923 (C-H), 2854, 1653 (C=O), 1583 (C=C), 1369, 1225 (C-O), 1170, 1109. *m/z*: = 426 (M^+), 357, 301, 289, 233, 177, 69; δ_H (400 MHz, CD_3OD) = 1.55 (s, 6H, C*H*$_3$ **12**), 1.57 (s, 6H, C*H*$_3$ **11**), 1.67 (s, 3H, CH_3 **17**), 1.73 (s, 3H, CH_3 **16**), 1.60–1.80 (m, mixture of resonances from **19** and **20**), 1.83–1.94 (m, 2H, **19**), 2.50-2.67 (m, 4H, C*H*$_2$ **8**), 3.09 (d, *J* = 6.78 Hz, 2H, C*H*$_2$ **13**), 4.14 (quin, *J* = 7.15 Hz, 1H, C*H* **18**), 4.77 (t, *J* = 7.65, 2H, CH **9**), 5.02 (t, *J* = 6.27, 1H, C*H* **14**); δ_C (100 MHz, CD_3OD) = 18.1 (CH_3 **16**), 18.3 (CH_3 **12**), 21.8 (CH_2 **13**), 26.2 (CH_3 **17**), 26.2 (CH_3 **11**), 27.3 (CH_2 **20**), 30.9 (CH_2 **19**), 38.9 (CH_2 **8**), 48.9 (CH **18**), 59.0 (C **6**), 108.7 (C **2**), 112.3 (C **4**), 119.4 (CH **9**), 123.5 (CH **14**), 132.7 (C **10**), 135.8 (C **15**), 174.4 (C **5**), 191.1 (C **3**), 198.2 (C **7**), 207.5 (C **1**); *Accurate Mass* (Negative ion mode, calculated for $[C_{27}H_{39}O_4]^-$ = 427.2843): Found 427.2844.

The synthesis of 3,5-Dihydroxy-4,6,6-tris-(3-methyl-but-2-enyl)-2-(cyclopentanecarbonyl)-cyclohexa-2,4-dienone **(1j)**

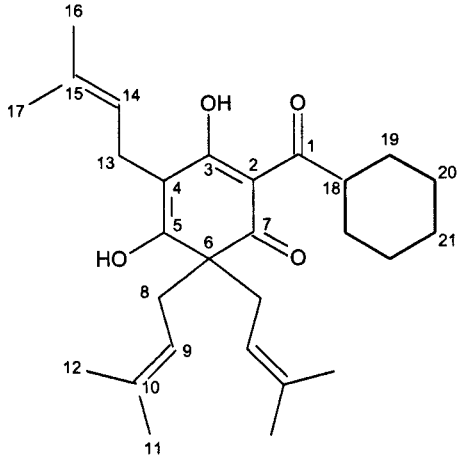

This was carried out as detailed for the synthesis of 3,5-Dihydroxy-4,6,6-tris-(3-methyl-but-2-enyl)-2-(3-methylbutyryl)-cyclohexa-2,4-dienone (lupulone) **1** with the following reagents and quantities:

- cyclohexyl(2,4,6-trihydroxyphenyl)methanone **3j** (0.797 g, 3.38 mmol, 1 eq)
- 3,3-dimethylallyl bromide **23** (1.4 ml, 12.0 mmol, 4 eq)
- Ammonia (100 ml)

The title compound **1j** was obtained as white crystals (0.566 g, 1.29 mmol, 38%). Mpt = 118.4-119.2 °C. ν_{max} (neat)/cm^{-1} = 3400 (O-H), 1651 (C=O), 1579 (C=C), 1448, 1365, 1195, 1102, 820; δ_H (400 MHz, CD_3OD) = 1.19-1.34 (m, 2H, C*H*$_2$ **21**), 1.35-1.45 (m, 4H, C*H*$_2$, **20**), 1.54 (s, 6H, C*H*$_3$ **12**), 1.57 (s, 6H, C*H*$_3$ **11**), 1.67 (s, 3H, C*H*$_3$ **17**), 1.73 (s, 3H, C*H*$_3$ **16**), 1.74-1.84 (m, 4H, **19**), 2.49-2.72 (m, 4H, C*H*$_2$ **8**), 3.09 (d, *J* = 6.78, 2H, C*H*$_2$ **13**), 3.60-3.83 (m, 1H, C*H* **18**), 4.76 (t, *J* = 7.15 Hz, 2H, C*H* **9**), 5.01 (t, *J* = 6.27 Hz, 1H, CH **14**); δ_C (100 MHz, CD_3OD) = 18.1 (**17**), 18.2 (**12**), 21.79 (**13**), 21.82 (**21**), 26.17 (**16**), 26.20 (**11**), 27.35 (**21**), 27.41 (**20**), 30.4 (**19**), 39.0 (**8**), 47.7 (**18**), 59.1 (**6**), 108.4 (**4**), 112.4 (**2**), 119.5

(**9**), 123.5 (**14**), 132.6 (**10**), 135.7 (**15**), 174.7 (**5**), 191.2 (**3**), 198.2 (**7**), 207.8 (**1**); *m/z*: = 440 (M^+), 371, 315, 303, 289, 259, 233, 177, 109, 83, 69, 55. *Accurate Mass* (Calculated for $[C_{28}H_{40}O_4]^+$ = 440.2921): Found 440.2919.

The synthesis of 3,5-Dihydroxy-4,6,6-tris-(3-methyl-but-2-enyl)-2-(benzoyl)-cyclohexa-2,4-dienone **(1k)**

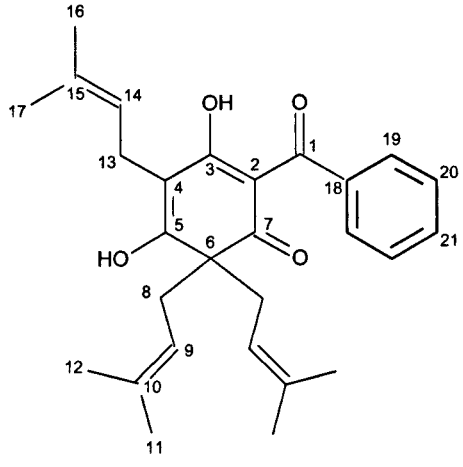

This was carried out as detailed for the synthesis of 3,5-Dihydroxy-4,6,6-tris-(3-methyl-but-2-enyl)-2-(3-methylbutyryl)-cyclohexa-2,4-dienone (lupulone) **1** with the following reagents and quantities:

- phenyl(2,4,6-trihydroxyphenyl)methanone **3k** (0.969 g, 4.21 mmol, 1 eq)
- 3,3-dimethylallyl bromide **23** (1.7 ml, 14.6 mmol, 3.5 eq)
- Ammonia (100 ml)

The title compound **1k** was obtained as yellow crystals (0.647 g, 1.49 mmol, 35%). Mpt = 140.1-141.3 °C; ν_{max} (neat)/cm^{-1} = 2965 (C-H), 2922, 1646 (C=O), 1454, 1340, 1187, 1032, 819; δ_H (400 MHz, CD_3OD) = 1.60 (d, *J* = 1.00 Hz, 6H, C*H*$_3$ **12**), 1.63 (d, *J* = 1.00 Hz, 6H, C*H*$_3$ **11**), 1.70 (d, *J* = 1.00 Hz, 3H, C*H*$_3$ **17**), 1.75 (s, 3H, C*H*$_3$ **16**), 2.61 (d, J = 7.28 Hz, 4H, C*H*$_2$ **8**), 3.14 (d, *J* = 6.78, 2H, C*H*$_2$ **13**), 4.87-4.91 (m, 2H, C*H* **9**), 5.07 (tt, *J* = 7.00, 1.29 Hz, 1H, CH **14**), 7.33-

7.39 (m, 2H, C*H* **19**), 7.39-7.43 (m, 2H, C*H* **20**), 7.44-7.49 (m, 1H, C*H* **21**); δ_C (100 MHz, CD_3OD) = 18.2 (CH_3 **17**), 18.3 (CH_3 **12**), 21.9 (CH_2 **13**), 26.2 (CH_3 **16**), 26.3 (CH_3 **11**), 38.6 (CH_2 **8**), 119.4 (CH **9**), 123.3 (CH **14**), 128.11 (CH **20**), 129.0 (CH **19**), 133.0 (C **10**), 136.2 (C **15**), 199.0 (C **1**) n.b. not all signals seen; weak spectrum due to low concentration of compound weakly soluble in methanol-D4. Spectra obtained in alternative deutrated solvents gives rise to tautomeric forms with spectra difficult to assign correctly; *m/z*: = 434 (M^+), 365, 349, 309, 297, 215, 177, 105, 81, 69, 53. *Accurate Mass* (Negative ion mode, calculated for $[C_{28}H_{33}O_4]^-$ = 433.2384): Found 433.2371.

The synthesis of 3,5-Dihydroxy-4,6,6-tris-(3-methyl-but-2-enyl)-2-(4-methoxybenzoyl)-cyclohexa-2,4-dienone **(1l)**

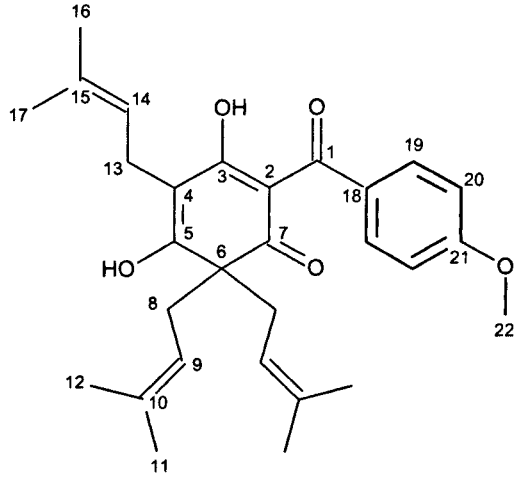

This was carried out as detailed for the synthesis of 3,5-Dihydroxy-4,6,6-tris-(3-methyl-but-2-enyl)-2-(3-methylbutyryl)-cyclohexa-2,4-dienone (lupulone) **1** with the following reagents and quantities:

- (4-methoxyphenyl)(2,4,6-trihydroxyphenyl)methanone **3l** (1.969 g, 7.57 mmol, 1 eq)
- 3,3-dimethylallyl bromide **23** (3.50 ml, 30.1 mmol, 3.9 eq)

- Ammonia (100 ml)

The title compound **1l** was obtained as a yellow powder (2.25 g, 4.85 mmol, 64%). Mpt = 147.3-148.9 °C. ν_{max} (neat)/cm^{-1} = 3436 (O-H), 1644 (C=O), 1605 (C=C), 1506, 1254 (C-O), 1174, 1029; δ_H (400 MHz, CD_3OD) = 1.61 (d, *J* = 0.88 Hz, 6H, C*H*$_3$ **12**), 1.62 (d, *J* = 0.82 Hz, 6H, C*H*$_3$ **11**), 1.69 (d, *J* = 0.88 Hz, 3H, C*H*$_3$ **17**), 1.74 (s, 3H, C*H*$_3$ **16**), 2.63 (d, J = 7.40 Hz, 4H, C*H*$_2$ **8**), 3.13 (d, *J* = 6.84, 2H, C*H*$_2$ **13**), 3.85 (s, 3H, C*H*$_3$ **22**), 4.88-4.91 (m, 2H, C*H* **9**), 5.06 (tt, *J* = 7.02, 1.33 Hz, 1H, CH **14**), 6.86-6.91 (m, 2H, C*H* **19**), 7.45-7.52 (m, 2H, C*H* **20**); δ_C (100 MHz, CD_3OD) = 18.0 (CH_3 **17**), 18.2 (CH_3 **12**), 21.9 (CH_2 **13**), 26.1 (CH_3 **16**), 26.2 (CH_3 **11**), 38.4 (CH_2 **8**), 56.0 (C **6**), 113.9 (C **4**), 119.4 (CH **9**), 123.3 (CH **14**), 132.0 (CH **19**), 132.8 (CH **20**), 133.0 (C **10**), 136.1 (C **15**), 197.5 (C **1**) n.b. not all signals seen; weak spectrum due to low concentration of compound weakly soluble in methanol-D4. Spectra obtained in alternative deutrated solvents gives rise to tautomeric forms with spectra difficult to assign correctly; *m/z*: = 464 (M^+), 396, 379, 341, 325, 233, 217, 189, 177, 135, 109, 91, 77, 55. *Accurate Mass* (Negative ion mode, calculated for $[C_{29}H_{35}O_5]^-$ = 463.2490): Found 463.2477.

The synthesis of 3,5-Dihydroxy-4,6,6-tris-(3-methyl-but-2-enyl)-2-(4-nitrobenzoyl)-cyclohexa-2,4-dienone **(1m)**

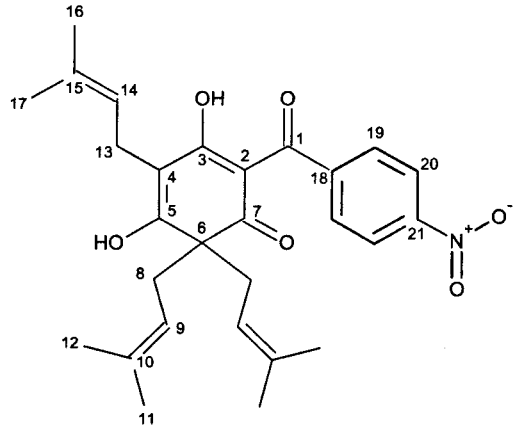

This was carried out as detailed for the synthesis of 3,5-Dihydroxy-4,6,6-tris-(3-methyl-but-2-enyl)-2-(3-methylbutyryl)-cyclohexa-2,4-dienone (lupulone) **1** with the following reagents and quantities:

- (4-nitrophenyl)(2,4,6-trihydroxyphenyl)methanone **3m** (1.201 g, 4.36 mmol, 1 eq)
- 3,3-dimethylallyl bromide **23** (2.0 ml, 17.2 mmol, 3.9 eq)
- Ammonia (100 ml)

The title compound **1m** was obtained as yellow crystals (0.523 g, 1.09 mmol, 25%). Mpt = 148.4-149.0 °C; ν_{max} (neat)/cm^{-1} = 2954 (C-H), 2923, 2853, 1692 (C=O), 1577 (C=C), 1456, 1347 (N=O), 1096, 797; δ_H (400 MHz, CD_3OD) = 1.59 (s, 6H, C*H*$_3$ **12**), 1.63 (s, 6H, C*H*$_3$ **11**), 1.70 (s, 3H, C*H*$_3$ **17**), 1.76 (s, 3H, C*H*$_3$ **16**), 2.49-2.67 (m, 4H, C*H*$_2$ **8**), 3.16 (d, *J* = 6.65, 2H, C*H*$_2$ **13**), 4.81-4.86 (m, 2H, C*H* **9**), 5.06 (t, *J* = 6.71 Hz, 1H, CH **14**), 7.51 (d, *J* = 8.78 Hz, 2H, C*H* **19**), 8.23 (d, *J* = 8.91 Hz, 2H, C*H* **20**); δ_C (100 MHz, CD_3OD) = 18.1 (CH_3 **17**), 18.3 (CH_3 **12**), 21.8 (CH_2 **13**), 26.2 (CH_3 **16**), 26.3 (CH_3 **11**), 38.8 (CH_2 **8**), 58.9 (C **6**), 112.4 (C **4**), 118.3 (C **2**), 119.2 (CH **9**), 123.0 (CH **20**), 124.1 (CH **14**), 129.3

(CH **19**), 133.2 (C **10**), 136.4 (C **15**), 148.0 (C **18**), 150.0 (C **21**), 177.0 (C **5**), 189.5 (C **3**), 197.1 (C **1**); *Accurate Mass* (Negative ion mode, calculated for $C_{28}H_{32}NO_6$ = 478.2235): Found 478.2229.

6.1.7 Synthesis of Generation of 2nd Generation β-Acids

The general reaction scheme is as follows:

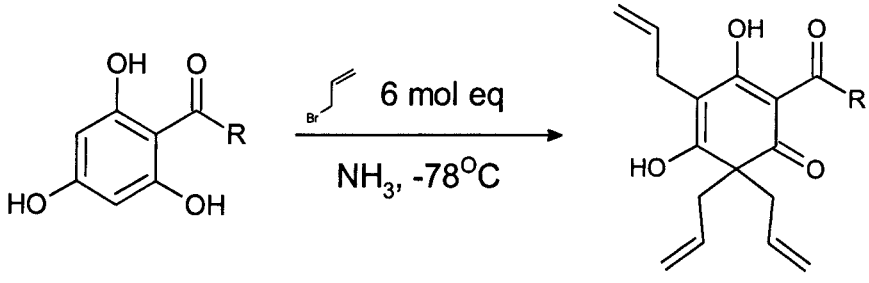

The synthesis of 3,5-dihydroxy-2-(3-methylbutanoyl)-4,6,6-tri(prop-2-en-1-yl)cyclohexa-2,4-dien-1-one **(42a)**

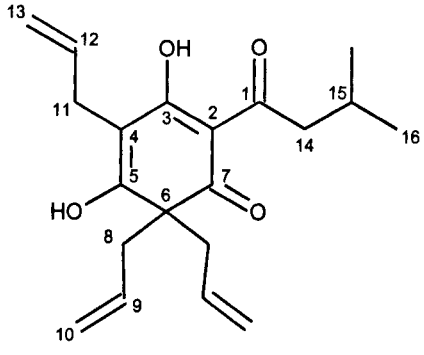

A 2-neck round bottomed flask (250 ml) equipped with a magnetic stirrer bar, nitrogen inlet and rubber septum was charged with sodium-dried ammonia (100 ml) at -78 °C. With stirring, 3-methyl-1-(2,4,6-trihydroxyphenyl)butan-1-one **3e** (1.72 g, 8.21 mmol, 1 eq) dissolved in diethyl ether (30 ml) was added dropwise *via* syringe, and the solution allowed to stir for 15 minutes. Allyl bromide **41** (4.3 ml, 6.01 g, 49.7 mmol, 6 eq) dissolved in diethyl ether (30 ml) was added dropwise *via* syringe and the reaction mixture was stirred at -78 °C for 5 hours.

The reaction mixture was warmed to room temperature overnight to allow the ammonia to carefully evaporate. The semi-solid was diluted in diethyl ether (50 ml), and washed successively with 10% HCl solution (2 x 30 ml), water (2 x 30 ml), brine (2 x 30 ml) and dried over sodium sulphate. The mixture was filtered and the solvent removed *in vacuo*.The crude material was purified by flash column chromatography (100% DCM).The solvent was removed *in vacuo* to give an oil which soon solidified. Recrystallisation from hexane gave white crystals (0.618 g, 1.79 mmol, 22 %). Mpt = 43.9-44.8 °C. ν_{max} (neat)/cm^{-1} = 3191 (O-H), 3079 (Ar-H), 2957, 2922 (C-H), 1641 (C=O), 1588, 1521 (C=C), 1455, 1360 (C-H), 1195, 1133 (C-O), 924 (=C-H); δ_H (400 MHz, CD_3OD) = 0.95 (d, *J* = 6.65 Hz, 3H, CH_3 **16**), 2.11 (quin, *J* = 6.73 Hz 1H, CH **15**), 2.53-2.72 (m, 4H, CH_2 **8**), 2.86 (d, *J* = 6.27, 2H CH_2 **14**), 3.16 (d, *J* = 5.40 Hz, 2H, CH_2 **11**), 4.86-5.08 (m, 6H, CH_2 *HSQC indicates overlapping signals for* **10** *and* **13**), 5.46 (ddt, *J* = 17.13, 9.98, 7.40 Hz, 2H, CH **9**), 5.74-5.87 (m, 1H, CH **12**); δ_C (100 MHz, CD_3OD) = 23.3 (CH_3 **16**), 26.6 (CH **11**), 27.1 (CH_2 **15**), 44.3 (CH_2 **8**), 50.1 (CH_2 **14**), 58.9 (C **6**), 109.4 (C **4**), 110.4 (C **2**), 115.2 (CH_2 **13**), 118.9 (CH_2 **10**), 133.5 (CH **9**), 136.4 (CH **12**), 174.0 (C **5**), 190.8 (C **3**), 197.2 (C **7**), 204.2 (C **1**); *m/z*: = 330 (M^+), 289, 261, 233, 205, 193, 177, 115, 109, 69, 57; *Accurate Mass* (Calculated for $C_{20}H_{26}O_4$ = 330.1826): Found 330.1830.

The synthesis of 3,5-dihydroxy-2-propanoyl-4,6,6-tri(prop-2-en-1-yl)cyclohexa-2,4-dien-1-one **(42b)**

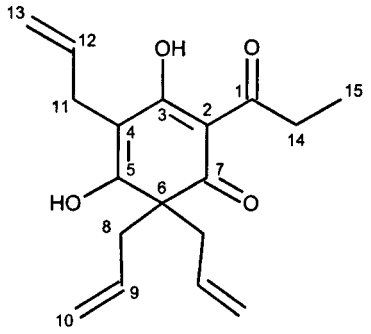

This was carried out as detailed for the synthesis of 3,5-dihydroxy-2-(3-methylbutanoyl)-4,6,6-tri(prop-2-en-1-yl)cyclohexa-2,4-dien-1-one **42a** with the following reagents and quantities:

- 1-(2,4,6-trihydroxyphenyl)propan-1-one **3b** (2.51 g, 13.8 mmol, 1 eq)
- Allyl bromide **41** (4.2 ml, 5.87g, 48.5 mmol, 6 eq)
- Ammonia (150 ml)

The title compound **42b** was obtained as white crystals (0.718 g, 2.18 mmol, 16 %). Mpt = 60.2-61.1 °C (Lit[60]. = 60 °C). ν_{max} (neat)/cm^{-1} = 3586 (O-H), 3079 (=C-H), 2923, 2854 (C-H), 1641 (C=O), 1584, 1519 (C=C), 1463, 1364 (C-H), 1225, 1189, 1167 (C-O), 917 (=C-H); δ_H (400 MHz, CD_3OD) = 1.11 (t, *J* = 7.3, 3H, CH_3 **15**), 2.54-2.72 (m, 4H, CH_2 **8**), 3.00 (q, *J* = 6.5 Hz, 2H CH_2 **14**), 3.16 (d, *J* = 5.4, 2H, CH_2 **11**), 4.82-5.07 (m, 6H, CH_2 *HSQC indicates overlapping signals for* **10** *and* **13**), 5.46 (ddt, *J* = 17.1, 10.0, 7.4, Hz, 2H, CH **9**); 5.74-5.88 (m, 1H, CH **12**); δ_C (100 MHz, CD_3OD) = 9.93 (CH_3 **15**), 26.5 (CH **11**), 35.3 (CH_3 **14**), 44.4 (CH_2 **8**), 59.0 (C **6**), 108.9 (C **4**), 110.1 (C **2**), 115.2 (CH_2 **13**), 118.9 (CH_2 **10**), 133.6 (CH **9**), 136.4 (CH **12**), 174.2 (C **5**), 190.4 (C **3**), 197.2 (C **7**), 205.8 (C **1**); *m/z*: = 302 (M^+), 272, 260, 205, 161, 128, 77, 67, 53; *Accurate Mass* (Calulated for $[C_{18}H_{22}O_4]^+$ = 302.1513): Found 302.1513.

The synthesis of 2-acetyl-3,5-dihydroxy-4,6,6-tri(prop-2-en-1-yl)cyclohexa-2,4-dien-1-one (**42c**)

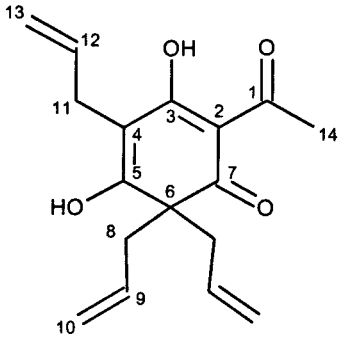

This was carried out as detailed for the synthesis of 3,5-dihydroxy-2-(3-methylbutanoyl)-4,6,6-tri(prop-2-en-1-yl)cyclohexa-2,4-dien-1-one **42a** with the following reagents and quantities:

- 1-(2,4,6-trihydroxyphenyl)ethanone **3a** (4.61 g, 24.8 mmol, 1 eq)
- Allyl bromide **41** (13 ml, 15.4 g, 127 mmol, 5 eq)
- Ammonia (50 ml)

The title compound **42c** was obtained as white crystals (3.67 g, 12.7 mmol, 51%). Mpt = 78.6-79.7 °C (Lit[61]. = 79 °C). ν_{max} (neat)/cm^{-1} = 3079 (=C-H), 2924, 2854 (C-H), 1649 (C=O), 1588, 1460 (C=C), 1243, 1197 (C-O), 926 (=C-H); δ_H (400 MHz, CD_3OD) = 2.23 (s, 3H, CH_3 **14**), 2.56-2.72 (m, 4H, CH_2 **8**), 3.25 (d, *J* = 5.5 Hz, 2H CH_2 **11**), 4.90-5.06 (m, 6H, CH_2 *HSQC indicates overlapping signals for* **10** *and* **13**), 5.47 (ddt, *J* = 17.1, 9.9, 7.4 Hz, 2H, CH **9**), 5.75-5.86 (m, 1H, CH **12**); δ_C (100 MHz, CD_3OD) = 26.5 (CH **11**), 29.2 (CH_3 **14**), 44.3 (CH_2 **8**), 59.0 (C **6**), 109.6 (C **4**), 110.2 (C **2**), 115.1 (CH_2 **13**), 119.0 (CH_2 **10**), 133.5 (CH **9**), 136.4 (CH **12**), 174.2 (C **5**), 190.3 (C **3**), 197.5 (C **7**), 201.8 (C **1**); *m/z*: = 288 (M^+), 273, 246, 228, 205, 191, 163, 91, 69, 53; *Accurate Mass* (calculated for $[C_{17}H_{20}O_4]^+$ = 288.1356): Found 288.1354.

The synthesis of 2-butanoyl-3,5-dihydroxy-4,6,6-tri(prop-2-en-1-yl)cyclohexa-2,4-dien-1-one **(42d)**

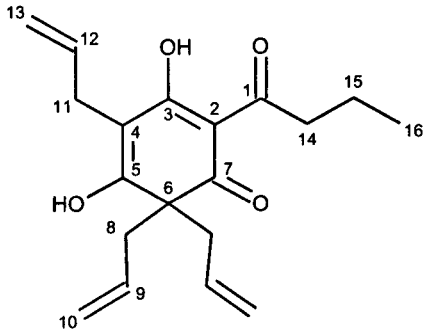

This was carried out as detailed for the synthesis of 3,5-dihydroxy-2-(3-methylbutanoyl)-4,6,6-tri(prop-2-en-1-yl)cyclohexa-2,4-dien-1-one **42a** with the following reagents and quantities:

- 1-(2,4,6-trihydroxyphenyl)butan-1-one **3c** (4.36 g, 22.3 mmol, 1eq)
- Allyl bromide **41** (11.5 ml, 16.1 g, 132 mmol, 6eq)
- Ammonia (200 ml)

The title compound **42d** was obtained as white crystals (3.46 g, 10.9 mmol, 49 %). Mpt = 55.2-56.4 °C. ν_{max} (neat)/cm^{-1} = 3080 (=C-H), 2924, 2854 (C-H), 1648 (C=O), 1582, 1523 (C=C), 1459, 1378 (C-H), 1218, 1193, 1107 (C-O), 917 (=C-H); δ_H (400 MHz, CD_3OD) = 0.97 (t, *J* = 7.4 Hz, 3H, CH_3 **16**), 1.63 (sxt, *J* = 7.4 Hz 2H, CH_2 **15**), 2.53-2.74 (m, 4H, CH_2 **8**), 2.95 (br. s, 2H CH_2 **14**), 3.16 (d, *J* = 5.3 Hz, 2H, CH_2 **11**), 4.92-5.10 (m, 6H, CH_2 *HSQC indicates overlapping signals for* **10** *and* **13**), 5.46 (ddt, *J* = 17.2, 10.0, 7.4, Hz, 2H, CH **9**), 5.73-5.90 (m, 1H, CH **12**); δ_C (100 MHz, CD_3OD) = 14.5 (CH_3 **16**), 19.7 (CH_2 **15**), 26.5 (CH **11**), 43.6 (CH_2 **14**), 44.3 (CH_2 **8**), 59.0 (C **6**), 109.1 (C **4**), 110.3 (C **2**), 115.1 (CH_2 **13**), 119.0 (CH_2 **10**), 133.5 (CH **9**), 136.4 (CH **12**), 174.0 (C **5**), 190.6 (C **3**), 197.1 (C **7**), 204.8 (C **1**); *m/z*: = 316 (M^+), 275, 233, 203, 188, 161, 115, 79, 55; *Accurate Mass* (Calculated for $C_{19}H_{24}O_4$ = 316.1669): Found 316.1673.

The synthesis of 3,5-dihydroxy-2-(2-methylpropanoyl)-4,6,6-tri(prop-2-en-1-yl)cyclohexa-2,4-dien-1-one **(42e)**

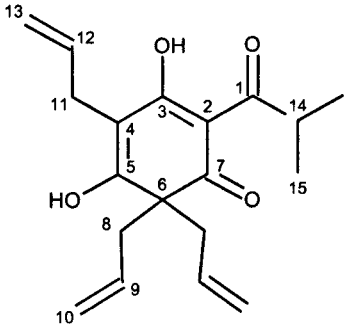

This was carried out as detailed for the synthesis of 3,5-dihydroxy-2-(3-methylbutanoyl)-4,6,6-tri(prop-2-en-1-yl)cyclohexa-2,4-dien-1-one **42a** with the following reagents and quantities:

- 2-methyl-1-(2,4,6-trihydroxyphenyl)propan-1-one **3d** (1.55 g, 7.88 mmol, 1 eq)
- Allyl bromide **41** (5.7 ml, 7.97 g, 65.9 mmol, 8 eq)
- Ammonia (100 ml)

The title compound **42e** was obtained as white crystals (0.964 g, 3.05 mmol, 39%). Mpt = 52.4-53.4 °C. ν_{max} (neat)/cm^{-1} = 3239 (O-H), 2980, 2936 (C-H), 1656 (C=O), 1584, 1519 (C=C), 1429, 1360 (C-H), 1226, 1160, 1125 (C-O), 922 (=C-H); δ_H (400 MHz, CD_3OD) = 1.10 (d, *J* = 6.8 Hz, 6H, CH_3 **15**), 2.54-2.73 (m, 4H, CH_2 **8**), 3.16 (d, *J* = 5.7 Hz, 2H, CH_2 **11**), 4.00 (dt, *J* = 12.9, 6.6, 1H CH **14**), 4.90-5.07 (m, 6H, CH_2 *HSQC indicates overlapping signals for* **10** *and* **13**), 5.46 (ddt, *J* = 17.1, 10.0, 7.4 Hz, 2H, CH **9**), 5.81 (ddt, *J* = 17.1, 10.2, 5.8, Hz, 2H, CH **12**); δ_C (100 MHz, CD_3OD) = 19.7 (CH_2 **15**), 26.6 (CH **11**), 37.4 (CH_2 **14**), 44.4 (CH_2 **8**), 59.1 (C **6**), 108.1 (C **4**), 110.3 (C **2**), 115.2 (CH_2 **13**), 119.0 (CH_2 **10**), 133.6 (CH **9**), 136.5 (CH **12**), 174.0 (C **5**), 191.0 (C **3**), 196.9 (C **7**), 209.3

(C **1**); *m/z*: = 316 (M^+), 275, 247, 204, 190, 161, 128, 91, 53; *Accurate Mass* (Calculated for $[C_{19}H_{24}O_4]^+$ = 316.1669): Found 316.1671.

The synthesis of 2-(cyclopropylcarbonyl)-3,5-dihydroxy-4,6,6-tri(prop-2-en-1-yl)cyclohexa-2,4-dien-1-one **(42f)**

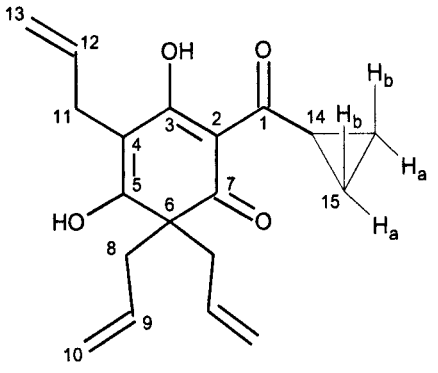

This was carried out as detailed for the synthesis of 3,5-dihydroxy-2-(3-methylbutanoyl)-4,6,6-tri(prop-2-en-1-yl)cyclohexa-2,4-dien-1-one **42a** with the following reagents and quantities:

- cyclopropyl(2,4,6-trihydroxyphenyl)methanone **3g** (3.50 g, 18.0 mmol, 1 eq)
- Allyl bromide **41** (9.4 ml, 13.1 g, 109 mmol, 6 eq)
- Ammonia (200 ml)

The title compound **42f** was obtained as white crystals (1.74 g, 5.53 mmol, 31%). Mpt 65.1-66.5 °C. ν_{max} (neat)/cm^{-1} = 3205 (O-H), 3081 (Ar-H), 2980, 2922 (C-H), 1639 (C=O), 1572, 1510 (C=C), 1436, 1315 (C-H), 1186, 1100 (C-O), 922 (=C-H); δ_H (400 MHz, CD_3OD) = 1.04 (m, 2H, CH_a **15**), 1.18 (m, 2H, CH_b **15**), 2.54-2.73 (m, 4H, CH_2 **8**), 3.16 (dt, *J* = 5.7, 1.7 Hz, 2H, CH_2 **11**), 3.61 (br. s, 1H CH **14**), 4.89-5.07 (m, 6H, CH_2 *HSQC indicates overlapping signals for* **10** *and* **13**); 5.40-5.59 (m, 2H, CH **9**), 5.80 (ddt, *J* = 17.2, 10.2, 5.8 Hz, 2H, CH **12**);

δ_C (100 MHz, CD_3OD) = 12.8 (CH_2 **15**), 18.3 (CH **14**); 26.6 (CH_2 **11**), 44.4 (CH_2 **8**), 59.1 (C **6**), 109.5 (C **4**), 109.9 (C **2**), 115.1 (CH_2 **13**), 118.9 (CH_2 **10**), 133.6 (CH **9**), 136.5 (C **12**), 173.7 (C **5**), 189.9 (C **3**), 197.7 (C **7**), 204.4 (C **1**); *m/z*: = 314 (M^+), 286, 273, 245, 203, 163, 135, 109, 91, 69, 53; *Accurate Mass* (Calculated for $[C_{19}H_{22}O_4]^+$ = 314.1513): Found 314.1514.

The synthesis of 2-(cyclopentylcarbonyl)-3,5-dihydroxy-4,6,6-tri(prop-2-en-1-yl)cyclohexa-2,4-dien-1-one **(42g)**

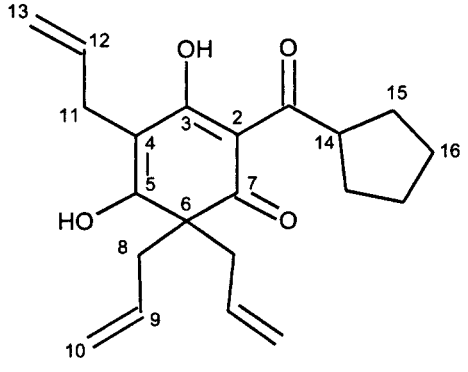

This was carried out as detailed for the synthesis of 3,5-dihydroxy-2-(3-methylbutanoyl)-4,6,6-tri(prop-2-en-1-yl)cyclohexa-2,4-dien-1-one **42a** with the following reagents and quantities:

- cyclopentyl(2,4,6-trihydroxyphenyl)methanone **3i** (2.88 g, 13.0 mmol, 1 eq)
- Allyl bromide **41** (4.5 ml, 6.29 g, 52.0 mmol, 4 eq)
- Ammonia (150 ml)

The title compound **42g** was obtained as white crystals (0.615 g, 1.79 mmol, 14%). Mpt = 57.7-59.1 °C. δ_H (400 MHz, CD_3OD) = 1.58-1.66 (m, 2H, CH **16**), 1.67-1.78 (m, 4H, CH *HSQC indicates overlapping signals for* **15** *and* **16**), 1.85-1.96 (m, 2H, CH **15**), 2.52-2.74 (m, 4H, CH_2 **8**), 3.16 (d, *J* = 5.5 Hz, 2H, CH_2

11), 4.11-4.22 (m, 1H, CH **14**), 4.88-5.07 (m, 6H, CH_2 *HSQC indicates overlapping signals for* **10** *and* **13**), 5.47 (ddt, *J* = 17.2, 10.1, 7.4, Hz, 2H, CH **9**), 5.76-5.88 (m, 1H, CH **12**); δ_C (100 MHz, CD_3OD) = 26.6 (CH **11**), 27.3 (CH_2 **16**), 30.9 (CH_2 **15**) 44.4 (CH_2 **8**), 48.9 (CH_2 **14**), 59.0 (C **6**), 108.6 (C **4**), 110.2 (C **2**), 115.1 (CH_2 **13**), 118.9 (CH_2 **10**), 133.6 (CH **9**), 136.5 (CH **12**), 173.8 (C **5**), 190.7 (C **3**), 197.0 (C **7**), 207.7 (C **1**); *Accurate Mass* (Positive ion mode, calculated for $[(C_{21}H_{26}O_4)H]^+$ = 343.1904): Found 343.1899.

6.1.8 Synthesis of 3rd Generation β-Acids Using Ring-Closing Metathesis

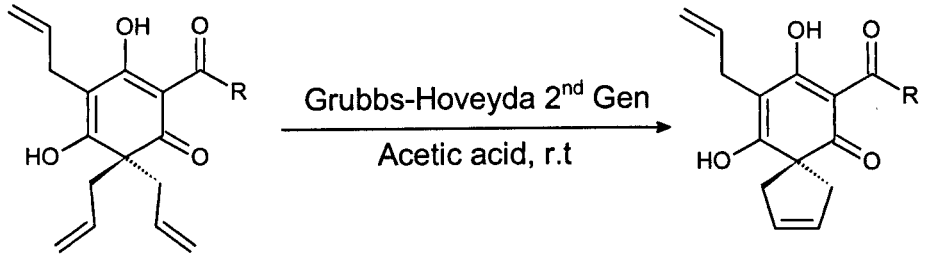

The synthesis of 7-acetyl-8,10-dihydroxy-9-(prop-2-en-1-yl)spiro[4.5]deca-2,7,9-trien-6-one (**50**)

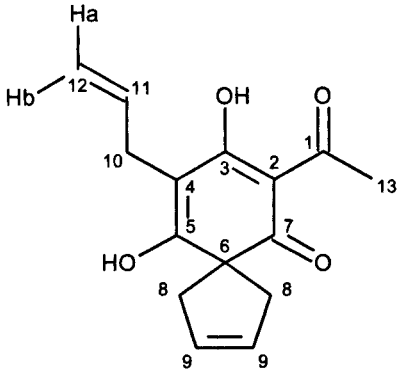

A 2-neck round bottomed flask (250 ml), equipped with a magnetic stirrer bar, a rubber septum and a gas-bubbler was charged with acetic acid (100 ml) and 2-acetyl-3,5-dihydroxy-4,6,6-tri(prop-2-en-1-yl)cyclohexa-2,4-dien-1-one **42c** (1.04

g, 3.59 mmol, 1 eq). Nitrogen gas was bubbled through the solvent *via* a long needle, with vigorous stirring, for 3 hours to remove dissolved oxygen gas. The bubbler was quickly replaced with a nitrogen inlet. Quickly and with a strong positive pressure of nitrogen gas, the rubber septum was removed and Hoveyda-Grubbs Catalyst 2nd Generation **49d** (0.0848 g, 0.135 mmol, 0.04 eq) was added in one portion. Septum returned, the reaction was monitored at half-hour intervals by TLC and GCMS to determine when the reaction end-point. Water (100 ml) was added and the product extracted into diethyl ether (100 ml). The organic layer was washed with water (3 x 100 ml), then brine (2 x 50 ml), and the solvent removed *in vacuo* to give a brown crude, purified by flash column chromatography (25% ethyl acetate : 75% petroleum ether) to give a light brown oil which solidified under high vacuum. Recrystallisation with hexane yielded white crystals (0.130 g, 0.499 mmol, 14 %). δ_H (400 MHz, CD_3OD) = 2.53 (s, 3H, CH_3 **13**), 2.73-2.90 (m, 4H, CH_2 **8**), 3.16 (dt, *J* = 5.8, 1.5 Hz, 2H CH_2 **11**), 4.94 (dq, *J* = 10.2, 1.5 Hz, 1H, CH_b **12**), 4.99 (dq, *J* = 17.1, 1.8 Hz, 1H, CH_a **12**), 5.67 (br.s, 2H, CH **9**), 5.84 (ddt, *J* = 17.1, 10.2, 5.8 Hz , 1H, CH **11**); *m/z*: = 260 (M^+), 245, 227, 218, 190, 177, 153, 107, 93, 77, 65, 53; *Accurate Mass* (Calculated for $[C_{15}H_{16}O_4]^+$ = 260.1043): Found 260.1041.

The synthesis of 7-(cyclopropylcarbonyl)-8,10-dihydroxy-9-(prop-2-en-1-yl)spiro[4.5]deca -2,7,9-trien-6-one **(50a)**

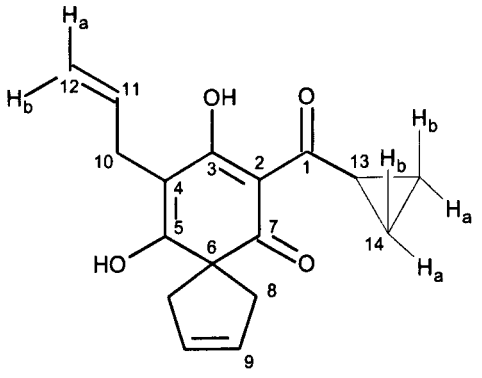

A 2-neck round bottomed flask (250 ml), equipped with a magnetic stirrer bar, a rubber septum and a gas-bubbler was charged with acetic acid (100 ml) and 2-(cyclopropylcarbonyl)-3,5-dihydroxy-4,6,6-tri(prop-2-en-1-yl)cyclohexa-2,4-dien-1-one **42f** (1.13 g, 3.59 mmol, 1 eq). Nitrogen gas was bubbled through the solvent *via* a long needle, with vigorous stirring, for 1 hour to remove dissolved oxygen gas. The bubbler was quickly replaced with a nitrogen inlet. Quickly and with a strong positive pressure of nitrogen gas, the rubber septum was removed and Hoveyda-Grubbs Catalyst 2nd Generation **49d** (0.0876 g, 0.140 mmol, 0.04 eq) was added in one portion and the septum returned. The reaction was monitored at half-hour intervals by TLC and GCMS to determine when the reaction end-point. Water (100 ml) was added and the product extracted into diethyl ether (100 ml). The organic layer was washed with water (3 x 100 ml), then brine (2 x 50 ml), and the solvent removed *in vacuo* to give a brown crude, purified by flash column chromatography (20% ethyl acetate : 80% petroleum ether) to give a light brown oil which solidified under high vacuum. Recrystallisation with hexane yielded white crystals (0.0115 g, 0.402 mmol, 11%). ν_{max} (neat)/cm^{-1} = 3334 (O-H). 2923 (C-H), 1631 (C=O), 1566, 1505

(C=C), 1426, 1329 (C-H), 1221, 1113 (C-O), 921 (=C-H); δ_H (400 MHz, CD_3OD) = 0.99-1.05 (m, 2H, CH_a **14**), 1.14-1.22 (m, 2H, CH_b **14**), 2.73-2.95 (m, 4H, CH_2 **8**), 3.15 (dt, *J* = 5.8, 1.5 Hz, 2H, CH_2 **10**), 3.47-3.56 (m, 1H, CH **13**), 4.95 (d, *J* = 9.8 Hz, 1H CH_b **12**), 4.99 (d, *J* = 16.9 Hz, 1H CH_a **12**), 5.96 (br.s, 2H, CH **9**), 5.84 (ddt, *J* = 16.9, 10.2, 5.6, Hz, 2H, CH **11**); δ_C (100 MHz, CD_3OD) = 12.5 (CH_2 **14**), 17.8 (CH **13**), 26.3 (CH_2 **10**), 46.5 (CH_2 **8**), 58.0 (C **6**), 105.8 (C **4**), 106.5 (C **2**), 114.7 (CH_2 **12**), 129.3 (CH **9**), 176.0 (C **5**), 189.5 (C **3**), 199.6 (C **7**), 205.2 (C **1**); *Accurate Mass* (Calculated for $C_{17}H_{18}O_4$ = 286.1200): Found 286.1198.

6.1.9 Lithio-cuprate Coupling of Allyl Bromides to 1,3,5-trimethoxybenzene

The general reaction scheme is as follows:

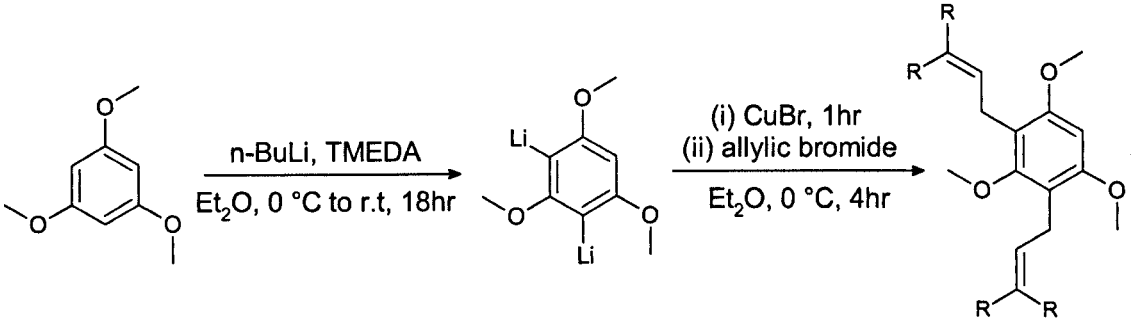

The synthesis of 1,3,5-trimethoxy-2,4-di(prop-2-en-1-yl)benzene **(56a)**

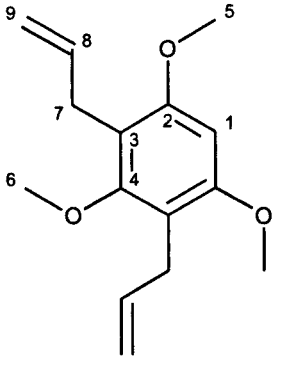

Into a round bottomed flask (250 ml) equipped with a nitrogen inlet and a rubber septum was added 1,3,5-trimethoxybenzene **38** (3.34 g, 18.7 mmol, 1eq) and diethyl ether (60 ml). Tetramethylethylenediamine (11.1 ml, 8.66 g, 74.5 mmol, 4eq) was added and the solution cooled in an ice bath. *n*-Butyl lithium (2.0 M solution in hexane, 37 ml, 74 mmol, 4eq) was added dropwise *via* syringe then allowed to slowly warm to room temperature and stirred for a further 18 hours. A separate 3-neck round bottomed flask, equipped with a magnetic stirrer bar, nitrogen inlet, a dropping funnel and a rubber septum was charged with copper (I) iodide (14.4 g, 75.6 mmol, 4eq), diethyl ether (20 ml), and cooled in an ice bath. The tan-yellow suspension of lithiated 1,3,5-trimethoxybenzene was transferred *via* cannula to the dropping funnel, and added slowly to the stirred suspension of CuI over 30 minutes. The mixture was stirred in an ice bath for a further 1 hour, then allyl bromide **41** (8 ml, 9.10 g, 75.2 mmol, 4eq) was added dropwise *via* syringe and the temperature maintained at 0 °C. After 4 hours, the reaction was quenched by addition of water (30 ml), then poured into saturated ammonium chloride solution (30 ml). The product was extracted 3 times into diethyl ether (50 ml), and the combined organic layers were washed with water (2 x 30 ml) and brine (30 ml) then dried over anhydrous sodium sulphate. The solvent was removed *in vacuo* and the resulting crude purified by flash column chromatography (20% ethyl acetate / 80% petroleum ether) to afford the product as a pale yellow oil (2.82 g, 11.4 mmol, 61%). ν_{max} (neat)/cm^{-1} = 3076 (Ar-H), 2936, 2835 (C-H), 1600 (C=C), 1455, 1406 (C-H), 1079 (C-O), 905 (=C-H). δ_H (400 MHz, CD_3OD) = 3.38 (dt, J = 5.98, 1.69 Hz, 4H, CH2 **7**); 3.72 (s, 3H, CH3 **6**); 3.83 (s, 6H, CH_3 **5**); 4.94-5.01 (m, 4H, CH_2 **9**); 6.01 (ddt, J = 17.00, 5.99 Hz, 2H, CH **8**); 6.32 (s, 1H, CH, **1**). δ_C (100 MHz, CD_3OD) = 28.0 (CH_2 **7**);

55.7 (CH_3 **5**); 62.0 (CH_3 **6**); 91.8 (CH **1**); 113.8 (C **4**); 114.0 (CH2 **9**); 137.7 (CH **8**); 157.3 (C **4**); 157.8 (C **3**). *m/z*: = 248 (M^+), 233, 217, 176, 161, 145, 128, 115, 103, 91, 77, 69, 53. *Accurate Mass* (calculated for $[C_{15}H_{20}O_3]^+$ = 248.1407): 248.1404.

The synthesis of 1,3,5-trimethoxy-2,4-bis(3-methylbut-2-en-1-yl)benzene **(56b)**

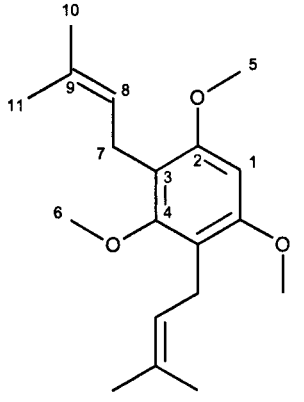

Into a round bottomed flask (250 ml) equipped with a nitrogen inlet and a rubber septum was added 1,3,5-trimethoxybenzene **38** (3.47 g, 20.7 mmol, 1eq) and diethyl ether (60 ml). Tetramethylethylenediamine (12.0 ml, 9.36 g, 80.5 mmol, 4eq) was added *via* syringe and the solution cooled in an ice bath. *n*-Butyl lithium (2.0 M solution in hexane, 40 ml, 80 mmol, 4eq) was added dropwise *via* syringe, allowed to slowly warm to room temperature, and stirred for a further 18 hours. Into a separate 3-neck round bottomed flask, equipped with a magnetic stirrer bar, nitrogen inlet, a dropping funnel and a rubber septum was added copper (I) iodide (15.8 g, 83.0 mmol, 4eq) and diethyl ether (20 ml), and cooled in an ice bath. The tan-yellow suspension of lithiated 1,3,5-trimethoxybenzene was transferred *via* cannula to the dropping funnel, and added slowly to the stirred suspension of CuI over 30 minutes. The mixture was stirred in an ice bath for a further 1 hour, before the dropwise addition of 3,3-

dimethylallyl bromide **23** (7.3 ml, 9.3 g, 63 mmol, 3eq). The reaction mixture was maintained at a cool temperature in the ice bath and monitored by TLC. After 4 hours, the reaction was quenched by addition of water (30 ml), then pouring into saturated ammonium chloride solution (30 ml). The product was extracted 3 times into diethyl ether (50 ml), which was washed with water (2 x 30 ml) and brine (30 ml) then dried over sodium sulphate. The solvent was removed *in vacuo* and the resulting crude purified by flash column chromatography (20% ethyl acetate / 80% petroleum ether) to afford the product as a pale yellow oil (3.50 g, 11.5 mmol, 56%). ν_{max} (neat)/cm^{-1} = 2922.4 (C-H), 1597 (C=C), 1454, 1435, 1406 (C-H), 1095, 1056 (C-O), 945, 804. δ_H (400 MHz, CD_3OD) = 1.67 (d, *J* = 1.13 Hz, 6H, CH_3 **11**); 1.77 (d, *J* = 0.88 Hz, CH_3 **10**); 3.30 (d, *J* = 6.78 Hz, 4H, CH_2 **7**); 3.70 (s, 3H, CH_3 **6**); 3.83 (s, 6H, CH_3 **5**); 5.19 (tdt, *J* = 6.82, 6.82, 2.81, 1.38 Hz, 2H, CH **8**); 6.31 (s, 1H, CH **1**) . δ_C (100 MHz, CD_3OD) = 17.8 (CH_3 **10**); 22.9 (CH_2 **7**); 25.7 (CH_3 **11**); 55.8 (CH_3 **5**); 61.6 (CH_3 **6**); 91.1 (CH **1**); 115.7 (C **4**); 124.0 (CH **8**); 130.6 (CH_2 **9**); 156.9 (C **4**); 157.5 (C **3**). *m/z*: = 304 (M^+), 233, 205, 191, 179, 145, 115, 91, 69, 55. *Accurate Mass* (calculated for $[C_{19}H_{28}O_3]^+$ = 304.2033): 304.2036.

6.2 Microbiology and Antibacterial Testing

6.2.1 Materials

Bacteria was taken from stocks held within the university, stored at -80 °C. Methicillin-resistant *Staphylococcus aureus* strains were acquired from London hospitals. Petri dishes measured 90 mm x 16.2 mm and were purchased from SLS. Ringers solution tablets, nutrient agar powder and Mueller-Hinton agar powder was purchased from Sigma Aldrich, and used as directed on the

packaging. All preparation and experimental work was performed in an aseptic environment, using equipment that was sterilised in an autoclave prior to use, or purchased as sterile, one-time-use items.

6.2.2 Preparation of Bacterial Suspensions

*Escherichia coli, Pseudomonas, Proteus, Staphylococcus epidermidis, Baccilus subtilis,*methicillin-sensitive *Staphylococcus aureus* (MSSA) and methicillin-resistant *Staphylococcus aureus* (MRSA) where subcultured from stocks taken from a -80 °C store. From each stock, a subculture was grown by inoculating a nutrient agar plate with an individual bacteria and incubating at 37 °C for 18 hours. From this subculture, a further subculture onto nutrient agar was performed using a defined streaking pattern (**Figure 76**) to grow well defined, individual colonies to use in the disc diffusion assay; again, the bacteria were incubated at 37 °C for 18 hours.

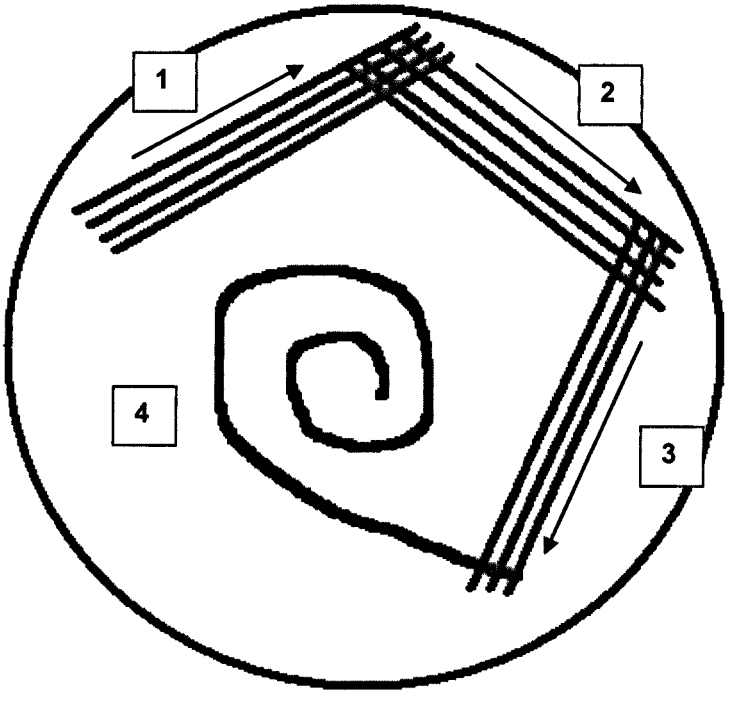

Figure 76: *Streaking pattern used to subculture bacteria before use in the disc diffusion assay*

Using a flame-sterilised loop, 3-5 colonies of a given bacteria where touched, and suspended in Ringers solution (5 ml). The turbidity of the suspension was adjusted to match that of a 0.5 McFarland Standard solution, either by the addition of bacteria or the addition of Ringer solution.

The Ringers suspensions of bacteria were discarded after use, and the bacteria re-subcultured onto fresh nutrient agar plates before the next experiment.

6.2.3 Preparation of the Infused Discs

Each compound was diluted in ethanol to produce a 0.05 M solution. From these stocks, 10 µL was taken and deposited on a filter-paper disc measuring 6 mm in diameter by use of a calibrated Gilson pipette. The ethanol was allowed to evaporate producing dry discs infused with an individual compound; enough discs were prepared to last the duration of the planned experiments, and when not used were stored under nitrogen in a freezer.

Mueller-Hinton agar was prepared according to the packaging instructions, and poured into petri dishes to a depth of 4 mm. These were then inoculated with a given bacteria from its respective Ringers suspension using a sterile cotton swab, ensuring full coverage of the plate was achieved. For each inoculated plate, two samples of compound-infused plate were placed on the agar, with a negative control (blank disc) and a positive control (ciprofloxacin 5 µg or vancomycin 5 µg discs) (**Figure 77**)

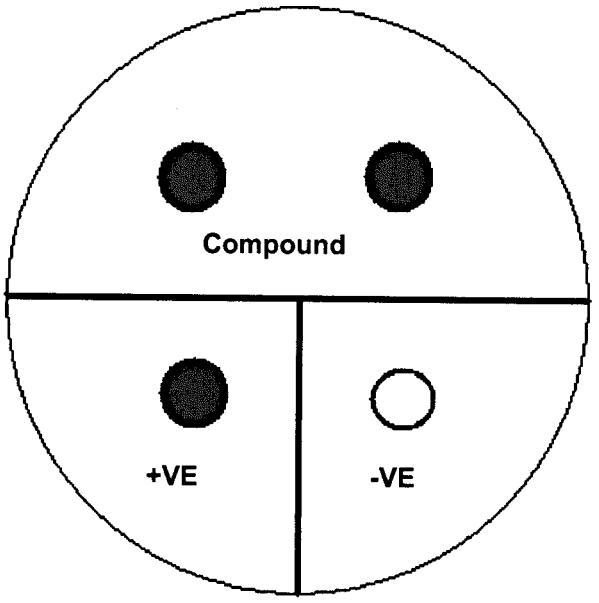

Figure 77: *Each inoculated agar plate had placed upon it two samples of a compound disc (top), a positive (+VE) control (commercially available antibiotic disc, bottom left) and a negative (-VE) control (blank disc, bottom right).*

The plates were incubated at 37 °C for 18 hours, and then the diameter (mm) of the zone where no bacteria had grown was measured using a metal rule. These experiments were performed in triplicate for each compound against each bacteria species, on successive days. The results were compiled, and the arithmetic mean with an associated standard deviation calculated.

Chapter Seven:

References

1. M. Van Cleemput, K. Cattoor, K. De Bosscher, G. Haegeman, D. De Keukeleire and A. Heyerick, *J Nat Prod*, 2009, **72**, 1220-1230.
2. K. Sakamoto and W. N. Konings, *International Journal of Food Microbiology*, 2003, **89**, 105-124.
3. G. Wang, L. Tian, N. Aziz, P. Broun, X. Dai, J. He, A. King, P. X. Zhao and R. A. Dixon, *Plant physiology*, 2008, **148**, 1254-1266.
4. Y. Okada and K. Ito, *Bioscience, Biotechnology, and Biochemistry*, 2001, **65**, 150-155.
5. Y. Tsurumaru, K. Sasaki, T. Miyawaki, Y. Uto, T. Momma, N. Umemoto, M. Momose and K. Yazaki, *Biochemical and Biophysical Research Communications*, 2012, **417**, 393-398.
6. F. Suen-Ying, K. W. M. Zuurbier, N. B. Paniego, J. J. C. Scheffer and R. Verpoorte, *Phytochemistry*, 1997, **44**, 1047-1053.
7. S. Hecht, K. Kammhuber, J. Reiner, A. Bacher and W. Eisenreich, *Phytochemistry*, 2004, **65**, 1057-1060.
8. K. W. M. Zuurbier, S.-Y. Fung, J. J. C. Scheffer and R. Verpoorte, *Phytochemistry*, 1998, **49**, 2315-2322.
9. K. W. M. Zuurbier, S.-Y. Fung, J. J. C. Scheffer and R. Verpoorte, *Phytochemistry*, 1995, **38**, 77-82.
10. B. J. Clarke and R. P. Hildebrand, *Journal of the Institute of Brewing*, 1965, **71**, 11.
11. O, Vitzthum, P. Hubert and W. Sirtl, US Patent 4104409, 1976.
12. C. J. Dahlberg, G. Harris, J. Urban, M. L. Tripp, J. S. Bland and B. J. Carroll, *Journal of Separation Science*, 2012, **35**, 1183-1189.
13. G. A. Howard, J. R. A. Pollock and A. R. Tatchell, *Journal of the Chemical Society (Resumed)*, 1955, 174.
14. M. Collins and D. R. J. Laws, *Journal of the Chemical Society, Perkin Transactions 1*, 1973, 2013.
15. G. Haseleu, D. Intelmann and T. Hofmann, *Food Chemistry*, 2009, **116**, 71-81.
16. D. Wright, *Journal of the Chemical Society (Resumed)*, 1963, 1769.
17. J. Coates, D. R. J. Laws and J. A. Elvidge, *Journal of the Chemical Society, Perkin Transactions 1*, 1974, 36.

18. E. Tyrrell, R. Archer, G. A. Skinner, K. Singh, K. Colston and C. Driver, *Phytochemistry Letters*, 2010, **3**, 17-23.
19. G. Haseleu, A. Lagemann, A. Stephan, D. Intelmann, A. Dunkel and T. Hofmann, *Journal of Agricultural and Food Chemistry*, 2010, **58**, 7930-7939.
20. P. James, T. Tynan, I. McMurrough and J. Byrne, *Journal of the Institute of Brewing*, 1990, **96**, 5.
21. M. Frobisher, *Fundamentals of microbiology : an introduction to the microorganisms with special reference to the procaryons*, 8th ed. edn., Saunders, 1968.
22. S. P. Denyer and W. B. P. m. Hugo, *Hugo and Russell's pharmaceutical microbiology*, 8th ed. edn., Wiley-Blackwell, Oxford, 2011.
23. http://micro.digitalproteus.com/, Accessed 31st July 2012.
24. D. M. Rollins and S. W. Joseph, http://www.life.umd.edu/classroom/bsci424/LabMaterialsMethods/GramStain.htm, Accessed 25th August, 2012.
25. W. J. Simpson, *Journal of the Institute of Brewing*, 1993, **99**, 405-411.
26. W. J. Simpson, *Journal of General Microbiology*, 1993, **139**, 1041-1045.
27. J. L. Shimwell, *Journal of the Institute of Brewing*, 1937, **43**, 111-118.
28. A. F. Schmalreck, M. Teuber, W. Reininger and A. Hartl, *Canadian Journal of Microbiology*, 1975, **21**, 205-212.
29. S. Bhattacharya, S. Virani, M. Zavro and G. J. Haas, *Economic Botany*, 2003, **57**, 118-125.
30. N. Yamaguchi, K. Satoh-Yamaguchi and M. Ono, *Phytomedicine*, 2009, **16**, 369-376.
31. A. E. Larson, R. R. Y. Yu, O. A. Lee, S. Price, G. J. Haas and E. A. Johnson, *International Journal of Food Microbiology*, 1996, **33**, 195-207.
32. K. Sakamoto, A. Margolles, H. W. v. Veen and W. N. Konings, *Journal of Bacteriology*, 2001, **183**, 5371-5375.
33. R. F. Pratt, *Journal of the Chemical Society, Perkin Transactions 2*, 2002, 851-861.
34. J. F. Fisher, S. O. Meroueh and S. Mobashery, *Chemical Reviews*, 2005, **105**, 395-424.
35. G. Wright, *Advanced Drug Delivery Reviews*, 2005, **57**, 1451-1470.

36. E. Lobkovsky, E. M. Billings, P. C. Moews, J. Rahil, R. F. Pratt and J. R. Knox, *Biochemistry*, 1994, **33**, 6762-6772.
37. Y. Utsui and T. Yokota, *Antimicrob Agents Chemother.*, 1985, **28**, 7.
38. Y. Tsurusako, K. Fukushima, K. Nishizaki, T. Takata, T. Ogawa, T. Nakashima, K. Sugata, S. Yorizane, T. Ogawara and Y. Masuda, *Acta oto-laryngologica. Supplementum*, 1999, **540**, 67-71.
39. F. D. Lowy, *Journal of Clinical Investigation*, 2003, **111**, 1265-1273.
40. P. C. Appelbaum, *International Journal of Antimicrobial Agents*, 2007, **30**, 398-408.
41. R. C. Moellering, *Clinical Infectious Diseases*, 2006, **42**, S3-S4.
42. MHRA, *PL 24701/0022-3*, http://www.mhra.gov.uk/home/groups/par/documents/websiteresources/con088014.pdf, Accessed 13th September, 2012.
43. http://www.cancerresearchuk.org/.
44. *All Cancers Combined - Key Facts*, http://www.cancerresearchuk.org/cancer-info/cancerstats/keyfacts/Allcancerscombined/, Accessed 16th November 2012, 2012.
45. *Breast Cancer - Key Facts*, http://www.cancerresearchuk.org/cancer-info/cancerstats/keyfacts/breast-cancer/, Accessed 16th November 2012, 2012.
46. *Breast Cancer Survival Statistics*, http://www.cancerresearchuk.org/cancer-info/cancerstats/types/breast/survival/#Trends, Accessed 16th November 2012, 2012.
47. *Prostate Cancer - Key Facts*, http://www.cancerresearchuk.org/cancer-info/cancerstats/keyfacts/prostate-cancer/, Accessed 16th November 2012, 2012.
48. *Prostate Cancer - Survival Statistics*, http://www.cancerresearchuk.org/cancer-info/cancerstats/types/prostate/survival/, Accessed 16th November 2012, 2012.
49. H. Tobe, M. Kubota, M. Yamaguchi, T. Kocha and T. Aoyagi, *Bioscience, Biotechnology and Biochemistry*, 1997, **61**, 1027-1029.

50. Y. Honma, H. Tobe, M. Makishima, A. Yokoyama and J. Okabe-Kado, *Leukemia Research*, 1998, **22**, 605-610.
51. D. D. Bikle, *Endocrine reviews*, 1992, **13**, 765-784.
52. T. E. Stephan, E. O. Ngo and L. M. Nutter, *Biochemical Pharmacology*, 1998, **55**, 505-514.
53. W. C. Su, *Japanese Journal of Clinical Oncology*, 2000, **30**, 562-567.
54. W.-J. Chen and J.-K. Lin, *Journal of Agricultural and Food Chemistry*, 2004, **52**, 55-64.
55. N. N. Danial and S. J. Korsmeyer, *Cell*, 2004, **116**, 205-219.
56. J. C. Sharpe, D. Arnoult and R. J. Youle, *Biochimica et Biophysica Acta (BBA) - Molecular Cell Research*, 2004, **1644**, 107-113.
57. A. H. Boulares, *Journal of Biological Chemistry*, 1999, **274**, 22932-22940.
58. V. Lamy, S. Roussi, M. Chaabi, F. Gosse, N. Schall, A. Lobstein and F. Raul, *Carcinogenesis*, 2007, **28**, 1575-1581.
59. J. P. Maye, D. Beddie and G. Pollach, European Patent 6893857, 2005.
60. D. L Seman, J. A. Hirschey, A. L. Milkowski and M. Barney, US Patent 2004/0175480, 2003.
61. R. J. H Wilson, R. J. Smith and G. Hass, US Patent 7910140, 2011.
62. J. P. May, US Patent 2004/0044087, 2003.
63. W. Riedl and J. Nickl, *Chemische Berichte*, 1956, **89**, 1838-1849.
64. M. Collins, D. R. J. Laws, J. D. McGuinness and J. A. Elvidge, *Journal of the Chemical Society C: Organic*, 1971, 3814-3818.
65. K. G. Drewett and D. R. J. Laws, *Journal of the Institute of Brewing*, 1970, **76**, 188-190.
66. C. Friedel and J. M. Crafts, *Comptes Rendus*, 1877, **84**, 4.
67. C. Friedel and J. M. Crafts, *Comptes Rendus*, 1877, **84**, 5.
68. K. Hoesch, *Berichte der deutschen chemischen Gesellschaft*, 1915, **48**, 1122-1133.
69. J. Houben, *Berichte der deutschen chemischen Gesellschaft (A and B Series)*, 1926, **59**, 2878-2891.
70. K. Venkataraman, S. R. Seth and K. C. Gulati, *Organic Syntheses*, 1943, **2**, 522-523.
71. E. K. Raja and D. A. Klumpp, *Tetrahedron Letters*, 2011, **52**, 5170-5172.
72. E. K. Raja and D. A. Klumpp, *Tetrahedron*, 2011, **67**, 4494-4497.

73. R. Salmon and I. V. Efremov, in *Encyclopedia of Reagents for Organic Synthesis*, John Wiley & Sons, Ltd, 2001.
74. R. J. Fessenden, J. S. Fessenden and M. W. Logue, *Organic Chemistry (Non-InfoTrac Version)*, Brooks/Cole, 1998.
75. *United States Pat.*, 1977.
76. O. R. Perlovskaya, M. I. Shilina and V. V. Smirnov, *Russian Journal of Coordination Chemistry*, 2001, **27**, 469-475.
77. N. O. Mahmoodi and M. Salehpour, *Journal of Heterocyclic Chemistry*, 2003, **40**, 875-878.
78. J. M. Notestein, L. R. Andrini, F. G. Requejo, A. Katz and E. Iglesia, *Journal of the American Chemical Society*, 2007, **129**, 15585-15595.
79. F. J. J. Bihel, H. Justiniano, M. Schmitt, M. Hellal, M. A. Ibrahim, C. Lugnier and J.-J. Bourguignon, *Bioorganic & Medicinal Chemistry Letters*, 2011, **21**, 6567-6572.
80. W. C. Still, M. Kahn and A. Mitra, *The Journal of Organic Chemistry*, 1978, **43**, 2923-2925.
81. M. Mondal, V. G. Puranik and N. P. Argade, *The Journal of Organic Chemistry*, 2007, **72**, 2068-2076.
82. R. H. Grubbs, *Tetrahedron*, 2004, **60**, 7117-7140.
83. P. Jean-Louis Hérisson and Y. Chauvin, *Die Makromolekulare Chemie*, 1971, **141**, 161-176.
84. T. J. Katz and J. McGinnis, *Journal of the American Chemical Society*, 1975, **97**, 1592-1594.
85. A. H. Hoveyda and A. R. Zhugralin, *Nature*, 2007, **450**, 243-251.
86. E. L. Dias, S. T. Nguyen and R. H. Grubbs, *Journal of the American Chemical Society*, 1997, **119**, 3887-3897.
87. M. S. Sanford, M. Ulman and R. H. Grubbs, *Journal of the American Chemical Society*, 2001, **123**, 749-750.
88. S. Seto, K. Yumoto, K. Okada, Y. Asahina, A. Iwane, M. Iwago, R. Terasawa, K. R. Shreder, K. Murakami and Y. Kohno, *Bioorganic & Medicinal Chemistry*, 2012, **20**, 1188-1200.
89. B. Blass, *ACS Medicinal Chemistry Letters*, 2012, **3**, 875-876.
90. I. W. Ashworth, I. H. Hillier, D. J. Nelson, J. M. Percy and M. A. Vincent, *Chemical Communications*, 2011, **47**, 5428.

91. F. Nuñez-Zarur, X. Solans-Monfort, L. Rodríguez-Santiago and M. Sodupe, *Organometallics*, 2012, 120522121803007.
92. R. L. Pederson, I. M. Fellows, T. A. Ung, H. Ishihara and S. P. Hajela, *Advanced Synthesis & Catalysis*, 2002, **344**, 728-735.
93. C. S. Adjiman, A. J. Clarke, G. Cooper and P. C. Taylor, *Chemical Communications*, 2008, 2806.
94. G. R. A. Adair and J. M. J. Williams, *Tetrahedron Letters*, 2005, **46**, 8233-8235.
95. N. J. Wise and J. M. J. Williams, *Tetrahedron Letters*, 2007, **48**, 3639-3641.
96. G. P. Crowther, R. J. Sundberg and A. M. Sarpeshkar, *The Journal of Organic Chemistry*, 1984, **49**, 4657-4663.
97. R. Casas, C. Cavé and J. d'Angelo, *Tetrahedron Letters*, 1995, **36**, 1039-1042.
98. H. Gilman, R. G. Jones and L. A. Woods, *The Journal of Organic Chemistry*, 1952, **17**, 1630-1634.
99. S. Woodward, *Chemical Society Reviews*, 2000, **29**, 393-401.
100. N. P. Lorenzen and E. Weiss, *Angewandte Chemie International Edition in English*, 1990, **29**, 300-302.
101. N. Asao, H. Tomeba and Y. Yamamoto, *Tetrahedron Letters*, 2005, **46**, 27-30.
102. K. Iio, K. Kobayashi and M. Matsunaga, *Polymers for Advanced Technologies*, 2007, **18**, 953-958.
103. P. Yuxing, Z. Jiawei, L. Jialin and C. Linfeng, *Chinese Science Bulletin*, 1997, **42**, 1544-1549.
104. B. Jackson, H. D. Locksley, F. Scheinmann and W. A. Wolstenholme, *Journal of the Chemical Society C: Organic*, 1971, 3791-3804.
105. *BSAC Methods for Antimicrobial Susceptibility Testing*, http://bsac.org.uk/wp-content/uploads/2012/02/Version-10.1-2011-final.pdf, Accessed May 21st 2011.
106. MHRA, *Public Assessment Report CIPROFLOXACIN 2MG/ML IV INFUSION (CIPROFLOXACIN) PL 20438/0004*, http://www.mhra.gov.uk/home/groups/l-

unit1/documents/websiteresources/con2024369.pdf, Accessed 13 September, 2012.

107. MHRA, *PL 32019/0023-6*, http://www.mhra.gov.uk/home/groups/par/documents/websiteresources/con082024.pdf, Accessed 13th September, 2012.
108. D. C. Hooper, *Drug resistance updates : reviews and commentaries in antimicrobial and anticancer chemotherapy*, 1999, **2**, 38-55.
109. J. Ruiz, *Journal of Antimicrobial Chemotherapy*, 2003, **51**, 1109-1117.
110. H. M. Blumberg, D. Rimland, D. J. Carroll, P. Terry and I. K. Wachsmuth, *Journal of Infectious Diseases*, 1991, **163**, 1279-1285.
111. S. M. Smith, R. H. Eng and F. Tecson-Tumang, *Antimicrobial agents and chemotherapy*, 1989, **33**, 181-184.
112. K. Sakamoto, H. W. Van Veen, H. Saito, H. Kobayashi and W. N. Konings, *Appl Environ Microbiol*, 2002, **68**, 5374-5378.
113. R. Dhillon, St. George's University of London, 2011.
114. D. Ramanathan, St George's University of London, 2011.
115. H. D. Soule, J. Vazguez, A. Long, S. Albert and M. Brennan, *Journal of the National Cancer Institute*, 1973, **51**, 1409-1416.
116. D. W. Koh, T. M. Dawson and V. L. Dawson, *Pharmacological Research*, 2005, **52**, 5-14.
117. E. Tyrrell, P. Brawn, M. Carew and I. Greenwood, *Tetrahedron Letters*, 2011, **52**, 369-372.
118. S. Nahm and S. M. Weinreb, *Tetrahedron Letters*, 1981, **22**, 3815-3818.
119. B. Qu and D. B. Collum, *The Journal of Organic Chemistry*, 2006, **71**, 7117-7119.
120. K. Hisler, R. Tripoli and J. A. Murphy, *Tetrahedron Letters*, 2006, **47**, 6293-6295.